Condensed tannins as *in vivo* antioxidants in *Populus tremula x tremuloides*

by

Geraldine Gourlay
Bachelor of Science (Honours), Dominican University, 2014
Graduate Certificate in Learning and Teaching in Higher Education, University of Victoria, 2017

A Dissertation Submitted in Partial Fulfillment
of the Requirements for the Degree of

DOCTOR OF PHILOSOPHY

in the Department of Biology

Supervisory Committee

Condensed tannins as *in vivo* antioxidants in *Populus tremula x tremuloides*

by

Geraldine Gourlay
Bachelor of Science (Honours), Dominican University, 2014
Graduate Certificate in Learning and Teaching in Higher Education, University of Victoria, 2017

Supervisory Committee

Dr. C. Peter Constabel (Department of Biology)
Co-Supervisor

Dr. Barbara Hawkins (Department of Biology)
Co-Supervisor

Dr. Jürgen Ehlting (Department of Biology)
Departmental Member

Dr. Trevor Lantz (Department of Environmental Studies)
Outside Member

Abstract

Supervisory Committee
Dr. C. Peter Constabel (Department of Biology)
Co-Supervisor
Dr. Barbara Hawkins (Department of Biology)
Co-Supervisor
Dr. Jürgen Ehlting (Department of Biology)
Departmental Member
Dr. Trevor Lantz (Department of Environmental Studies)
Outside Member

Plants are exposed to diverse environmental stresses, which can lead to the accumulation of harmful reactive oxygen species (ROS). To prevent cellular damage, plants have evolved diverse antioxidant compounds and mechanisms to scavenge and remove ROS. My research aimed to determine if condensed tannins (CTs) function as *in vivo* antioxidants in plants. CTs are abundant plant secondary metabolites and are well-known for their strong *in vitro* antioxidant activity, but their function as antioxidants *in planta* has not previously been investigated. I used transgenic hybrid poplar (*Populus tremula x tremuloides*) with high (MYB134- and MYB115-overexpressing) and low (MYB134-RNAi) leaf CT content. Three different abiotic stresses were used to induce oxidative stress in the plants: methyl viologen (MV), drought, or UV-B stress. Oxidative stress can damage the plant's photosystems, and this damage was assessed using chlorophyll fluorescence. I employed light-adapted (*Fq'/Fm'*) and dark-adapted (*Fv/Fm*) parameters of chlorophyll fluorescence and monitored photosystem II function during each stress. Under all three stresses, the high-CT transgenics retained greater chlorophyll fluorescence, demonstrating reduced photosystem II damage, compared to wild-type plants. Oxidative damage was measured by quantifying malondialdehyde (MDA), and hydrogen peroxide (H_2O_2) was quantified as a measure of ROS accumulation. High-CT plants consistently accumulated less H_2O_2 and MDA than wild-type plants before and after each stress. MYB134-RNAi plants showed the converse effects, as predicted by lower CT concentrations, with reduced photosystem function and increased levels of H_2O_2 and MDA compared to wild-type following each stress. Overall, this work demonstrates that CTs can function as *in planta*

antioxidants and can aid in protection against oxidative damage. My work provides the first evidence for an antioxidant function of CTs in living plants exposed to stress.

Table of Contents

List of Tables

List of Figures

Acknowledgments

I would like to first thank my supervisors Dr. C. Peter Constabel and Dr. Barbara Hawkins for their unending support, guidance, and trust as we uncovered the connection between condensed tannins and antioxidative functions. I am grateful for the freedom throughout my project to try different assays or explore a little deeper in one direction even if the data did not support further expedition at the time – sometimes stubbornness can pay off. Thanks to the both of you, I have learned so much over the last five years and I am eternally grateful for the experience, knowledge, and skills I have gained.

I express my deepest gratitude to my committee members: Drs. Trevor Lantz and Jürgen Ehlting. Thank you both being very patient as I muddled my way through explaining ANOVAs. Thank you to Dr. Will Hintz for your support over the years.

I extend a warm thanks to the Constabel lab for their encouragement and indulgence with my endless questions when trying out a new assay. Thanks, too, for the hugs or high-fives shared with me when things were not going as smoothly as hoped or just because. I also acknowledge all the students (both graduate and undergraduate), faculty, and staff within the Centre for Forest Biology for their generous support, kindness, and insightful discussions over the years.

A special thanks to Brad Binges and Peter Gourlay for their crucial assistance throughout my project with assistance with the greenhouse, my plants, and my crazy light and water schedules, as well as being a constant companion in and out of the greenhouse. A warm thanks to Samantha Robbins for her having the utmost patience in training me on the fluorometer and being the repository for all my questions about “how” or “why” or “what if”.

This work has been generously funded through the NSERC CREATE program in Forests and Climate Change, as well as the University of Victoria through graduate scholarships and my entrance scholarship my first semester. Lastly, Chapter 4 was partially funded through the German Academic Exchange (DAAD) to whom I express my deepest thanks for a wonderful experience at Helmholtz Zentrum in Munich, Germany with Dr. Jörg-Peter Schnitzler and his amazing team.

Chapter 1 : General Introduction

1.1 The biology of *Populus*

The genus *Populus* includes poplars, aspens, and cottonwoods (hereafter referred to collectively as poplars) (Farmer, 1996). Poplars are widespread deciduous trees distributed across the Northern Hemisphere (Brunner *et al.*, 2004) and many are considered keystone species in their ecosystems (Wullschleger *et al.*, 2013). Poplars are dioecious, wind-pollinated trees that live in habitats ranging from arid to riparian (Bradshaw *et al.*, 2000). They can be vegetatively propagated (Bradshaw *et al.*, 2000). Poplars are known to multiply through root suckering (shoots sprouting from lateral roots close to the surface) which is a key trait for poplars that produces clones of the parent tree (Braatne *et al.*, 1996).

Populus is a very diverse genus with 29 species (Slavov and Zhelev, 2010). There are six distinct sections of poplar classified on the basis of genetics, morphology, and ecology: Abaso, Turanga, Leucoides, Aigeiros, Tacamahaca, and Populus (Slavov and Zhelev, 2010). Species within a particular section can be crossed with other species in that section, but inter-section crossing is not as common (Stanton *et al.*, 2010). *Populus tremula* and *Populus tremuloides* are two species of poplar (Section Populus), the former native to western Eurasia/north Africa and the latter from North America. The two species have been actively hybridized for poplar research and breeding, and several resulting hybrids are of particular interest for both forestry and research. My work involves one specific hybrid: *Populus tremula x tremuloides* (clone INRA-353-38; Appendix 1). Another species of interest is *Populus euphratica* (Section Turanga) from Asia, due to its well-known drought resistance (Bogeat-Triboulot *et al*., 2007). *Populus davidiana* (Section Populus) is a Korean aspen that is also recognized for being drought tolerant (Zhang *et al.*, 2004). *Populus balsamifera*, *P. trichocarpa,* and *P. angustifolia* (Section Tacamahaca) from North America with *P. nigra* (Section Aigeiros) from Europe all reproduce asexually through root suckering and via rooting of shoots from broken branches or trunks, which is unique to these species (Slavov and Zhelev, 2010). Depending on their location, poplar trees can grow in a diverse range of habitats from hot and arid deserts in northern and central Africa and central Asia, to boreal and temperate forests in North America and Europe (Slavov

and Zhelev, 2010). Poplar trees have a short-rotation period which is useful in forestry work (Ellis *et al.*, 2010).

Following the genome sequencing for *Populus trichocarpa* (Tuskan *et al.*, 2006), *Populus* became a model organism for woody plants as this genus has numerous desirable biological traits. These include a modest genome size, a suitability for genetic transformation and vegetative propagation, and a shorter generation time than other tree species (Ellis *et al.*, 2010). Overall, poplars exhibit many attributes such as adaptations to diverse environments which makes them useful in research.

1.2 Poplars synthesize a suite of phenolic compounds

Poplars produce a wide range of phenolic compounds. Phenolics are compounds with a six-carbon ring and hydroxyl groups that extend from the ring. Phenolics have diverse roles in plants acting as anti-fungal compounds, UV-screens, herbivore deterrents, plant defense compounds, and pigments (Dixon *et al.*, 2005). The phenolic pathway underpins lignin biosynthesis for plant cell walls (Saito *et al*., 2013). Examples of phenolics commonly found in *Populus* are hydroxy cinnamate esters, phenolic glycosides (including salicinoids), aromatic acids, flavonoids (including flavanones, flavonols, and dihydroflavonols), and chalcones (Ristivojević *et al.*, 2015). Salicinoids are a specialized group of phenolic glycosides with strong anti-herbivory activity (Boeckler *et al.*, 2011; Boeckler *et al.*, 2014). In poplar, flavonoids also include anthocyanins that can protect plants against the damaging effects of UV-B (Gould, 2004; Mellway *et al.*, 2009). Flavanones and flavonols are also thought to play a role in response to UV-B stress (Shirley, 1996). Dihydroflavonols are found in the resin and heartwoods of some trees and are thought to exhibit antifungal and antimicrobial properties (Ristivojević *et al.*, 2015). The flavonoid genes in *Populus* have been fully characterized (Tsai *et al.*, 2006).

Condensed tannins (CTs), also known as proanthocyanidins, are widespread secondary metabolites composed of oligomers and polymers of flavan-3-ols, most commonly epicatechin and catechin (Hagerman, 2002). Tannins are defined by their ability to precipitate proteins (Quideau *et al.*, 2011). CTs are synthesized from the phenylpropanoid and flavonoid pathway (Figure 1.1; Dixon *et al.*, 2005) and like most phenolics, are stored within the vacuole (Quideau

et al., 2011). The flavan-3-ols are generally linked between C8 and C4 by a carbon-carbon bond and have a heterocyclic ring system that is derived from polyketides (A-ring) and phenylalanine (B-ring) (Figure 1.2; Hagerman, 2002). Their B-ring usually contains hydroxyl groups that are critical for their properties and functions, such as metal chelation and antioxidant activity (Hagerman *et al.*, 1998). The greater the number of hydroxyl groups, the better the ability of the compound to chelate and function as an antioxidant (Hagerman *et al.*, 1998). CTs are present in the bark, leaves, seeds, and fruits of many woody species (Dixon *et al.*, 2005). For seeds, CTs can be deposited in the seed coat as protection against pests and microbes (Debeaujon *et al*., 2003; Gonzalez *et al*., 2016). In fruits such as grape (*Vitis vinifera*), CTs are synthesized before ripening (Kennedy *et al.*, 2001) at which point anthocyanins begin to accumulate, providing the berry colour (Bogs *et al.*, 2005; Dixon *et al.*, 2005; Fournand *et al.*, 2006). CT structures are diverse and differ based on stereochemistry, interflavan linkage, degree of polymerization, and the hydroxylation pattern (Constabel *et al.*, 2014). CTs can make up nearly 25% of dry weight in leaf tissues (Lindroth and Hwang, 1996) in species such as poplar and *Eucalyptus*. They are also induced by several biotic and abiotic stresses. CTs have been shown to be induced in poplar by UV-B and wounding (Mellway *et al*., 2009), herbivory (Peters and Constabel, 2002), nitrogen deficiency (Harding *et al.*, 2005), pathogens (Ullah *et al.*, 2017), and in *Eucalyptus* by drought (McKiernan *et al.*, 2015). Although stress induction of CTs does not demonstrate a protective role against a given stress, it is often a first indicator of a plant response to stress. The diverse biological and ecological roles of CTs are further described, below.

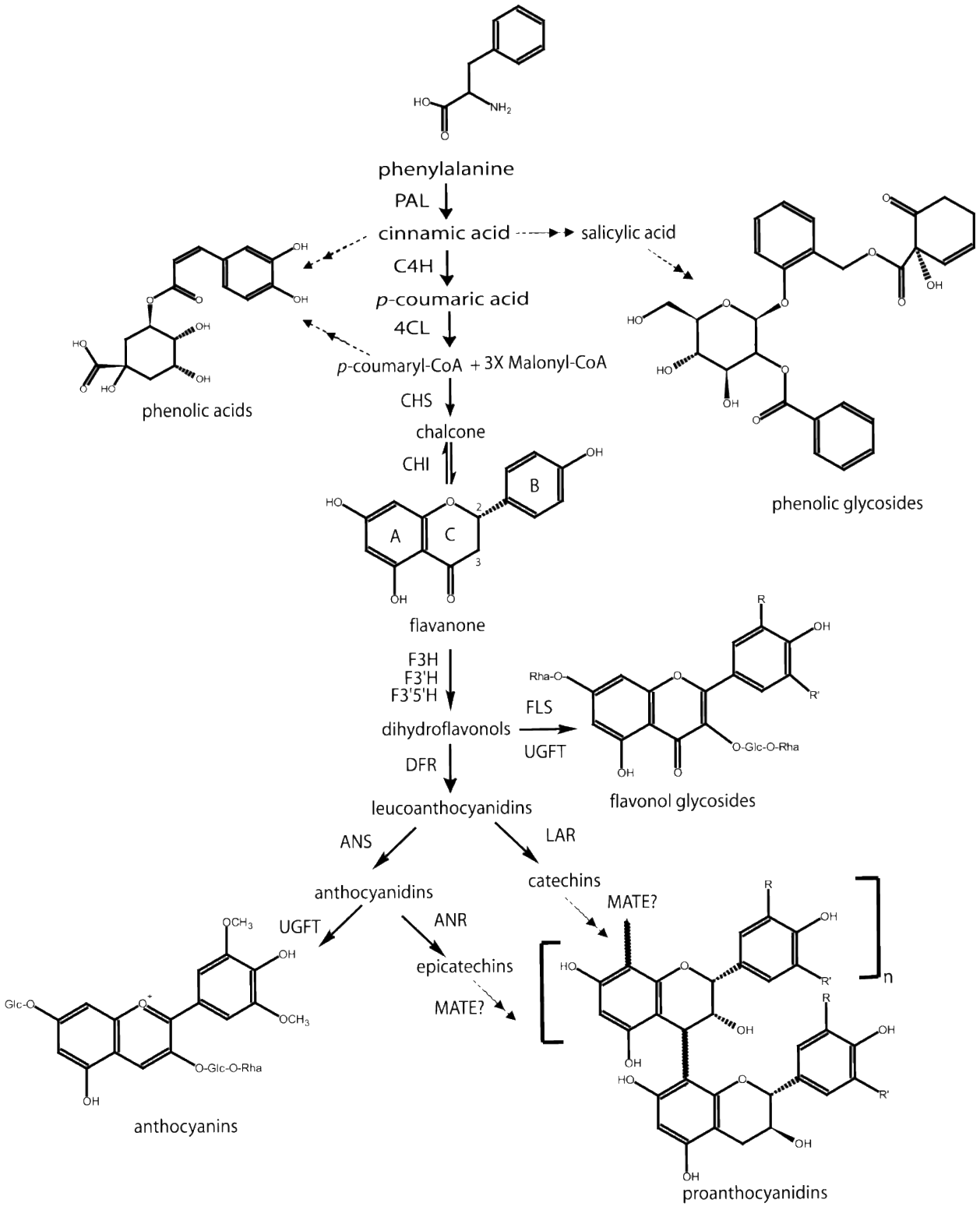

Figure 1.1: The general flavonoid synthesis pathway (from Mellway *et al*., 2009).

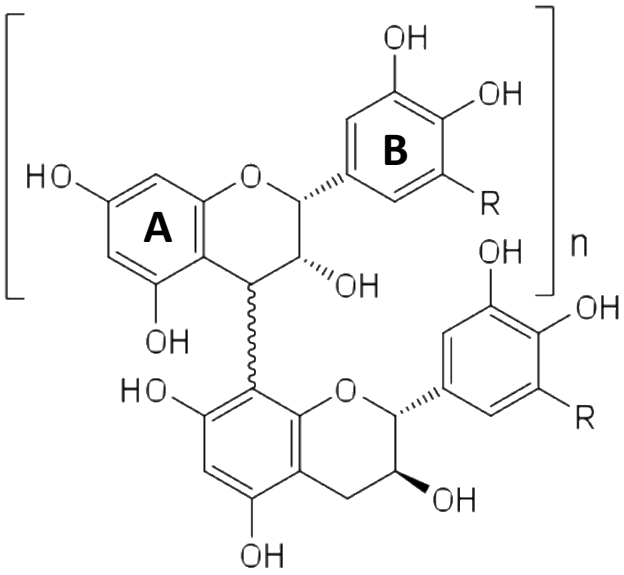

Figure 1.2: Structure of a condensed tannin.

1.3 Transcriptional regulation of CT biosynthesis by MYB transcription factors

The biosynthesis of phenolic and flavonoid compounds is largely controlled by transcription factors (TFs) called MYBs. Plant MYB TFs are encoded by large gene families (Xu *et al.*, 2015), and the poplar genome contains 192 MYB genes. However, MYBs that specifically regulate the synthesis of CTs have been characterized, and include both activators and repressors (Mellway *et al.*, 2009; James *et al.*, 2017; Ma *et al.,* 2018). MYB TFs that regulate CT biosynthesis require two co-activators to function: a WD-repeat 40 protein (WD40) and a basic-helix-loop-helix (bHLH) (Ramsay and Glover, 2005). Together, those three components make up the MBW complex necessary for the regulation of genes associated with CT biosynthesis. It is the MYB TFs that determine the specificity of the MBW complex and therefore are crucial regulators of CT biosynthesis (Ma and Constabel, 2019).

Overexpressing the MYB TFs specific for CT biosynthesis results in a marked over-accumulation of CTs, but not other flavonoids. Specifically, overexpressing MYB115 (James *et al.*, 2017) and MYB134 (Mellway *et al.*, 2009) yield high-CT transgenic poplar with up to 50-

times more CTs than wild-type. These transgenics are important tools for investigating the function of CTs *in planta*, and are used extensively in my work.

1.4 Condensed tannin functions

1.4.1 Condensed tannins as herbivore feeding deterrents

Early work proposed the hypothesis that CTs were a constitutive defense for woody species against herbivores. This idea was based on the ability of CTs to precipitate proteins in the guts of herbivores and the negative correlations observed between herbivore (*Operophtera brumata,* winter moth) performance and the level of CTs in the foliage of *Quercus robur* (oak) (Feeny, 1968). Additionally, CTs have been shown to accumulate following herbivory in *Populus* suggesting they could be an inducible defense (Osier and Lindroth, 2001; Peters and Constabel, 2002; Kosola *et al*., 2006).

Recent work has not been successful in consistently replicating the work of Feeny (1968). Although CTs can have negative effects on some insect herbivores, those effects are not due to their ability to bind dietary and digestive proteins (Constabel *et al.*, 2014). CTs precipitate proteins only under acidic conditions and the guts of caterpillars (Lepidopterans) have a pH 8-10 (Barbehenn *et al.*, 2009; Barbehenn and Constabel, 2011). Instead, CTs appear to exhibit more of a toxic effect on herbivores (Barbehenn and Constabel, 2011). This toxic effect is due to the CTs being oxidized in the insect gut and forming semiquinone radicals (Barbehenn and Constabel, 2011). In general, there is only limited evidence that CTs have a deterrent or antinutrient effect on insect herbivores.

Vertebrate guts are acidic, and at high concentrations, CTs have been shown to be effective anti-herbivore compounds (Stevens and Hume, 2004). When vertebrates consume leaf material that contains high levels of CTs, those CTs will bind to nutritive proteins within the gut of the vertebrate herbivore and reduce available nitrogen. This has been shown to significantly impact the health, performance, and survival of the vertebrates (Wallis *et al.*, 2012). In summary, CTs are antinutrient defenses against vertebrates but their role against insect herbivores is not clear.

1.4.2 Antimicrobial and antifungal properties of condensed tannins

CTs have been shown to act as general antimicrobial and antifungal compounds. CTs inhibit fungal growth by complexing with enzymes and by chelating heavy metal ions (*e.g.* Fe^{3+}) which are necessary for the function of metalloenzymes (Scalbert, 1991). The chelate formed between metal ions and CTs could also function as a physical barrier around the root, preventing any fungal growth (Treutter, 2006). CTs also have *in vitro* antimicrobial activity by disrupting cellular function by binding to the cell walls of bacteria (Smith *et al.*, 2005). Ullah *et al.* (2017) found that transgenic poplars with enhanced CT concentrations were less susceptible to *Melamposora* leaf rust, suggesting that CTs can function as antifungal compounds. Assefa *et al*. (2017) found that CTs from forage plants had antimicrobial activity against *Escherichia coli* and *Staphylococcus aureus.* Peters and Constabel (2002) hypothesized that the accumulation of CTs in wounded poplar leaves is to protect the wounded leaf from infection from pathogens.

Due to their strong antimicrobial activity, CTs have been considered as an alternative to antibiotics in the poultry industry (Redondo *et al.*, 2014). Peng *et al.* (2018) found that CTs from purple prairie clover inhibited growth of bacteria and fungi during ensiling. However, the effect appeared to be species-specific due to variation in microbial populations in the microbiome (Peng *et al.*, 2018). CTs are very beneficial for ruminant animals because they can lower the overall gut parasite load and help reduce the chance of bloating (Constabel *et al.*, 2014).

1.4.3 Condensed tannins in nutrient decomposition

As forest tree foliage usually contains large amounts of CTs, leaf litter in forests is often high in CTs. CTs in the leaves inhibit the decomposition and decay of leaf litter by microbes and fungi in the soil. Previously, CTs have been shown to negatively influence the rate of leaf decay in montane forests (Hättenschwiler *et al.*, 2003). It was found that root CT concentrations were inversely correlated with N-concentration, and high concentrations of CTs led to reduced rates of decomposition (Hättenschwiler *et al.*, 2003). Different concentrations of CTs in leaf litter were found to influence the rates of litter decay in different *Populus* species (Fremont poplar, Narrowleaf poplar, and some hybrid poplars) (Schweitzer *et al.*, 2004). CTs are known to influence the rate of nitrogen mineralization, as well as the decomposition process (Constabel

et al., 2014; Shay *et al.*, 2018). There are five means by which CTs could alter litter decomposition in forest soils: microbe toxicity, deactivating microbial exoenzymes, coating compounds in the soil thereby preventing their decomposition, forming protein-tannin complexes that are resistant to decomposition, and being resistant to decomposition on their own (Kraus *et al*., 2003). In *Quercus laevis* (turkey oak), the composition of leaf litter from randomly selected individuals of *Q. laevis* greatly influenced the nutrient cycling over the three-year field study (Madritch and Hunter, 2005). Work by Madritch and Lindroth (2015) showed that elevated concentrations of CTs increased the overall total nitrogen recovered by *Populus tremuloides* following defoliation by *Lymantria dispar* (gypsy moth). During defoliation and herbivory attacks, CTs are upregulated and trees with higher levels of CTs recover more nitrogen than trees with lower levels of CTs (Madritch and Lindroth, 2015). Therefore, the CTs play an indirect role in nutrient cycling. CTs were significant in affecting the litter chemistry and altering the overall nutrient dynamics within the soil by affecting carbon and nitrogen changes in the leaf litter (Madritch and Hunter, 2005). Consequently, there is strong evidence that CTs impact decomposition and nutrient cycling in forest soils. How this benefits trees has not yet been demonstrated. It has been suggested that inhibition of mineralization gives trees and their mycorrhizal symbionts, which can assimilate organic nitrogen, a competitive advantage over other tree species (Constabel *et al.*, 2014).

1.4.4 Heavy metal chelation by condensed tannins

A phenyl (B) ring containing two or more hydroxyl groups facilitates heavy metal chelation by phenolic compounds (Quideau *et al.*, 2011). Due to their numerous *ortho*-hydroxyl groups, CTs have the capacity to chelate heavy metal ions such as iron (Fe), copper (Cu), zinc (Zn), and aluminum (Al) (Hagerman *et al.*, 1998; Oo *et al.*, 2009; Constabel *et al.*, 2014). One mechanism proposed for CTs chelating heavy metals is through ion exchange between the *ortho*-hydroxyls and the metal cations leading to the formation of a chelate (Oo *et al.*, 2009). The interaction between CTs and heavy metals would be primarily through the flavonoid B-rings, and therefore the overall structure of the B-ring will play a role in how well CTs can chelate heavy metals. But, this heavy metal chelation, in particular of Cu and Fe, supports the hypothesis that CTs can

prevent the transition metal-catalyzed generation of free radicals in plant cells (Rice-Evans *et al.*, 1997). For instance, in the camphor tree (*Cinnamomum camphora*), CTs accumulate in cells that shield the growing root cells, which minimizes the toxic effect of heavy metals within the soil interfering with root growth (Osawa *et al.*, 2011).

1.4.5 Condensed tannins in human diets

In addition to possible functions in plants, CTs are well-established as strong dietary antioxidants for humans (Dixon *et al.*, 2005). CTs are found in many foods and beverages including wine, tea, cereals, fruits, nuts, and vegetables (Prior and Gu, 2005). Diets high in CTs have been associated with decreased risks of cardiovascular diseases, cancer, and some neurodegenerative diseases (Fraga *et al.*, 2010). CTs have also been shown to have cardioprotective effects by minimizing the oxidation of low-density lipoprotein (Santos-Buelga and Scalbert, 2000; Prior and Gu, 2005). A diet rich in CTs may benefit someone suffering from iron-related diseases (Santos-Buelga and Scalbert, 2000) or to lower blood glucose levels and aid in managing diabetes (Kumari and Jain, 2012).

1.4.6 The antioxidant capacity of condensed tannins

Condensed tannins have been shown to exhibit strong *in vitro* antioxidant activity. This is based on the proximity of aromatic rings with hydroxyl groups and the *ortho*-hydroxylation pattern on the B- ring (Hagerman *et al.*, 1998). The polymeric structure of CTs, with their large number of hydroxyl groups, further facilitates scavenging and quenching of reactive oxygen species (ROS) (Figure 1.2; Hagerman *et al.*, 1998). Two main mechanisms by which CTs are thought to directly quench ROS are: hydrogen atom transfer or single-electron transfer (Quideau *et al.*, 2011). In both mechanisms, the CTs would donate either a hydrogen or an electron to stabilize the ROS, generating a stable phenoxy radical that does not react with the ROS or with lipids, thereby stopping the radical chain reaction (Quideau *et al*., 2011). *In vitro* studies have concluded that CTs are stronger antioxidants than vitamin C or vitamin E, both of which are considered standard antioxidants (Rice-Evans *et al.*, 1996). The *ortho*-dihydroxy organization in the B-ring

of the CT compound is essential in the strength of the antioxidant activity (Burda and Oleszek, 2001). In addition to scavenging and quenching ROS directly, CTs are thought to serve as antioxidants by chelating Fe^{2+} and preventing the Fenton reaction. The Fenton reaction occurs when hydrogen peroxide and Fe^{2+} interact and generate a hydroxyl radical (Quideau *et al.*, 2011), the most damaging of all ROS (Demidchik, 2015). However, studies thus far have been done *in vitro,* and my dissertation will examine the effects of CTs as antioxidants *in planta* following exposure to different abiotic stresses.

1.5 General abiotic stress effects, production of ROS, and plant responses

Plants are exposed to a diverse array of stresses over the course of their lifespan, and as sessile organisms they must have mechanisms to cope with stresses in the environment. Abiotic stress is any stress imposed by a non-living agent. Stress can have immediate biochemical and physiological effects and may result in a reduction in vegetative or reproductive growth, impaired development or death of plants. For example, under drought stress, plant cells cannot expand fully because of dehydration and this can lead to a reduction in overall plant growth (Cramer *et al*., 2011). Salt stress leads to cytotoxicity due to an accumulation of ions which can interfere with nutrient uptake (Lutts *et al.*, 1996). During freezing stress, ice crystals are formed in the extracellular space, which may lead to rupture or dehydration of unacclimated cells (Schulz *et al.*, 2015).

One common feature of several abiotic stresses is the generation of ROS which cause oxidative stress in a plant. ROS include hydrogen peroxide (H_2O_2), singlet oxygen ($^1O_2$), superoxide (O_2^-), and the hydroxyl radical (HO*) (Apel and Hirt, 2004). Singlet oxygen and superoxide can be generated in the chloroplasts due to electrons being diverted from the electron transport chain to molecular oxygen under high light or drought stress (Krieger-Liszkay, 2005). H_2O_2 is formed from the dismutation of superoxide and the hydroxyl radical is formed by H_2O_2 interacting with Fe^{2+} in the Fenton reaction (Dat *et al.*, 2000; del Río, 2015). If ROS concentrations become too high, they can result in damage to proteins, DNA, and lipids (lipid peroxidation) (Farmer and Mueller, 2013) within the plant. ROS, specifically H_2O_2, have also been shown to be involved in signaling and can influence gene expression, ABA signaling,

programmed cell death, and root hair growth (Smirnoff and Anaud, 2019). Upon exposure to a specific environmental condition (*e.g.* wounding, high light), the changes in gene expression can be seen in leaves not immediately impacted by the condition, and H_2O_2 is thought to play a role in transmitting that signal throughout the plant (Smirnoff and Anaud, 2019).

Plants can respond to abiotic stresses in part by the production of antioxidant molecules and enzymes that detoxify and remove the ROS produced. Two key enzymes for maintaining the ROS homeostasis in plants and preventing lipid peroxidation are: superoxide dismutase which converts superoxide to H_2O_2 (Bowler *et al*., 1992) and catalase which converts H_2O_2 to water (Aebi, 1984). Small compounds that function as antioxidants and protect against oxidative stress include ascorbate, glutathione, and α-tocopherol (del Río, 2015). Additionally, other compounds such as small phenolics also serve as antioxidants (Rice-Evans *et al.*, 1997). The end products of the flavonoid pathway, CTs and anthocyanins, are strong antioxidants *in vitro* as mentioned above (Rice-Evans *et al.*, 1997).

Some flavonoids have been recently shown to function as *in planta* antioxidants, but this function has not been thoroughly tested, except in a few cases. In particular, work has been done investigating the *in vivo* antioxidant function of anthocyanins. *Arabidopsis* plants overexpressing MYB12 had an increased accumulation of anthocyanins and this protected the plants during oxidative stress generated by methyl viologen and drought stress by scavenging ROS (Nakabayashi *et al.*, 2014). Utilizing *Arabidopsis* overexpressing different UDP-glycosyltransferases, Li *et al.* (2017) found that the overexpression led to increases in anthocyanin accumulation and this contributed to plant tolerance to drought, salt, and cold stress. While anthocyanins appear to function as *in vivo* antioxidants in plants, the possibility that CTs, which are vacuolar compounds like anthocyanins (Agati *et al.*, 2012), function as *in planta* antioxidants, has not been tested. My PhD work aims to fill this information gap and to address the important question of whether or not CTs function as *in-planta* antioxidants.

1.6 Research objectives

The key question of my research is: can CTs function as *in vivo* antioxidants in poplar trees and act as a defense against abiotic stress? Rice-Evans *et al.* (1997), Hagerman *et al.* (1998) and many others have previously established that CTs have strong *in vitro* antioxidant activity.

Testing the *in vivo* function of CTs as antioxidants may be important to understand why some species of trees (*e.g.* poplars, *Eucalyptus*) induce CTs following certain stresses. The Constabel lab has previously generated transgenic poplars with high concentrations of CTs (Mellway *et al.*, 2009; James *et al.*, 2017). Low-CT poplar were generated as part of this dissertation (Chapter 3) in the hybrid *Populus tremula x tremuloides* which naturally accumulates high concentrations of leaf CTs. These plants allowed me to address, for the first time, the critical question of CT function.

I selected three types of ROS-generating stresses. Drought and UV-B stress were chosen because they are known to generate ROS, and are encountered by poplars under natural conditions. Additionally, drought and UV-B generate ROS by distinct mechanisms, which allowed me to include both indirect and direct-ROS producing stresses. I also used methyl viologen (MV) to more precisely control ROS production and oxidative stress in the plants (Bus and Gibson, 1984).

The general approach throughout this work was to use both physiological and biochemical techniques to measure the impacts of stress in poplar leaves. These techniques include chlorophyll fluorescence, biochemical analysis, antioxidant assays, oxidative biomarker assays, and ROS quantification methods.

In Chapter 2, I first confirm that the concentration of CTs was positively correlated with antioxidant capacity in our high-CT transgenics; that is, with elevated CT concentrations the plants also showed high antioxidant activity. Next, I used the herbicide methyl viologen (MV) as a controlled method to generate oxidative stress as a first test of whether CTs can act as protective antioxidants *in vivo*. Because MV can be administered to individual leaves via the transpiration stream, I was able to generate ROS and cause oxidative stress in the leaves under carefully controlled conditions. This chapter has been published in Tree Physiology 39: 345-355 (Gourlay and Constabel, 2019).

The focus of Chapter 3 is the characterization of low-CT MYB134-RNAi transgenics and their use as additional tool for studying the function of CTs as *in vivo* antioxidants. I demonstrated that these transgenics have little accumulation of CTs under stressful conditions. I also performed additional studies, including transcriptomic and HPLC analysis as well as

morphological measurements, to confirm that no other biochemical pathways were disrupted (Appendix 2, 3), and that only the CT pathway was affected in these plants. These plants were exposed to MV to test if the low-CT transgenics are more susceptible than the high-CT transgenics. These experiments allowed us to complete our investigation of how plants with differing levels of CTs survive ROS produced by MV. This chapter has been submitted to the Journal of Experimental Botany (Gourlay *et al.*, 2019).

Chapter 4 addresses the question: "Do condensed tannins in poplar saplings protect against ROS produced during drought and UV-B exposure?", and investigates stresses commonly encountered by trees in the field. Using both high- and low-CT transgenics, I test the hypothesis that high-CT transgenic plants are better protected against these ROS-producing abiotic stresses. Chapter 4 focuses on how the different high- and low-CT transgenic lines performed under drought and how the high-CT plants tolerated UV-B stress. I travelled to Germany for these experiments and carried out all the work described, including the UV-B experiments in sun simulation chambers at the Environmental Simulation Unit at Helmholtz Zentrum in Munich. This chapter will be submitted to New Phytologist.

The final discussion in Chapter 5 ties together the main results and key conclusions from each of the experimental chapters (Chapters 2-4) in the light of what is known about CTs and stress tolerance. I also address the implications and significance of my research for future work with CTs.

My work directly addresses the question: do CTs function as *in vivo* antioxidants in poplar trees and protect against ROS-producing abiotic stresses? I use the information collected from high- and low-CT transgenics under three ROS-producing abiotic stresses to demonstrate a novel role for a well-known compound. This is the first time CTs have been shown to function as *in vivo* antioxidants in plants. This new function may explain why many types of stress act to induce CTs in certain plants.

Chapter 2 : Condensed tannins are inducible antioxidants and protect hybrid poplar against oxidative stress

(This chapter is published as Gourlay and Constabel (2019) in Tree Physiology **39**: 345-355)

2.1 Introduction

Plants produce a plethora of phenolic secondary plant metabolites that help them adapt to a wide array of biotic and abiotic stresses. Globally, the most abundant secondary plant metabolites are the condensed tannins (CTs), polymeric flavonoids found throughout the plant kingdom. They are especially prevalent in roots, bark and leaves of woody plants, where they can constitute as much as 25% of tissue dry weight (Barbehenn and Constabel, 2011). In herbaceous plants, CTs are found primarily in the seed coat, where they are cross-linked to other cellular constituents and help protect the seed. By contrast, in leaves of trees and woody plants, they appear to have different roles, and can function as anti-microbial defense compounds and anti-herbivore defenses. In leaf litter and forest soils, CTs inhibit microbial processes such as nutrient cycling and decomposition (Constabel *et al*., 2014). Because of their abundance in seeds and many fruit, they are a significant part of the human diet (Prior and Gu, 2005). Importantly, a diet high in CTs is linked to reduced risk of cardio-vascular disease, neurodegenerative diseases and metabolic syndrome; this association has stimulated much research into CTs (Santos-Buelga and Scalbert, 2000; Prior and Gu, 2005).

Like many other flavonoids and phenolics, CTs have a strong antioxidant capacity *in vitro* (Rice-Evans *et al.*, 1997; Hagerman *et al.*, 1998; Barbehenn *et al*., 2006). The presence of a catecholic B-ring is typical of most CTs and the key factor determining their antioxidant capacity (Rice-Evans *et al.*, 1996; Quideau *et al*., 2011). This capacity is further enhanced by the polymerization of flavan-3-ols into the larger CTs (Rice-Evans *et al*., 1996; Hagerman *et al.,* 1998). Condensed tannins and flavonoids are proposed to act as antioxidants via H-atom transfer or single-electron transfer mechanisms (Seyoum *et al.,* 2006; Quideau *et al.,* 2011).

Despite many studies demonstrating high antioxidant capacity of CTs *in vitro*, it is not known if CTs can act as cellular antioxidants. Exposure to stressful conditions enhances the

accumulation of reactive oxygen species (ROS) in plant tissues and cause oxidative stress. While ROS are by-products of normal metabolism, their levels increase following drought, salt stress, nutrient deficiency, exposure to excess light and UV-B, and other stresses (Demidchik, 2015). Such conditions cause disruption of the photosystems, resulting in leakage of electrons from the photosynthetic electron transport chain to O_2 and creating superoxide anions (O_2^-). Under normal conditions, superoxide can be detoxified by superoxide dismutase and converted to H_2O_2 (Gill and Tuteja, 2010), which is further metabolized by catalase or ascorbate peroxidase (Noctor and Foyer, 1998). Other ROS commonly found in plants are singlet oxygen ($^1O_2$) and the hydroxyl radical (•OH). The latter is produced by the Fenton reaction involving H_2O_2 and iron (Fe) and is highly toxic. Oxidative stress causes membrane damage and leads to lipid peroxide formation. In the presence of transition metals such as copper (Cu) or Fe, these peroxides participate in cyclical reactions resulting in further ROS generation (Dat *et al*., 2000; Gill and Tuteja, 2010; Demidchik, 2015). In addition to the enzymes that directly remove ROS, plants also produce small molecules that have the ability to quench ROS. These include water soluble antioxidants such as glutathione and ascorbic acid, and the lipid-soluble α-tocopherols and carotenoids that detoxify ROS in membranes (Gill and Tuteja, 2010). Enzymatic systems to regenerate these substances are also a critical component of plant adaptation to oxidative stress.

Experimentally, oxidative stress and ROS can be generated in plants using methyl viologen (MV), an herbicide with the trade name Paraquat. Methyl viologen interrupts photosynthetic electron flow and accepts excited electrons from photosystem I, which are subsequently donated to molecular oxygen, generating superoxide. At high concentrations, MV generates sufficient ROS to cause cell death and ultimately kill the plant. At non-lethal concentrations, MV can be used to generate ROS in order to study plant responses and tolerance to oxidative stress (Bus and Gibson, 1984). Methyl viologen application thus allows for precise control of oxidative stress under controlled conditions.

Photosynthetic membranes and proteins are particularly sensitive to oxidative stress, and measuring chlorophyll fluorescence is a useful approach for assessing plant health (Baker and Rosenqvist, 2004). Chlorophyll fluorescence measurements detect photosystem

damage by determining how much light is productively used for photochemistry, rather than dissipated as heat or fluorescence (Maxwell and Johnson, 2000). Measurements can be taken on intact plants and provide a non-destructive measure of plant health in real time (Maxwell and Johnson, 2000; Baker, 2008). This approach has been used to determine the effects of abiotic stresses such as salt, drought, high temperature and UV-B (Allakhverdiev *et al.,* 1996; Utkhao and Yingjajaval, 2015; Czégény *et al.,* 2016).

Previously, we discovered that high light, UV-B irradiation, and pathogen infection all induce CT synthesis and accumulation in poplar leaves (Mellway *et al*., 2009). Similarly, other groups have shown that drought stress induces CTs in some trees including poplar (Popović *et al.*, 2016), eucalyptus (McKiernan *et al*., 2015), and *Casuarina equisetifolia* (Zhang *et al.*, 2012). Reactive oxygen species accumulation is a common feature of all these stresses; this suggests that CT accumulation could be an adaptive response to oxidative stress, especially in tree leaves with abundant CTs. Poplar and aspen trees (*Populus* spp.) accumulate CTs in leaves and other tissues and are thus useful experimental systems for studying these compounds (Constabel and Lindroth, 2010). Furthermore, some hybrids of *Populus* can be genetically transformed using *Agrobacterium* (Brunner *et al.*, 2004), and several *Populus* genomes have been sequenced (Tuskan *et al*., 2006; Wullschleger *et al.*, 2013), facilitating a molecular approach to ecophysiological questions.

During previous work on the transcriptional regulation of CTs, we generated transgenic poplar (*Populus*) plants that accumulate high concentrations of CTs by overexpressing MYB134 and MYB115 transcription factors (Mellway *et al.,* 2009; James *et al.,* 2017). These plants are excellent tools for testing CT function. Here, we use MYB115- and MYB134-overexpressing transgenics to demonstrate that high-CT plants have enhanced antioxidant capacity, and that leaves from these plants show improved tolerance to MV-induced oxidative stress.

2.2 Materials and Methods

2.2.1 Plant growth conditions and treatment

Populus tremula x P. tremuloides (clone INRA 353-38) wild-type and transgenic MYB134- and MYB115-overexpressing plantlets (Mellway *et al.,* 2009; James *et al.,* 2017) were maintained and micropropagated in tissue culture on Lloyd and McCown's Woody Plant Media (WPM; Caisson) supplemented with 1 µM indole-3-butyric acid (IBA). Prior to experiments, tissue culture plantlets were transferred to soil and acclimated in a mist chamber for 4 weeks (Appendix 4.1), then planted in 1-gallon pots with a peat moss-based soil-less mix (Sunshine Mix 4, Sungro®, Seba Beach, AB, Canada) with additional slow-release fertilizer as described by Major and Constabel (2006). Plants were kept in the greenhouse under 16 h days with supplemental lights to extend day length (Appendix 4.2). Temperatures ranged from 18 °C to 26 °C. Plants were 2 months old with 15-20 leaves when used for experiments.

For high light treatments, 8-week old plants in pots were moved to an open-top area (Appendix 4.3) and exposed to natural sunlight for 2 weeks during the summer months (June - August) in Victoria, BC, Canada (48.4634 °N, 123.3117 °W). Pots for outdoor plants were kept in saucers and watered three times daily. The average light intensity was 835 µmol m^{-2} s^{-1} of light for the 2-week experimental duration. Plants were rotated every other day to minimize light differences.

For nitrogen (N) deficiency treatments, greenhouse plants were grown in standard soil-less mix as above, but without additional slow-release fertilizer. These plants were watered with Long Ashton nutrient solution (Hewitt, 1966) with standard nitrogen concentration (10 mM) for 2 weeks. The plants were then subjected to three different nitrogen levels (10 mM, 1 mM, or 0.1 mM) for an additional 2 months. Nitrogen concentrations were modulated by fertilizing the plants daily with 100 ml of Long Ashton nutrient solution with modified NH_4NO_3 concentrations (10 mM, 1 mM, or 0.1 mM).

2.2.2 Methyl viologen treatment

Multiple independently transformed MYB134- and MYB115-overexpressing poplar lines (Mellway *et al*., 2009; James *et al.,* 2017) were used for experiments, with wild-type poplar plants servings as controls. Five individual clonal replicates of each transgenic line were used as a source of leaves in each experiment, with duplicate experimental leaves excised from each plant from within the leaf plastochron index 10-12 range. Detached leaves were placed in parafilmed 50 ml conical tubes with the petiole submerged in 200 µM MV or water (Schwanz and Polle, 2001; Appendix 4.4). The leaves were placed in a growth chamber equipped with LED lighting (GreenPowerLED production module DR/B 150_110V, Philips, Markham, Ont., Canada) set for a 16 h photoperiod. The light fixture in the chamber was placed so that all leaves received 200 µmol m^{-2} s^{-1} of light. Tubes were randomized within the chamber and organized to avoid shading. Solutions were replaced as needed after 12 h.

2.2.3 Chlorophyll fluorescence

Chlorophyll fluorescence measurements were taken using an OPTI-Sciences Modulated Chlorophyll Fluorometer OS1p (Opti-Sciences, Inc., Hudson, NH, USA). We measured *Fv/Fm,* a dark-adapted parameter that indicates maximum quantum efficiency of photosystem II photochemistry (Baker, 2008; Murchie and Lawson, 2013). Dark adapter clips were placed on two similar locations across the leaves and the chamber was darkened for 30 min, after which fluorescence measurements were taken at each dark adapter clip site. All experiments were started early in the morning and at the same time of day for each replicated experiment. After the last fluorescence measurements, 1.5 cm diameter leaf discs were excised and stained according to protocols below. Multiple independent experiments using two independently transformed lines of each high-CT MYB overexpressor types were performed.

2.2.4 Staining and image analysis

3,3'-Diaminobenzidine (DAB) staining of leaf discs was performed following Daudi and O'Brien (2012). Two leaf discs (1.5 cm diameter) were excised from each leaf per

treatment per plant using a cork borer and placed abaxial side down on DAB staining solution in 24-well plates. The plates were covered in aluminum foil, placed in a desiccator, and mild vacuum was applied for 5 min for infiltration. Following incubation on a shaking incubator in the dark at 100 rpm for 2.5 h, discs were cleared using 3:1:1 of 100% EtOH:glycerol:acetic acid (Daudi and O'Brien, 2012). Stained leaf discs were stable in clearing solution for up to three days at 4 °C. Nitroblue tetrazolium (NBT) staining was performed following Wohlgemuth *et al.* (2002), and leaf discs were handled as above but stained for only 30 min. Stained leaf discs were scanned using an EPSON Perfection V700 Photo scanner and stained areas quantified using WINRHIZO version 2009c (Regent Instruments Canada, Inc., Quebec City, QC, Canada). The images were scanned at 600 dpi on a solid white or yellow background for DAB and NBT stained discs, respectively. The software was then used to quantify leaf disc areas that were stained. Each color category was manually defined within the software for a given experiment using at least 12 representative colored spots for each category. These were manually chosen to cover the range of coloration observed in stained and unstained areas of the discs.

2.2.5 Extraction and butanol-HCl condensed tannin assay

The butanol-HCl assay (Porter *et al*., 1986) was used to quantify condensed tannins as described previously (Yoshida *et al.,* 2015). Twenty-five milligrams of ground freeze-dried tissue was extracted in 1.5 ml of 100% MeOH and homogenized in 2-ml CryoTubes with four steel beads using a Precellys tissue homogenizer (Bertin Technologies, Rockville, MD, USA) for 2 x 45 s at 5000 rpm followed by centrifugation of 10 min at 15,000*g*. Extractions were repeated twice more with an additional 1 ml MeOH. For the assay, 66.7 µl iron reagent (2% w/v $FeNH_4(SO_4)_2$ in 2N HCl) and 2 ml butanol-HCl (95:5 v/v) was added to 500 µl of MeOH extract. After vortexing, 200 µl of the mixture was removed as the unheated blank. The remaining assay mixture was heated to 95 °C in a water bath for 1 h, cooled to room temperature, and the A_{550} of 200 µl of the mixture read in 96-well plates using a PerkinElmer Victor X5 2030 Multilabel Plate Reader (Turku, Finland). The A_{550} unheated aliquots was subtracted from that of the heated aliquots for background correction. Tannin concentration was calculated using purified poplar condensed tannin as a standard (Mellway *et al.,* 2009).

2.2.6 Antioxidant assays

The 2-diphenyl-1-picrylhydrazl (DPPH) assay is based on a stable radical cation that acts as the reactive species and changes colour in the presence of antioxidant molecules (Blois 1958; Nakajima *et al.,* 2004). Briefly, 50 µM of DPPH solution was made in 100% MeOH. Two milliliters of this solution was pipetted into the appropriate number of cuvettes (4 ml spectrophotometric plastic cuvettes, Fisher Scientific, Ottawa, Ont., Canada) and initial A_{517} read on a spectrophotometer (ThermoSpectronic Genesys 10uv Scanning spectrophotometer, ThermoFisher Scientific, Waltham, MA, USA). Twenty microliters of methanolic plant extract was added to each cuvette. After incubation at room temperature in the dark for 4 h, A_{517} was measured again. The final absorbance was subtracted from initial absorbance and results were expressed relative to a Trolox (Sigma Aldrich, Oakville, Ont., Canada) standard as Trolox equivalent antioxidant capacity (TEAC) (Re *et al.,* 1999).

The ABTS (2,2'-azinobis-(3-ethyl-benzothiazoline-6-sulfonic acid) assay was adapted from Re *et al.* (1999). Equal portions of 7 mM ABTS and 2.45 mM potassium persulfate were mixed in water and at room temperature in the dark for 12 - 16 h to generate the stable radical $ABTS^+$. This $ABTS^+$ solution was diluted with MeOH to an A_{734} of 0.70 (+/- 0.02). Ten microliters of methanolic plant extract was pipetted into a 4 ml plastic cuvette and 1 ml of the ABTS solution was added. Initial absorbance was measured after mixing and the cuvettes incubated at room temperature in the dark for 45 min. Final absorbance was measured and subtracted from the initial absorbance, and the results were expressed as TEAC.

The Ferric reducing antioxidant power (FRAP) assay was adapted from Benzie and Strain (1996). A FRAP working solution was prepared with 0.3 M acetate buffer pH 3.6, 10 mM TPTZ (2,4,6-tripyridyl-triazine) diluted in 40 mM HCl, and 20 mM $FeCl_3 \cdot 6H_2O$ at 10:1:1. Fifty microliters of methanolic plant extract was added to a 4 ml plastic cuvette and placed directly in a 37 °C water bath. The FRAP working solution (2.95 ml) was added to each plastic cuvette. After 4 min, A_{593} was measured and antioxidant activity was calculated as TEAC.

2.2.7 Hydrogen peroxide quantification assay

Twenty milligrams of fresh tissue was ground in a chilled mortar and pestle with 1.5 ml of 20 mM potassium phosphate buffer, pH 6.5 (Cha *et al.*, 2015) and 10% polyvinyl polypyrrolidone (PVPP). The slurry was incubated on ice for 15 min and mixed by inversion every 5 min, then centrifuged at 10,000*g* for 15 min at 4 °C. The supernatant was transferred to fresh tubes. Hydrogen peroxide concentration was determined in 50 µl of extract using the AmplexRed Hydrogen Peroxide/Peroxidase Assay Kit (Fisher Scientific) according to the manufacturer's instructions.

2.2.8 Statistical analyses

For all experiments, data were analyzed using *t*-tests, or analysis of variance (ANOVA) and Tukey honest significant difference (HSD) post-hoc tests in R (https://www.r-project.org); details are presented in the figure legends. Pearson correlation coefficients were calculated using R.

2.3 Results

2.3.1 High light stress and nitrogen deficiency induce antioxidant capacity and CTs in poplar leaves

Previous work had demonstrated the induction of CTs by high light stress and nitrogen deficiency, treatments that cause oxidative stress in leaves. We produced high light stress by exposing greenhouse-grown plants to natural sunlight for two weeks. This treatment stimulated a 14-fold increase in foliar CT concentration (Figure 2.1). The antioxidant capacity showed a parallel response; Trolox equivalent antioxidant (TEAC) increased from 10 mg/g^{-1} dry weight to 80 mg/g^{-1} dry weight (Figure 2.1).

We also tested the plant response to nitrogen deficiency. This treatment was previously shown to induce accumulation of phenylpropanoids including CTs in poplar (Harding *et al.,* 2005; Hikosaka *et al.*, 2005). To determine if this treatment also induces antioxidant activity, we irrigated plants grown in soil-less peat mix with nutrient solutions with two levels of reduced nitrogen concentration. Plants grown at 0.1 mM nitrogen showed a 4- to 5-fold greater CT content than those grown at 10 mM nitrogen (Figure 2.2). Plants irrigated with 1.0 mM nitrogen showed an intermediate response. The antioxidant capacity of the extracts again closely mirrored the CT concentration, suggesting that CTs are the major contributors to extractable antioxidant capacity in nitrogen-deficient leaves. For both stress treatments, the correlation of CT content and antioxidant activity was tested directly using Pearson correlation analysis; the correlation coefficients were 0.972 ($P < 0.001$) and for high light stress and nitrogen deficiency, respectively.

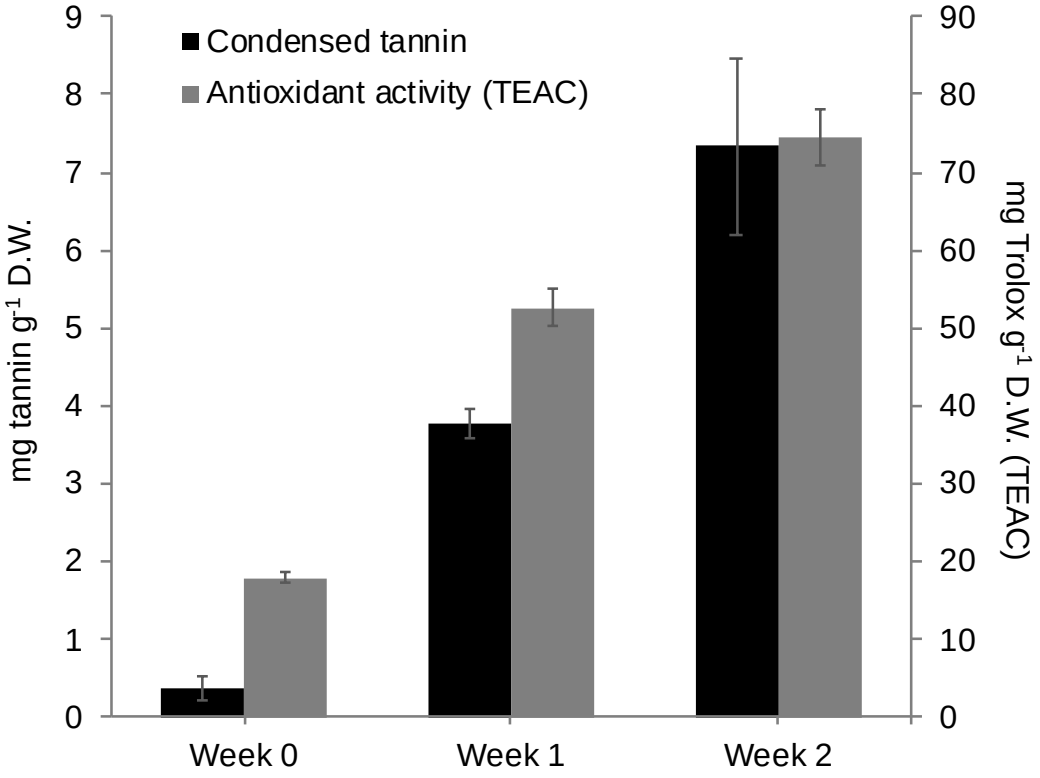

Figure 2.1: Induction of condensed tannins and antioxidant activity in hybrid *Populus* leaves under high light stress. Plants were exposed to natural sunlight and leaves of LPI 10-12 were harvested and extracted as described in the Methods. Week 0 samples were taken prior to high light treatment. Black bars represent condensed tannins assayed by the butanol:HCl method and grey bars represent antioxidant activity assayed by the DPPH assay and expressed as Trolox equivalent antioxidant capacity (TEAC). All data points represent the means of four independently treated plants, and all treatments are significantly different from week 0 (two-way ANOVA; $P < 0.001$). Error bars represent SE.

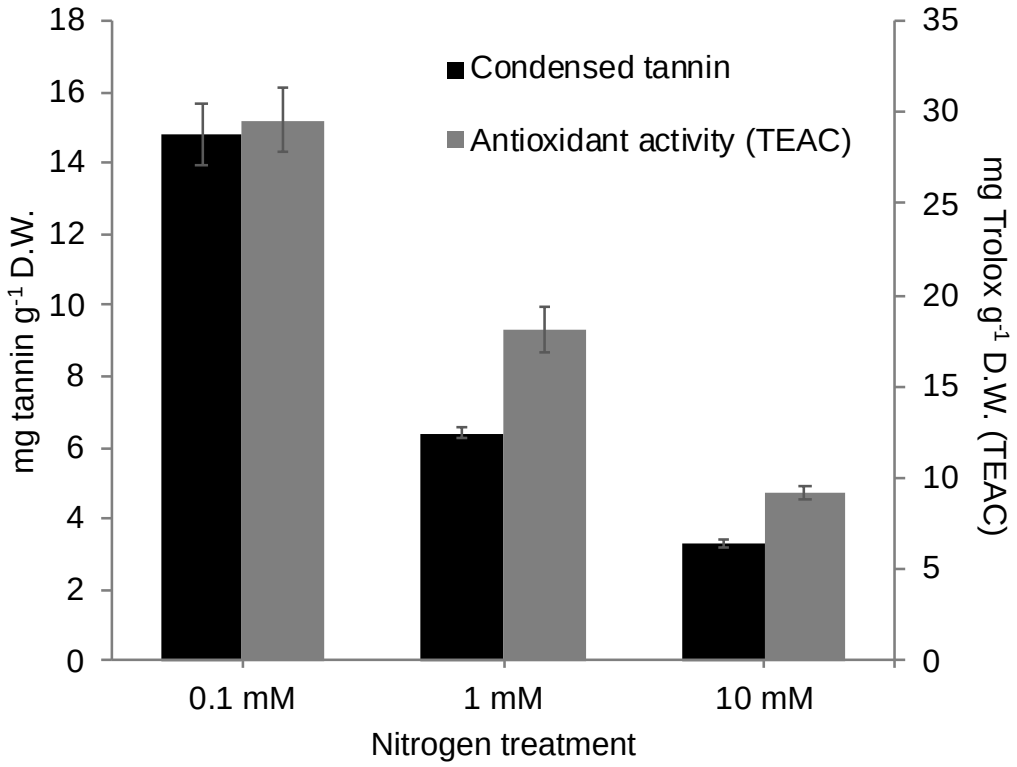

Figure 2.2: Induction of condensed tannins and antioxidant activity in hybrid *Populus* leaves under reduced nitrogen availability. Black bars represent condensed tannins assayed by the butanol:HCl method and grey bars represent antioxidant activity assayed by the DPPH assay and expressed as Trolox equivalent antioxidant capacity (TEAC). All data points represent the means of four independently treated plants, and all treatments are significantly different from 10 mM nitrogen (two-way ANOVA; $P < 0.001$). Error bars represent SE.

2.3.2 High tannin transgenic poplars have greatly enhanced antioxidant capacity

The two stress treatments applied above induce not only CTs but also other flavonoids and phenolics (Harding *et al.*, 2005; Mellway *et al.*, 2009). To test the role of CTs in determining leaf antioxidant capacity in the absence of these confounding factors, we made use of previously generated high-CT transgenic poplar lines. These transgenics had been produced by overexpressing poplar *MYB134* and *MYB115* genes, which encode transcription factors that activate the CT pathway (Mellway *et al*., 2009; James *et al.*, 2017). Under normal greenhouse conditions, both MYB115 and MYB134 overexpressor plants (MYB115OE and MYB134OE, respectively) have 50-fold greater CT content than control plants (Figure 2.3A), but only minor shifts in other flavonoids (Mellway *et al.,* 2009; James *et al.,* 2017). The pattern of antioxidant activity as measured by the DPPH assay again mirrored CT concentrations; MYB115 overexpressors had slightly higher CTs and antioxidant capacity, however.

We also performed additional antioxidant assays using these extracts. The ABTS and FRAP assays measure antioxidant activity using a stable cation and generation of a ferrous complex, respectively (Benzie and Strain 1996; Re *et al.,* 1999). These tests showed almost identical trends in antioxidant activity as the DPPH assay (Figure 2.3). We noted that all three assays measured low but detectable antioxidant activity in controls. Nevertheless, Pearson correlation coefficients for the three measures of antioxidant activity with CT content were greater than 0.99 ($P < 0.001$) in all cases. Together, these data suggest that the majority of the antioxidant activity in the transgenics is due to the high concentration of CTs.

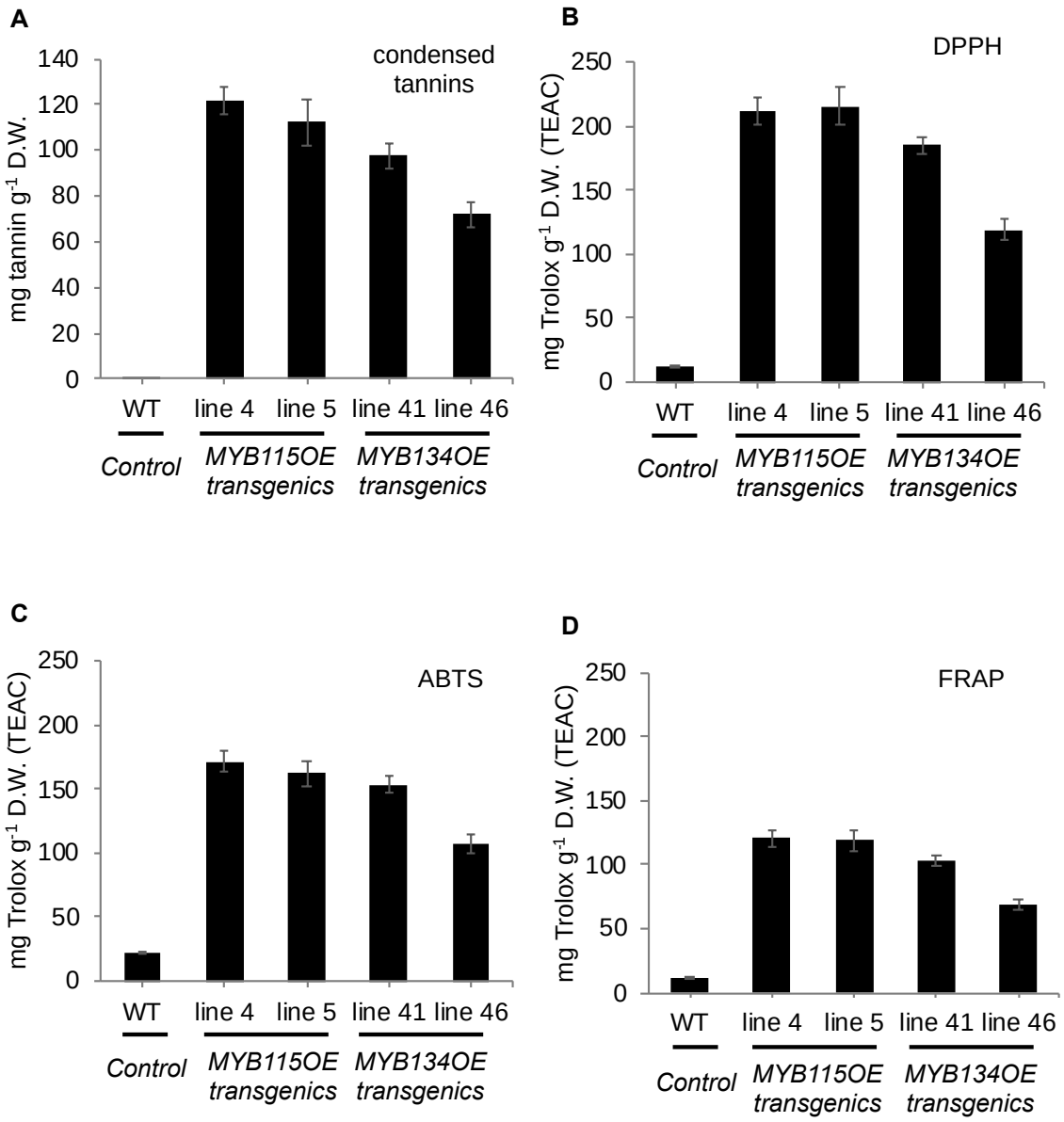

Figure 2.3: ABTS, DPPH, and FRAP antioxidant activity in extracts of high-condensed tannin (CT) MYB134- and MYB115-overexpressing poplar. Plants were grown under normal greenhouse conditions and leaves of LPI 10-12 were harvested and extracted as outlined in the Methods. Two independently transformed lines of each type of high-CT transgenic poplar were tested, and each data point is the mean of eight clonally replicated plants. Condensed tannin concentrations (A) were measured by butanol:HCl method, and antioxidant activity was determined by DPPH assay (B), ABTS assay (C), and FRAP assay (D) as outlined in the Methods. Antioxidant capacity is expressed as Trolox equivalents (TEAC). All transgenic leaf data points are significantly different from controls (*t* test; $P < 0.001$). Error bars represent SE.

2.3.3 *In vivo* protective effects of high-CT concentrations against oxidative stress generated by methyl viologen treatment of poplar leaves

As a next step, we devised experiments to test if CTs can act as antioxidants *in vivo* and protect against oxidative stress. In order to produce ROS in plant tissue under controlled conditions, we treated excised leaves with the herbicide methyl viologen (MV), also known as Paraquat. Methyl viologen competes with ferredoxin for electrons during photosynthetic electron transport (Nelson and Ben-Shem, 2004), and is commonly used as a means to directly generate ROS and produce oxidative stress in plants. A solution of MV was applied in the transpiration stream of detached leaves in environmental chambers in the light. Under these conditions, 12 - 16 ml of test solution was taken up within the 24 h experimental period. To assess leaf damage by oxidative stress and ROS, chlorophyll fluorescence measurements were taken at various time intervals. Preliminary experiments indicated that 200 µM MV exposure led to a reduction in photosystem II function within 24 h, followed by rapidly progressing necrosis. This concentration was therefore used in subsequent experiments. Two independently transformed MYB134 overexpressor lines and two MYB115 overexpressor lines were compared with wild-type leaves in several separate experiments, each with five replicates per treatment (water or MV). *Fv/Fm* was reduced in all leaves within 4 h as a result of leaf excision, but remained constant after this time point in water treated leaves (Figure 2.4). In wild-type plants, MV treatment caused a further steep decline in *Fv/Fm* that continued until the end of the experiment; in high-CT transgenics, however, this decline was significantly dampened, and leaves retained greater PSII function throughout the 24 h experimental period. The same pattern was observed for both MYB115 and MYB134 overexpressors (Figure 2.4): in all cases, high-CT lines were at least partially protected from the effects of MV. These data were supported by visual observations of necrosis: wild-type leaves treated with MV consistently showed faster necrosis development and larger lesions than the high-CT transgenics (Figure 2.5). All experimental combinations of MYB overexpressor lines were repeated at least four times, and all produced similar results.

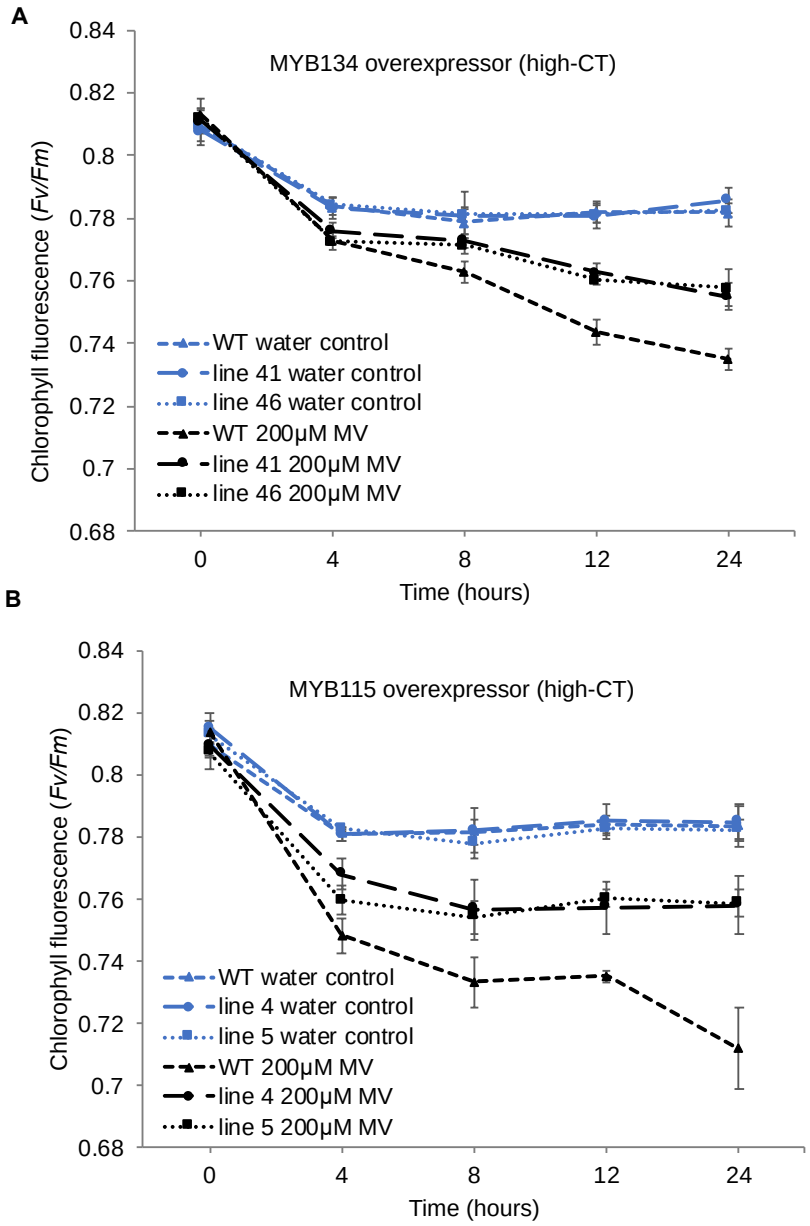

Figure 2.4: Effect of methyl viologen on chlorophyll fluorescence (*Fv/Fm*) in high-condensed tannin (CT) transgenic poplar and control leaves. Excised mature hybrid *Populus* leaves were exposed to methyl viologen through their petioles for 24 h, and chlorophyll fluorescence measured as described under Methods. Two MYB134 overexpressing high-CT transgenic lines (line 41 and line 46; panel A) and two MYB115 overexpressing high-CT transgenic lines (line 4 and line 5; panel B) are shown. The blue lines show water control treatments while the black lines are methyl viologen treated. All data points represent the means of five independently treated leaves. The interaction between genotypes over time is statistically significantly different in the methyl viologen treated group ($P < 0.01$) and was n.s. in the water control group (two-way ANOVA). Data points show means ± SE.

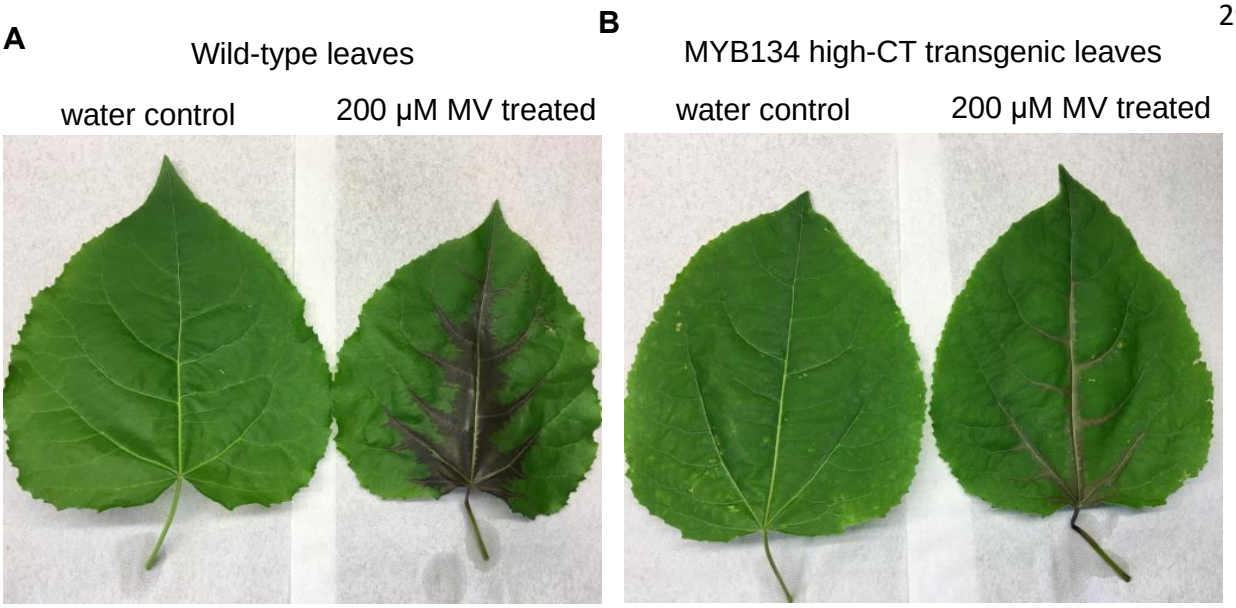

Figure 2.5: Representative images showing necrotic high-condensed tannin (CT) transgenic and control leaves after methyl viologen treatment. Mature hybrid *Populus* leaves were exposed to either 200 µM methyl viologen or water via the transpiration stream for 24 h. Two wild-type leaves (WT, panel A) and two MYB134 high-CT transgenic leaves (panel B) are shown.

The greater tolerance of MYB overexpressor transgenics to MV suggested that these lines should also accumulate lower concentrations of ROS. We therefore stained for H_2O_2 and O_2^-, using 3,3'-diaminobenzidine (DAB) and nitroblue tetrazolium (NBT), respectively, in leaf discs excised from the leaves of the experimental plants. The DAB staining for H_2O_2 was most apparent in leaf veins of MV-treated leaves (Figure 2.6A), but no staining was visible in water treated controls (data not shown). Importantly, DAB-stain was clearly more prevalent in the wild-type control compared to the high-CT transgenic lines. Quantification of DAB stain in the leaf discs using imaging software confirmed the lower extent of browning in the high-CT transgenics (Figure 2.6C). Similarly, wild-type leaf discs were stained more intensely with NBT than the high-CT leaf discs, indicating greater levels of superoxide (Figure 2.6B). Image analysis again confirmed the visual differences (Figure 2.6D). These results clearly indicated that high-CT transgenics had accumulated less hydrogen peroxide and superoxide levels after MV treatment than control lines (Figure 2.6). Staining was repeatable in all MV experiments performed, and identical results were obtained with the MYB115-overexpressing high-CT genotype (Supplemental Figure 2.1).

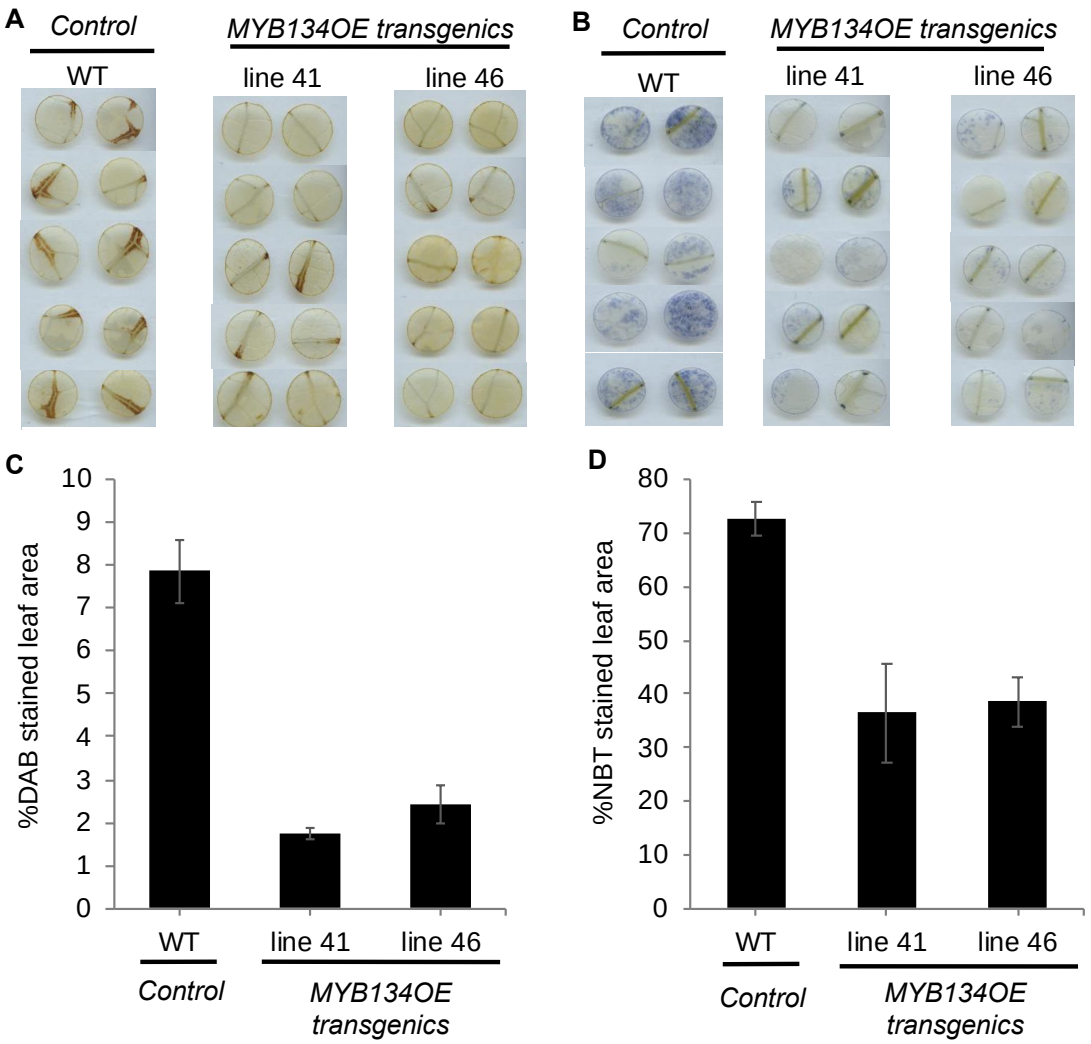

Figure 2.6: Leaf discs stained for hydrogen peroxide and superoxide in high-condensed tannin (CT) transgenic and control poplar leaves after methyl viologen treatment. Leaf discs were harvested from high-CT MYB134OE and wild-type (WT) leaves treated with methyl viologen (MV) as described under Methods. Hydrogen peroxide and superoxide were visualized with 3,3'-diaminobenzidine (DAB; panel A) and nitroblue tetrazolium (NBT, panel B). An image analyzing protocol (WhinRhizo) was used to quantify specific ROS staining by DAB (panel C) and NBT (panel D). All data points represent the means of five independently treated leaves. Staining in all MYB134 overexpressor transgenics was significantly different than the control line at $P < 0.001$ and $P < 0.01$ for DAB and NBT, respectively (*t* test). Error bars represent SE.

In addition, we confirmed the DAB staining results by quantifying H_2O_2 in leaf extracts. All high-CT leaves contained significantly less H_2O_2 after MV treatment compared with wild-type (Figure 2.7). Overall, our data indicate reduced production of H_2O_2 and O_2^- in high-CT transgenics, confirming that high-CT concentrations protect poplar leaves against ROS accumulation and oxidative stress induced by MV.

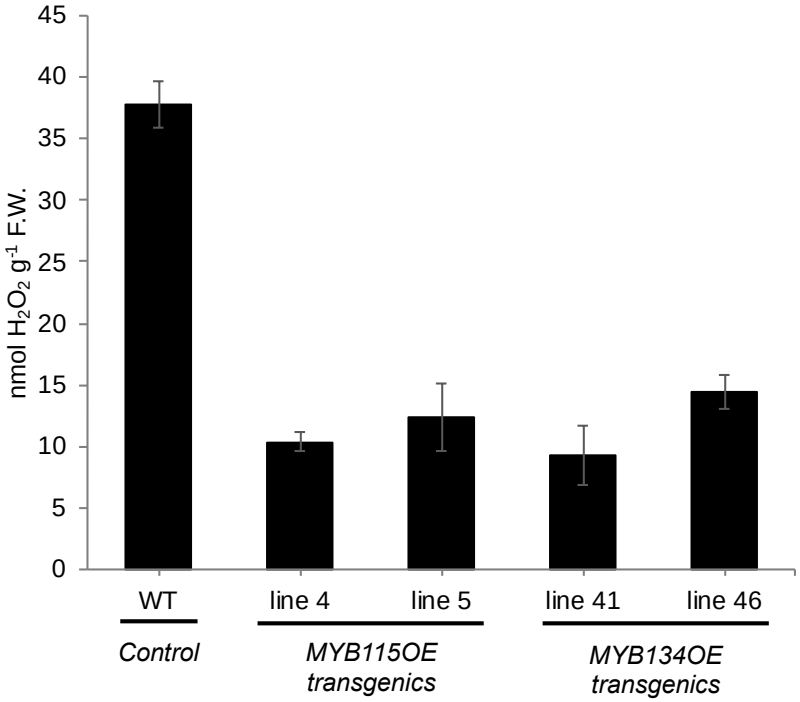

Figure 2.7: Hydrogen peroxide quantification in high-condensed tannin (CT) transgenic poplar and control leaves after methyl viologen (MV) treatment. Hydrogen peroxide (H_2O_2) levels were quantified from leaf extracts using AmplexRed Hydrogen Peroxide/Peroxidase assay kit as described in Methods. All data points represent the means of three independently treated leaves. H_2O_2 concentration in all high CT transgenic samples are significantly different from the control line (*t* test; $P < 0.01$). Error bars represent SE.

2.4 Discussion

The antioxidant capacity of CTs in solution well known (Hagerman *et al.,* 1998; Quideau *et al.,* 2011), but whether they can act as antioxidants in leaves and whole plants has not yet been rigorously tested. Jia *et al.* (2012) demonstrated that CT-deficient mutant *Arabidopsis* seeds, when exposed to extreme oxidative stress, produced more ROS than wild-type seeds; however, *Arabidopsis* does not accumulate CTs in leaves or other vegetative tissues affected by oxidative stress. Here we demonstrate that in poplar saplings, abiotic stress treatment leads to simultaneous increases in both CT content and antioxidant activity in leaves. We further demonstrate that transgenic poplar engineered for high-CT accumulation are more resistant to the oxidative damage caused by MV, an oxidative stress-inducing herbicide. The high-CT transgenics showed reduced leaf necrosis and photosystem II damage, as well as lower levels of H_2O_2 and superoxide, demonstrating a direct link between high CTs in leaves and protection against the effects of oxidative stress.

Our work builds on our previous biochemical and molecular characterization of MYB134- and MYB115-overexpressing poplars, which both showed a strong increase in CT content, but no substantial increases in other phenolics (Mellway *et al.,* 2009; James *et al.*, 2017). Transcriptomic analysis confirmed that the major impact was on the CT pathway and its regulators. Importantly, no known antioxidant enzymes or other pathways were induced (James *et al.,* 2017). We are therefore confident that the antioxidant activity and tolerance to MV observed in the transgenics is due to the high CT content, in particular since we obtained the same results using two different MYB transcription factors.

2.4.1 High-CT poplar transgenics have enhanced resistance to methyl viologen

High-CT transgenic leaves sustained significantly less photosynthetic damage by MV than wild-type leaves. To demonstrate this, we monitored *Fv/Fm*, a dark-adapted chlorophyll fluorescence parameter that indicates the maximum photochemistry possible if all reaction centers in photosystem II are open and can accept electrons. Although our assays used detached leaves to apply MV via the transpiration stream, the protective effects of CTs can be

expected to be equally effective in whole plants. For example, plant assays with transgenic plants applying MV at similar concentrations as ours have shown the same effects on *Fv/Fm* values. For example, Kim *et al.* (2011) observed that potato plants treated with up to 300 µM MV showed reduced *Fv/Fm*, but in plants overexpressing 2-cysteine peroxiredoxin this impact was much less severe. Similarly, poplar leaf discs from plants overexpressing *gshI*, the gene encoding γ-glutamylcysteine synthetase, showed less change in *Fv/Fm* under MV treatment than control leaf discs (Bittsánszky *et al*., 2006). Our demonstration that high-CT transgenics are more resistant to oxidative stress by MV is thus similar to previous work on other antioxidant systems in plants. Plants contain multiple systems for responding to oxidative stresses; given that trees are long-lived and have different evolutionary strategies, we propose that in trees CTs act as additional antioxidants in adaptation against stress.

Further support for this idea comes from work on anthocyanins, which are also end-products of the flavonoid pathway and show strong *in vitro* antioxidant capacity (Hagerman *et al.*, 1998; Hernández *et al.,* 2009). They are biosynthetically related to the CTs and often have an *ortho*-hydroxylated flavonoid B-ring, a key feature for phenolic antioxidants (Hagerman *et al.,* 1998; Quideau *et al.,* 2011). Similar to our data on high-CT transgenics, high-anthocyanin mutants of *Arabidopsis* are better protected against ROS generated by MV than wild-type plants (Nakabayashi *et al.,* 2014). Elevated anthocyanin concentrations also help to mitigate the effects of another ROS-generating stress, water deficit. It is thus possible that CTs could improve the tolerance of poplar to drought.

The ability of anthocyanins to act as *in vivo* antioxidants in plants is an important parallel to our work, since like the CTs, anthocyanins accumulate in the vacuole (Hernández *et al.,* 2009; Agati *et al.,* 2012). By contrast, ROS are typically generated in chloroplasts and mitochondria, and the mechanisms by which vacuolar antioxidants can have protective effects for the cell still needs to be established. Reactive oxygen species are generally short-lived, but H_2O_2 is long-lived enough to be able to cross membranes and enter the vacuole (Dat *et al.,* 2000, Agati *et al.,* 2012). Vacuoles also contain peroxidases and ascorbate, and it has been suggested that a vacuolar peroxidase/flavonoid/ascorbate system can remove H_2O_2 in this compartment (Agati *et al.,* 2012). The potential mechanisms for antioxidant activity of CTs include H-atom transfer

and the single-electron transfer processes that result in chain-breaking radicals (Quideau *et al.,* 2011). Alternatively, it could be the Fe-chelating properties of the CTs that are important (Santos-Buelga and Scalbert, 2000; Quideau *et al.,* 2011). H_2O_2 readily reacts with Fe, and the resulting Fenton reaction produces hydroxyl radicals, highly destructive ROS (Mittler, 2017). Fe chelation is an attractive hypothesis since it could occur in the vacuole. Further research is needed to test which of these mechanisms could underlie our results.

2.4.2 Stress induction of CTs and antioxidant activity

The antioxidant effects of CTs provide a unifying rationale for the observation that multiple biotic and abiotic stresses can induce CT biosynthesis in poplar and other trees. In the current work, we noted a close correlation of CT concentration and antioxidant activity following both light stress and nitrogen deficiency treatments. Induction of CTs by high light was also observed in apple and larch (Gesell *et al.*, 2014; Yan *et al*., 2014). Transferring plants from the greenhouse to natural sunlight exposes them to an increased intensity of visible wavelengths, as well as to UV-B (Mellway *et al.*, 2009). Oxidative stress is produced by high intensity light because more energy is absorbed than can be used for photochemistry, allowing high-energy electrons from the photosystems to react with atmospheric oxygen and produce ROS (Demmig-Adams and Adams, 1992; Takagi *et al.,* 2016). UV-B exposure also leads to ROS production, via damage to the D1 protein of photosystem II, resulting in a large burst of ROS (Jenkins, 2009). Our data suggest that the increase of CTs in response to these stresses adds antioxidant capacity to the cells, which can help to reduce tissue damage caused by ROS. The induction of CTs by other stresses could have similar effects.

We also observed an induction of CTs and a parallel increase in antioxidant activity when plants were stressed with nitrogen deficiency (Figure 2.2). The enhanced synthesis of CTs and phenolics under reduced nitrogen supply has been observed in many different trees including pine, eucalyptus, and oak (Kraus *et al.,* 2004; Hikosaka *et al.,* 2005). Similar to our work, Harding *et al.* (2005) have shown that in hydroponically grown poplar, CTs were induced by reduced nitrogen. It was also demonstrated that under nitrogen-limiting conditions,

transcription factors regulating flavonoids in poplar were upregulated, indicating that the induction of the flavonoid pathway by nitrogen deficiency is regulated transcriptionally (Harding *et al.,* 2005).

The inverse relationship of nitrogen supply and phenylpropanoid accumulation has intrigued plant physiologists for decades, but to date no convincing physiological explanation has been proposed. The carbon-nutrient balance hypothesis is sometimes invoked, and posits that a nutrient deficiency will impact growth more than photosynthesis, leading to an excess of carbon-based metabolites including phenolic secondary metabolites (Bryant *et al*., 1983). Although some studies are consistent with this hypothesis, its assumptions ignore the ability of plants to directly regulate the biosynthesis of secondary metabolites, and it is now largely discredited (Hamilton *et al.,* 2001). We propose an alternative explanation for the stimulation of phenylpropanoids by N deficiency: nitrogen deficiency brings on a reduction in photosynthetic capacity, due to the high nitrogen requirement of chlorophyll and photosynthetic proteins (Kant *et al.*, 2011). This leaves the photosystems more susceptible to photodamage by excess light, effectively causing high light stress and generation of ROS in leaves. Zhang *et al.* (2014) demonstrated enhanced levels of H_2O_2 in poplar under nitrogen deficiency, consistent with this idea. Nitrogen deficiency can therefore be seen as acting as an ROS producing-stress, to which the plant responds with synthesis of antioxidant CTs.

2.4.3 Conclusions

In conclusion, our work shows that high foliar CTs in poplar can protect against oxidative stress from MV. Further, we propose that both light stress and nitrogen deficiency induce CT synthesis as a mechanism for mitigating the ROS produced under these conditions. Our previous work showed the induction of CTs in poplar by very different environmental stresses, for example herbivory, biotrophic pathogens, UV-B, and high light stress (Mellway *et al.*, 2009). The current work, demonstrating an *in planta* antioxidant activity of CTs, provides an underlying rationale for these observations, since these are ROS-generating stresses and CT synthesis can now be seen as an adaptive plant response to oxidative stress. This interpretation predicts that our

high-CT poplar should also be more resistant to other ROS-producing conditions, for example, drought stress. Since trees and woody plants accumulate substantial concentrations of CTs, determining their role in abiotic stress resistance would have broad implications for environmental and forest sciences.

2.5 Supplemental Material

2.5.1 Supplemental figures

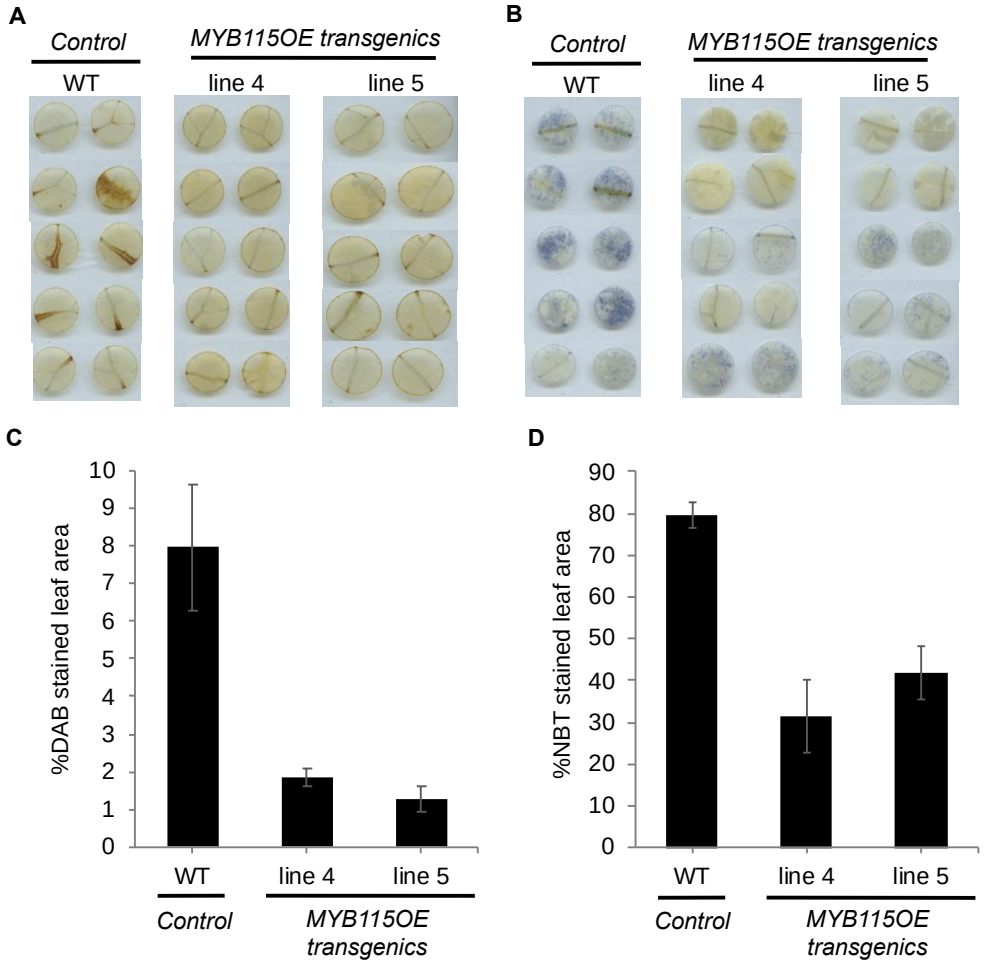

Supplemental Figure 2.1: Leaf discs stained for hydrogen peroxide and superoxide in high-CT MYB115 overexpressing and control poplar leaves after methyl viologen treatment. Leaf discs were harvested from high-CT MYB115OE and wild-type (WT) leaves treated with methyl viologen (MV) as described under Methods. Hydrogen peroxide and superoxide were visualized with 3,3'-diaminobenzidine (DAB; panel A) and nitroblue tetrazolium (NBT, panel B). An image analyzing protocol (WinRhizo) was used to quantify specific ROS staining by DAB (panel C) and NBT (panel D). All data points represent the means of five independently treated leaves. Staining in all MYB115 overexpressor transgenics was significantly different than the control line at $P < 0.01$ and $P < 0.001$ for DAB and NBT, respectively (*t* test). Error bars represent SE.

Chapter 3 : RNAi suppression of *MYB134* in transgenic poplar inhibits biosynthesis of leaf CTs and increases susceptibility to oxidative stress

(This chapter has been submitted to the Journal of Experimental Botany in August 2019 with authors Gourlay G, Ma D, Schmidt A, and Constabel CP. I carried out all experiments and devised experiments with CPC. AS generated initial construct to generate transgenics. DM modified construct and generated the MYB134-RNAi lines and performed the RNASeq. This manuscript is referred to as "Gourlay *et al.*, 2019" throughout the text.)

3.1 Introduction

Plants produce a diverse array of secondary metabolites that help them adapt to adverse and stressful environmental conditions. An important class of these secondary metabolites are the phenolics, which include the coumarins, hydroxycinnamate esters, phenolic acids and flavonoids. The condensed tannins (CTs, or proanthocyanidins) belong to the flavonoids, and are considered one of the most widespread secondary metabolites in the plant kingdom. They are especially abundant in woody plants (Quideau *et al*., 2011). They are also found in many edible fruits and seeds, and dietary CTs are associated with a reduced risk of cardio-vascular disease and neurodegenerative disease (Santos-Buelga and Scalbert, 2000; Prior and Gu, 2005).

Condensed tannins are a structurally varied set of compounds with diverse ecological functions. They play important roles as anti-herbivore compounds against vertebrates and some insects (Barbehenn and Constabel, 2011). Furthermore, they are antimicrobial and can contribute to pathogen defense, for example, in the interaction of *Populus* - *Melampsora* leaf rust interaction (Ullah *et al*., 2017). In forest soils, the CTs slow leaf litter decomposition and nutrient release; this can have benefits for plants which rely on mycorrhizae for nutrient acquisition (Constabel *et al*., 2014; Shay *et al*., 2018). In poplar, CTs are induced by a multitude of environmental stresses including high light, UV-B, herbivory, pathogens, and nitrogen deficiency (Harding *et al*., 2005; Mellway *et al*., 2009), suggesting a general role in plant adaptation. It is established that CTs are excellent *in vitro* antioxidants (Hagerman *et al*., 1998),

and recently we reported that they are also able to protect leaves against oxidative stress *in vivo* (Gourlay and Constabel, 2019).

CTs are end products of the well-characterized flavonoid pathway (Dixon *et al.,* 2005). They are derived from the flavan-3-ols (+)-catechin (2,3- *cis*-flavan-3-ol) and (-)-epicatechin (2,3-*trans*-flavan-3-ol), generally forming polymeric molecules that are linked by C4-C8 carbon-carbon bonds (Hagerman, 2002; Dixon *et al.*, 2005). The enzymes involved in CT biosynthesis can be divided into 'early' and 'late' flavonoid biosynthetic genes: chalcone synthase (*CHS*), chalcone isomerase (*CHI*), and flavanone-3-hydroxylase (*F3H*) are early in CT biosynthesis, whereas dihydroflavonol reductase (*DFR*), leucoanthocyanidin reductase (*LAR*), anthocyanidin reductase (*ANR*), and anthocyanidin synthase (*ANS*) are considered to be late flavonoid genes (Dixon *et al.,* 2005; Tsai *et al*., 2006). *LAR* and *ANR* are CT-specific enzymes.

Flavonoid biosynthesis is regulated by MYB transcription factors, which are encoded by large gene families in plants. The R2R3-MYBs are the most abundant subfamily of MYBs in plants; they regulate both developmental processes as well as metabolism. Many MYBs have been characterized, and specific MYBs that control synthesis of lignin, anthocyanins, flavonols, and CTs are known (Ramsey and Glover, 2005; Liu *et al*., 2015). The CT- and anthocyanin-specific MYBs require basic-helix-loop-helix (bHLH) and WD-repeat (WDR) co-activators, which comprise the so-called MBW complex (Ramsay and Glover, 2005; Ma and Constabel, 2019). However, the MYB partners determine the specificity of the complex and are thus the key for directing expression of CT biosynthesis.

In poplar, 192 R2R3-MYBs and five 3R-MYBs have been identified (Wilkins *et al*., 2009). CT-specific MYBs have been described in a variety of plants, but are most comprehensively studied in *Vitis* spp., *Medicago* spp., and poplar (Constabel, 2018). Many CT-accumulating plants have two CT-specific MYBs, a TT2-type and MYBPA1-type (Constabel, 2018). In poplar, these are represented by MYB134 and MYB115 (Mellway *et al*., 2009; James *et al*., 2017). Both MYB134 and MYB115 interact with poplar bHLH131 in a MBW complex, and appear to act redundantly (James *et al.*, 2017). Furthermore, promoter activation and transgenic experiments indicate that they both regulate each other's promoters and thus provide positive feedback for CT induction (James *et al*., 2017). Overexpression of either MYB gene in transgenic poplar leads

to a strong overaccumulation of CTs, but no major change in most other flavonoids (Mellway *et al*., 2009; James *et al*., 2017). These overexpressor plants have helped define MYB function, including identifying downstream MYB repressors of the flavonoid pathway (Ma *et al*., 2018; Ma and Constabel, 2019). Our current understanding is that both MYB activators and repressors function in a network of positive and negative regulatory feedback loops, which prevent overaccumulation of CTs or which may fine-tune expression in specific tissues or in response to stress. The high-CT MYB overexpressor plants have also been invaluable tools for better defining the ecological and physiological functions of foliar CTs in poplar (Boeckler *et al.*, 2014; Gourlay and Constabel, 2019).

Here we focus on the MYB134 CT activator in poplar. While MYB overexpressor plants have provided much insight, it can be difficult to separate primary and secondary effects of overexpression. Thus, to further define the function of MYB134, mutants or knockdowns are needed. RNA-interference (RNAi) is a powerful tool to achieve such knockdowns in transgenic plants, and can be useful in systems where CRISPR has not yet been established (Waterhouse and Helliwell, 2003; Wang *et al*., 2019*b*). Introducing constructs that generate double-stranded RNA and hairpin structures into a plant triggers a molecular response that ultimately results in the degradation of the endogenous transcript and thus silences expression of the target gene (Waterhouse and Helliwell, 2003). RNAi has been employed in a diverse array of species, including trees such as *Pinus radiata* and *Populus* spp. (Coleman *et al*., 2008; Tian *et al.,* 2013). Many of these RNAi experiments target the lignin pathway; however, trees also produce large amounts of other phenolic metabolites, in particular the CTs. Since a number of poplar hybrids are amenable to *Agrobacterium*-mediated genetic transformation (Brunner *et al*., 2004; Meilan and Ma, 2006), silencing of the CT pathway via RNAi would provide insight into the regulation and functions of these important metabolites.

Here we use RNAi to knock down the *MYB134* gene in *Populus tremula × P. tremuloides*, a poplar hybrid that is well suited for studying the CT pathway as it shows strong CT-induction by environmental stress (Mellway *et al*., 2009; James *et al*., 2017). We carry out both transcriptomic and physiological experiments on MYB134 knockdown plants. Our transcriptomic data confirm the specificity of MYB134 for the CT pathway, and provide insight

into the functions of the poplar MYB CT activators. We also demonstrate the utility of these CT knock-down plants by demonstrating their enhanced susceptibility to methyl viologen-induced oxidative stress and corroborating the role of CTs as *in vivo* antioxidants.

3.2 Materials and Methods

3.2.1 Vector construction and plant transformation

To construct a MYB134-RNAi vector, the MYB134 coding sequence containing 169 base pairs was cloned and inserted into the pTRAIN plasmid (Leveé *et al*., 2009) in sense and antisense orientations (Ullah *et al*., 2017). The sense and antisense MYB134 fragment together with ubiquitin promoter and terminator sequence were then subcloned from the pTRAIN vector and inserted into the pMDC32 binary vector (using HindIII sites). The pMDC32 vector was moved into the *Agrobacterium tumefaciens* strain GV3101::pMP90 by electroporation. *Populus tremula x P. tremuloides* (clone INRA 353–38) leaves were transformed as described previously (James *et al.*, 2017). Transformed lines were selected on shoot-inducing and rooting medium with hygromycin B (Sigma-Aldrich, Oakville, ON, Canada). Positive transformants were confirmed by RT qPCR of *MYB134* expression. The RNAi plants were initially generated by David Ma and Tieling Zhang in the Constabel lab.

3.2.2 RNA extraction and RT-qPCR analysis

Total RNA was extracted from poplar leaves as previously described (Yoshida *et al*., 2015). RNA was then treated with RQ1 DNase (Promega, Madison, WI, USA) to degrade genomic DNA and cDNA was synthesized using Superscript II reverse transcriptase (Invitrogen, Carlsbad, CA, USA) following the manufacturer's instructions. RT-qPCR was performed in 20µl reactions using 4µl of homemade qPCR master mix on a CFX96 Real Time system (Bio-Rad). The master mix consisted of (final concentrations): 24.1 mM Tris-HCl, 25.9 mM Tris-base, 25 mM KCl, 1.5 mM $MgCl_2$, 0.5% Tween 20, 4% glycerol, 0.83 mM dNTP, 5X EVAGreen SYBR (Biotium) in a total volume of 2 ml. MYB134 (Potri.006G221800) transcript abundance data were normalized using

the geometric mean of poplar elongation factor (EF1b; Potri.001G224700) and ubiquitin (UBQ10; Potri.014G115100) expression (Yoshida *et al*., 2015).

3.2.3 RNA-seq analysis

Total RNA was extracted as described above. cDNA library construction for RNA-seq was carried out as described previously (Ma *et al.*, 2018). Briefly, mRNA was purified from total RNA using a Mag-JET enrichment kit (ThermoScientific, Waltham, MA, USA). The mRNA was fragmented by heating the samples at 94 °C for 5 min. cDNA libraries with adaptors were constructed using NEB Next ultra RNA Library Prep Kit for Illumina (NEB), and the GeneJET NGS Cleanup Kit (ThermoScientific) was used to remove extra adaptors. Primers for RNA-seq were added to cDNA fragments using a NEBNext Multiplex Oligo kit (NEB). Fragments of approximately 350 nucleotides in length were purified using the MagJET NGS Cleanup and Size Selection Kit (ThermoScientific). Six libraries at the same concentrations (250 ng/mL each) were pooled and sequenced in one lane at the McGill University/GenomeQuebec Innovation Center (http://gqinnovation center.com) using an Illumina HiSeq 2000 system. Sequence alignment was performed using HISAT2 (version 2.1.0) and Cufflinks (version 2.2.1) (Pertea *et al*., 2016). The *P. tremula* genome sequence was used as the reference genome (Sjödin *et al.*, 2009; http://popgenie. org/). Cuffdiff was used to analyze the differentially expressed genes. DESeq package in R (version 3.4.0) was used to generate the final differentially expressed gene table (Anders and Huber, 2010). Differentially expressed genes are genes that are determined using a negative binomial generalized linear models; the estimates of dispersion and logarithmic fold changes incorporate data-driven prior distributions. A reference transcriptome from *P. tremula* (Sjödin *et al*., 2009; http://popgenie.org/) was used to assign gene annotations, in conjunction with Phytozome (http://phytozome.jgi.doe.gov) and NCBI (https://www.ncbi.nlm.nih.gov/). Flavonoid genes are named according to Tsai *et al.* (2006). The RNA-seq analysis was carried out by David Ma in the Constabel lab.

3.2.4 Plant growth conditions and experimental treatments

Populus tremula x Populus tremuloides (clone INRA 353-38) wild-type and transgenic MYB134-RNAi plantlets were maintained and micropropagated in tissue culture on Lloyd and McCown's Woody Plant Media (WPM; Caisson) with 1 µM indole-3-butyric acid (IBA). Prior to experiments, tissue culture plantlets were transferred to soil and acclimated in a mist chamber for four weeks, then planted in one-gallon pots with a peat moss-based soil-less mix (Sunshine Mix 4, Victoria, BC) with additional slow-release fertilizer as described by Major and Constabel (2006). Plants were kept in the greenhouse under 16 h days with supplemental lights to extend day length. Temperatures ranged from 18 °C to 26 °C. Plants were two months old with 15-20 leaves when used for experiments.

For natural sunlight treatments, eight-week old plants in pots were moved to an open-top area and exposed to natural sunlight for two weeks during the summer months (June - August) in Victoria, B.C., Canada. To prevent drying, potted outdoor plants were placed in saucers and watered three times daily. The average daily light intensity was 835 or 675 µmol m^{-2} s^{-1} of light for 2015 and 2016, respectively for the two-week experimental duration. Plants were rotated every other day to minimize light differences. Leaf samples were harvested, flash frozen in liquid nitrogen, stored at -80°C, and ground into a fine powder by mortar and pestle. An aliquot was freeze-dried prior to extraction for phenolic analysis.

For methyl jasmonate (MeJa) treatment, plants were sprayed with a 0.2% MeJa solution on days 0, 2, 4, and 6 for a ten-day induction experiment. MeJa (Sigma Aldrich) was first diluted to 10% in EtOH, then diluted to 0.2% with 0.1% Tween/water. Both sides of leaves were sprayed using a plant mister to the point of run-off. MeJa was used to stimulate CT biosynthesis as levels of CTs are low under greenhouse conditions.

Methyl viologen treatment on detached leaves was carried out as described previously (Gourlay and Constabel, 2019). Four independently transformed MYB134-RNAi poplar lines were used for experiments, and wild-type poplar plants served as controls. Three individual clonal replicates of each transgenic line were used as a source of leaves in each experiment. Two leaves were excised from leaf plastochron index (LPI) 10-12. Chlorophyll fluorescence

measurements on detached leaves were carried out as previously described (Gourlay and Constabel, 2019).

To harvest roots, plant shoots were removed, and the root balls were thoroughly washed, and soil particles removed using mesh sieves of different sizes. Three age classes of root tissue were sampled from each plant. Root tip was defined as the first 2 cm of a root behind the white tip. Fibrous roots were defined as white, thin, non-lignified roots. Woody roots consisted of larger, lignified (>0.75-1 cm in diameter) roots. All of each separate root zone was harvested and pooled from one plant, flash frozen in liquid nitrogen, and stored at -80 °C until ready to be processed further. There was a minimum of three replicates per line.

After fluorescence measurements at the last time point, leaves were harvested to measure hydrogen peroxide levels. Three replicate experiments using four different MYB134-RNAi transgenic lines were performed.

3.2.5 Phytochemical extraction and analysis

Twenty-five milligrams of ground, freeze-dried tissue was extracted in 1.5 ml of 100% MeOH and homogenized in 2-ml CryoTubes with four steel beads using a Precellys tissue homogenizer (Bertin Technologies, ESBE Ontario) for 2 x 45 s at 5000 shakes per min followed by centrifugation of 10 min at 15,000g. Extractions were repeated twice more with an additional 1 ml MeOH, giving 3.5 ml of total plant extract. The butanol-HCl method (Porter *et al*., 1986) was used for CT analysis as outlined in Gourlay and Constabel (2019). For HPLC-UV analysis, 3 ml of methanol extract (described above) was dried using a SpeedVac (ThermoSavant SC110A) and resuspended in 100% HPLC-grade MeOH to a final concentration of 50 mg tissue/ml methanol. The sample run and analysis was performed according to Ma *et al.* (2018) using a System Gold 126 HPLC system with autosampler and System Gold 168 detector (Beckman Coulter, Missassauga, ON, Canada) equipped with a Kinetics C18 column (150 x 4.6 mm, 2.6 µm; Phenomenex Torrance, CA, USA). The gradient profile to separate compounds was 5% B (0–5 min), 5% to 14% B (5–11 min), 14% to 38% B (11–40 min), 38% to 100% B (40–47

min), and 5% B (47–49 min). Rutin (Sigma Aldrich) and salicortin (from Richard Lindroth) were used as standards.

Antioxidant capacity of plant extracts was assayed by the DPPH (2-diphenyl-1-picrylhydrazl) antioxidant assay (Gourlay and Constabel, 2019). Hydrogen peroxide levels in plant tissues were measured as described in Gourlay and Constabel (2019).

3.2.6 Statistical analyses

Data were analyzed using *t*-tests or analysis of variance (one- or two-way ANOVA) with factors for genotype, time, and treatment and Tukey honest significant difference (HSD) post-hoc tests in R (https://www.r-project.org).

3.3 Results

3.3.1 MYB134-RNAi transformants show suppression of induced CT synthesis

Generated MYB134-RNAi transgenics were screened for suppression of CTs. As *in vitro* plantlets typically express MYB134 at very low levels and do not accumulate measurable CTs, they were acclimated and moved to the greenhouse and subsequently exposed to natural sunlight to stimulate CT synthesis (Mellway *et al*., 2009). Under these conditions, significant differences in CT content between wild-type and transgenic lines were observed (Figure 3.1). In wild-type plants, CT concentrations reached between 2-7 mg tannin/g D.W. (dry weight), while transgenic lines expressing the MYB134-RNAi construct accumulated 0.5-2 mg tannin/g D.W. (Figure 3.1). We selected four transgenic lines (RNAi line 3, 7, 22, and 24) for further study. In a separate experiment, RT-qPCR analysis confirmed that the MYB134 transcript was significantly reduced in all selected MYB134-RNAi lines as expected and correlated with reduced CTs (Figure 3.2). The total antioxidant capacity in the MYB134-RNAi plants was also lower relative to wild-type after two weeks of natural sunlight (Figure 3.2C), although the difference from wild-type plants was not as great compared to MYB134 relative expression and CT concentration.

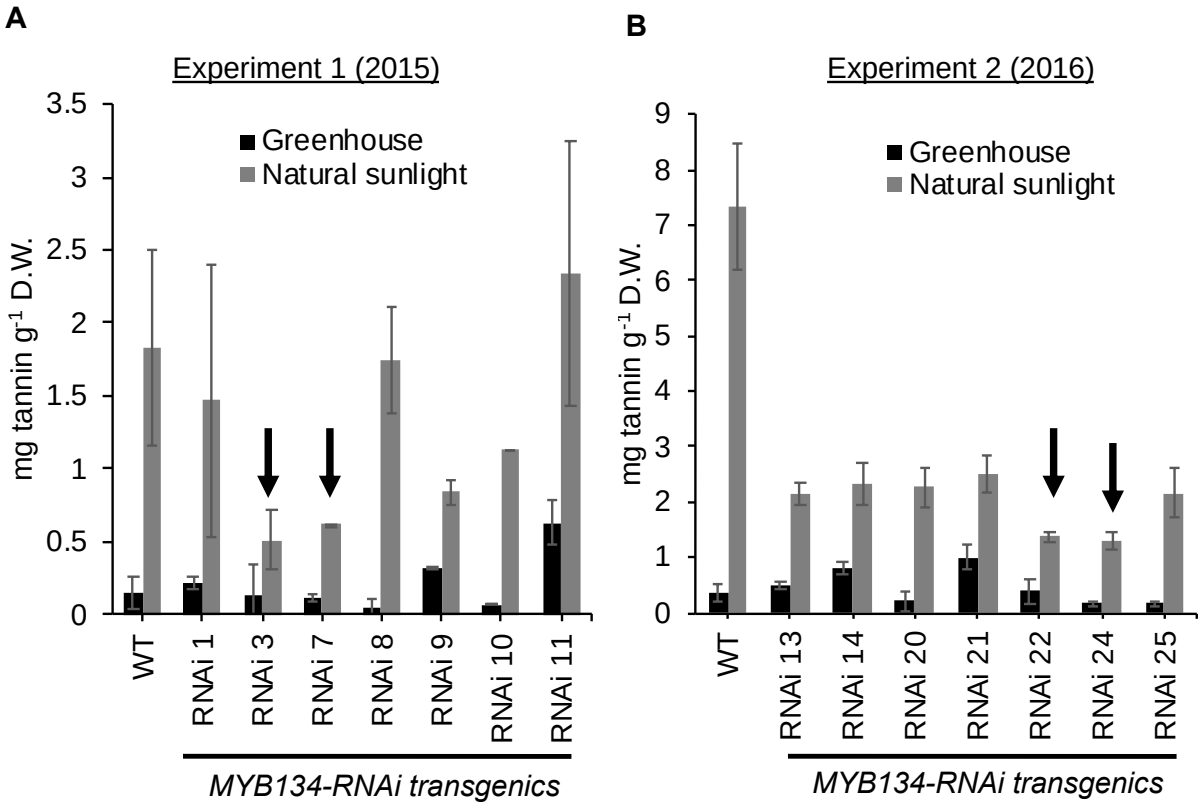

Figure 3.1: Preliminary selection of successful MYB134-RNAi lines with reduced tannin concentrations after exposure to high light stress. Plants were exposed to natural sunlight and leaves of LPI 10-12 were harvested and extracted as described in the Methods. Greenhouse samples were taken prior to natural sunlight treatment. Black bars represent condensed tannin concentrations prior to natural sunlight stress, and the grey bars represent condensed tannin concentrations after two weeks of natural sunlight. All data points represent the means of three independently treated plants in (A), and four independently treated plants in (B). Arrows represent lines that were selected as strong reductions in condensed tannin concentrations. All RNAi lines except 1, 8, and 11 are significantly different from controls after two weeks of natural sunlight (two-way ANOVA; $p < 0.001$). Error bars represent SE.

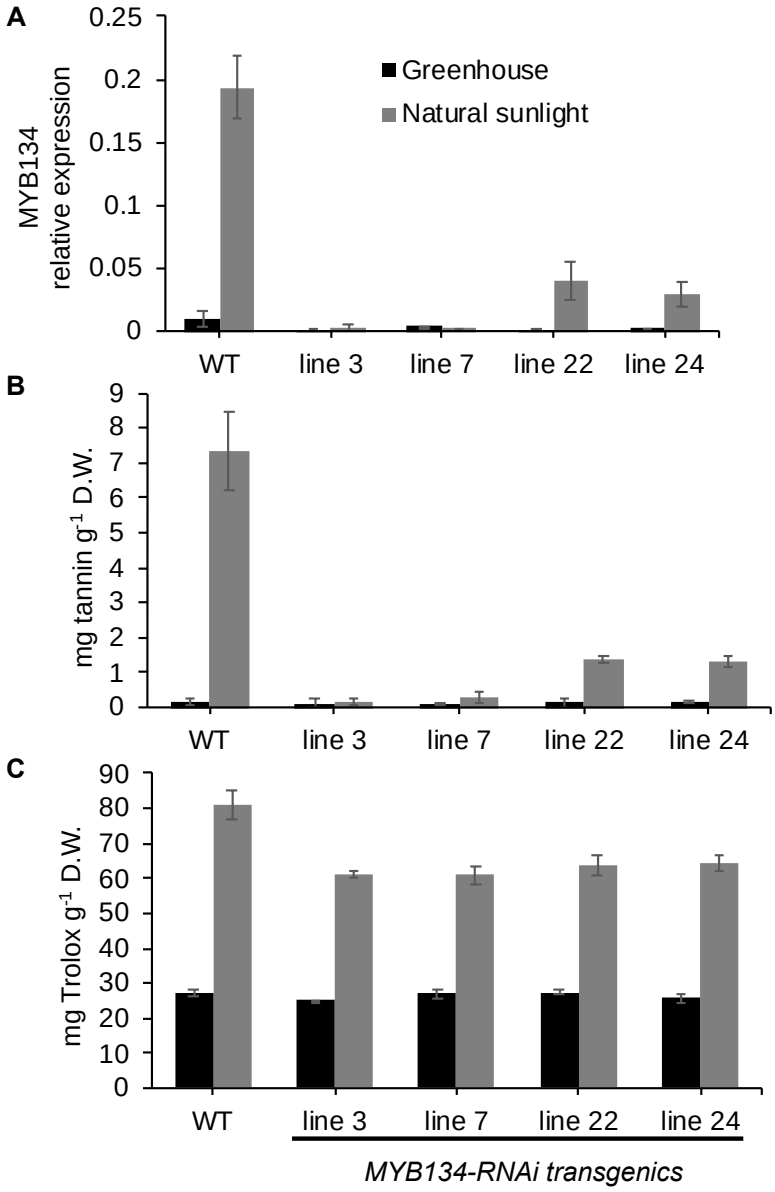

Figure 3.2: Induction of condensed tannins by natural sunlight is strongly suppressed in MYB134-RNAi transgenic poplar. After exposing plants to natural sunlight stress for two weeks in a different experiment, tissue was harvested and RNA was extracted and prepared for qPCR or dried and analyzed for CTs and antioxidant activity as described in the Methods. Black bars represent before natural sunlight stress, and gray bars represent after two weeks of natural sunlight. Two housekeeping genes were used to normalize the qPCR data: UBQ10 and Ef1β (panel A). Panel B is CT levels and panel C is antioxidant activity measured against Trolox as a standard. All data points represent the means of four independently treated plants. For all three panels, values in WT after two weeks outside were significantly higher than all four MYB134-RNAi lines ($p < 0.001$), but there was no significant difference between the lines before natural sunlight stress. Error bars represent SE; replicated twice.

3.3.2 RNA-seq analysis of MYB134-RNAi transgenics shows specific down-regulation of flavonoid pathway enzyme genes and transcription factors

To confirm the effect of the MYB134-RNAi construct on CT biosynthesis genes, we carried out transcriptome analysis by RNA-seq. RNA was isolated from three natural sunlight-induced leaf samples of wild-type and a representative MYB134-RNAi line (line 24), and the corresponding cDNA was analyzed by RNA-seq. Sequence alignment of reads was performed using HISAT2 and Cufflinks with *P. tremula* as reference genome, and Cuffdiff was used to identify differentially expressed genes. Using a threshold of log-fold change of at least 2 and a q-value < 0.05, a total of 61 genes were found to be differentially expressed between MYB134-RNAi line 24 and wild-type (Supplemental Table 3.1). Almost all differential genes showed reduced expression in the MYB134-RNAi plants. Of the 20 most strongly downregulated genes, 15 were flavonoid or CT-related genes, indicating that an effect of the RNAi suppression of MYB134 was focused on the CT pathway (Table 3.1; Supplemental Table 3.1). Down-regulated genes encoded CT-specific enzymes (*LAR, ANR*) as well as general flavonoid pathway genes (*DFR, CHS*). The most repressed flavonoid gene was LAR1 (0.023-fold) followed by DFR1 (0.036-fold).

In addition to flavonoid pathway genes, several MYB transcription factors or their co-factors were down-regulated in the MYB134-RNAi line. Surprisingly, this included MYB115, the other major CT regulator, and MYB201, a closely related but uncharacterized poplar MYB (James *et al.,* 2017). The RNAi plants also showed reduced expression of a MYB of unknown function (MYB009) and two WD-40 repeat proteins which form part of the MBW complexes (James *et al*., 2017). Therefore, the majority of the down-regulated genes were linked to flavonoid biosynthesis or its regulation.

We also compared the major soluble phenolics found in poplar in MYB134-RNAi and wild-type leaves using HPLC (Supplemental Table 3.2). We analyzed both control and natural sunlight-induced leaf samples. As expected, under natural sunlight, compared to the controls, MYB134-RNAi lines contained significantly less catechin in both replicate experiments, consistent with its role as a precursor to polymeric CTs. By contrast, the flavonol rutin was not affected in the RNAi lines (Supplemental Table 3.2). Interestingly, salicortin and tremulacin,

major phenolic glycosides found in the Salicaceae, were unchanged in the RNAi plants relative to controls.

Table 3.1: Selected flavonoid-related genes showing differential expression exposed to natural sunlight (at least two-fold change and q-values < 0.05).

			MYB134-RNAi	
Potri number[a]	**Potra number**	**Gene[b]**	**Fold-change**	***q*-value**
Flavonoid pathway enzymes				
Potri|008G116500	Potra002388g18184	LAR1[c]	0.023	8.36E-40
Potri|002G033600	Potra194092g28921	DFR1	0.036	3.73E-45
Potri|015G050200	Potra000121g00397	LAR3	0.038	2.30E-10
Potri|009G069100	Potra001804g14599	F3'5'H1	0.042	3.02E-28
Potri|014G019200	Potra166498g27221	Cytochrome b5	0.043	6.48E-30
Potri|003G176800	Potra161624g34003	CHS4	0.066	2.83E-19
Potri|005G113900	Potra000959g07878	F3H3	0.080	1.87E-27
Potri|009G133300	Potra000887g07160	Flavonoid 3-*O*-gal transferase-like	0.107	4.08E-09
Potri|004G030700	Potra001988g15626	ANR1	0.08	3.04E-26
Potri|014G019200	Potra000729g05732	Cytochrome b5	0.081	5.48E-06
Potri|009G133300	Potra000887g07161	Flavonoid 3-*O*-gal transferase-like	0.107	4.31E-04
Potri|003G176800	Potra010177g26513	CHS4	0.148	2.67E-13
Potri|005G113900	Potra000959g07878	F3H3	0.166	5.95E-05
Potri|001G051600	Potra002245g17252	CHS3	0.170	3.62E-12
Potri|005G229500	Potra001823g14702	DFR2	0.183	3.82E-04
Potri|010G129800	Potra002406g18301	LAR2	0.218	3.83E-10
Potri|019G057800	Potra000801g06348	CHI-like2	0.259	2.74E-04
Potri|003G176700	Potra179565g34898	CHS4	0.293	5.60E-06
Potri|013G073300	Potra009997g26466	F3'H1	0.334	1.42E-10
Potri|014G145100	Potra000539g03787	CHS1	0.334	4.04E-03
Potri|010G213000	Potra000854g35638	CHI1	0.346	3.18E-03
Potri|005G113900	Potra002038g15935	F3H3	0.415	6.29E-06
Phenylpropanoid pathway enzymes				
Potri|006G178700	Potra000682g05284	Cinnamoyl-CoA reductase-like	0.029	3.95E-29
Transcription factors[d]				
Potri|002G173900	Potra003711g22520	MYB115	0.030	1.49E-28
Potri|006G209000	Potra000895g07258	WD-40 repeat protein	0.072	6.77E-15
Potri|016G075800	Potra003770g22777	WD-40 repeat protein	0.076	7.37E-14
Potri|006G221800	Potra001661g13641	MYB134	0.102	7.36E-06
Potri|001G086700	Potra001048g08913	MYB009	0.210	1.17E-05
Potri|014G100800	Potra001051g08951	MYB201	0.395	8.83E-04
Putative transporters				
Potri|005G207500	Potra000524g03567	MATE transporter (TT12-like)	0.067	3.68E-14
Potri|002G055100	Potra183086g28278	MATE transporter (TT12-like)	0.143	6.77E-15

[a] Potri numbers as used in Phytozome were converted from Potra numbers on Popgenie (http://popgenie.org/)

[b] Gene names and annotation were used as defined by Tsai *et al*. (2006), and used in Yoshida *et al*. (2015), James *et al*. (2017), and Ma *et al*. (2018)

[c] Gene abbreviations for flavonoid gene are as follows. LAR, leucoanthocyanidin reductase; DFR, dihydroflavonol reductase; F3'5'H, flavonol-3',5'-hydroxylase, CHS, chalcone synthase; F3H, flavonoid-3-hydroxylase; CHIL, chalcone isomerase-like; ANR, anthocyanidin reductase; CHS, chalcone isomerase-like, CHI, chalcone isomerase

[d] Transcription factor names by Wilkins *et al*. (2009).

3.3.3 RNAi suppression of MYB134 does not affect root CT content

We also investigated the effect of MYB134 suppression on poplar roots. Under greenhouse conditions, *P. tremula × P. tremuloides* roots accumulate CTs at much higher concentration than leaves (Westley, 2015). Roots were separated into three zones: root tip (the apical 2 cm of white root tips), fibrous roots (thin, small, non-lignified roots), and woody roots (larger lignified, >0.75-1 cm in diameter). Consistent with our previous observations, CT content was highest in root tips and younger roots (Figure 3.3). We observed no significant differences in CT concentrations between MYB134-RNAi and control lines for any of the root zones. The higher variation in CT concentrations within the root tip zone was due to difficulty in obtaining roots of consistent tissue age.

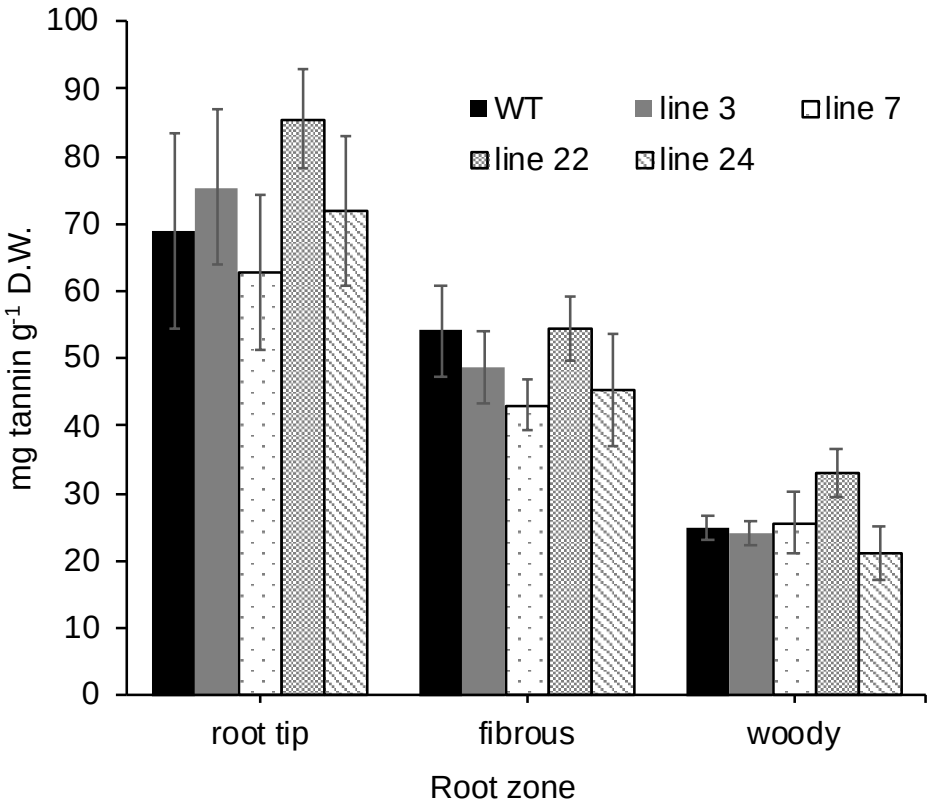

Figure 3.3: MYB134-RNAi expression is not manifested in the roots of transgenic poplar after two weeks of natural sunlight. Plants were grown under normal greenhouse conditions before being placed in natural sunlight for two weeks. Four independently transformed MYB134-RNAi lines as well as WT were tested, and each data point is the mean of four individual plants. Three different root zones were harvested and condensed tannins were extracted as outlined in the Methods. There are no statistical differences between WT and any of the MYB134-RNAi lines. Error bars represent SE.

3.3.4 Methyl jasmonate induces MYB134 and enhances RNAi-suppression

Methyl jasmonate (MeJa) is commonly used as a defense signaling compound to induce herbivore defense responses in plants. In poplar, this response includes the induction of CT biosynthesis and accumulation in leaves (Peters and Constabel, 2002). We tested MeJa treatment of control and MYB134-RNAi poplars in the greenhouse to determine if the effects of MYB134-RNAi suppression could be observed in the greenhouse without moving plants into natural sunlight. As previously observed, under greenhouse conditions plants have a very low CT content (0.3-0.4 mg tannin/g D.W.) (Figure 3.4). Following MeJa treatment, this increased to 1.1 mg CT/g D.W. in wild-type plants, but in MYB134-RNAi plants, CT content remained at 0.3-0.5 mg CT/g D.W. The differential responses were also observed in MYB134 transcript abundance, which increased much more in the wild-type than in the RNAi lines (Figure 3.4). This experiment suggested that MeJa would be a useful fool for testing the impact of RNAi-suppression of CTs on plant resistance to oxidative stress.

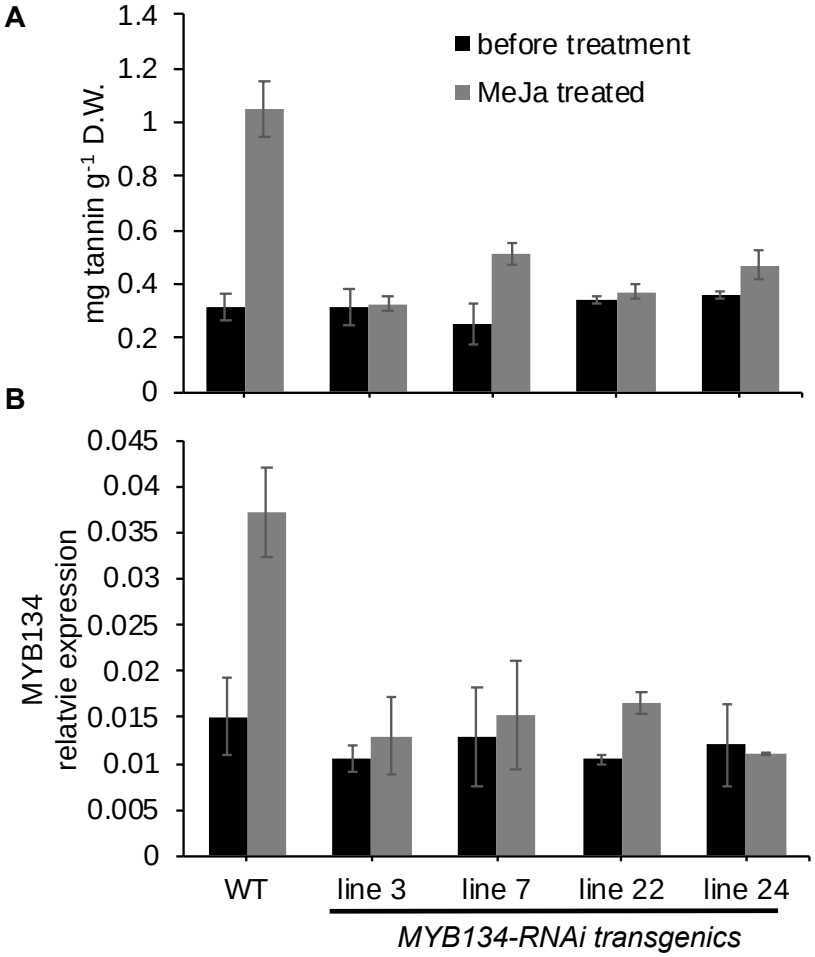

Figure 3.4: MYB134-RNAi hybrid poplar leaf extracts have a reduced capacity for tannin induction by methyl jasmonate (MeJa) spraying. Plants were grown under normal greenhouse conditions and leaves of LPI 10-12 were harvested and extracted according to the Methods. Plants were sprayed with MeJa every two days for four total treatments over ten days. Black bars represent samples taken prior to MeJa spraying, and grey bars represent samples taken after ten days of MeJa spraying. Four independently transformed RNAi lines were tested, and each data point is the mean of four plants. Condensed tannin concentrations (A) were measured by butanol:HCl method, and transcript levels were determined using qPCR MYB134 (B) as outlined in the Methods. Housekeeping gene levels were similar for all poplar lines (UBQ10 and Ef1β). After spraying with MeJa, WT CT and MYB134 transcript levels are significantly higher than any MYB134-RNAi line levels (two-way ANOVA; $p < 0.001$). Error bars represent SE; replicated three times.

3.3.5 MYB134-RNAi lines show enhanced susceptibility to oxidative stress

The successful generation of RNAi plants with reduced CT content provided the opportunity to test the impact of RNAi suppression on oxidative stress resistance *in planta*. Our recent results had demonstrated that high-CT MYB134-overexpressing poplar leaves are better protected against oxidative stress generated by methyl viologen (MV), manifested as enhanced protection of photosystem II (PSII) function, and reduced superoxide and hydrogen peroxide (H_2O_2) accumulation (Gourlay and Constabel, 2019). Since leaf extracts from MYB134-RNAi plants show reduced antioxidant activity in the DPPH assay (Figure 3.2), we predicted that MYB134-RNAi leaves should be more sensitive to MV. To test this hypothesis, leaves from MeJa-induced MYB134-RNAi and wild-type plants were subjected to MV treatment as described previously (Gourlay and Constabel, 2019). Excised leaves were placed in solutions of MV or water for up to 24 h. Both wild-type and transgenic leaves took up similar amounts of solution (approximately 12-15 ml). At various time intervals, chlorophyll fluorescence was used to assess leaf damage by oxidative stress. We monitored *Fv/Fm*, which reflects the efficiency of PSII in a dark-adapted state. All plants showed a decrease in *Fv/Fm* chlorophyll fluorescence in response to MV exposure over the 24 h period; however, the MYB134-RNAi lines all showed a significantly steeper decline compared to wild-type or water-treated controls (two-way ANOVA; $p < 0.01$) (Figure 3.5A). Therefore, we conclude that MYB134 suppression led to an increase in susceptibility to MV.

This was confirmed by quantifying leaf H_2O_2 levels, a key reactive oxygen species (ROS) that can be assayed directly in leaf extracts. All MYB134-RNAi lines contained significantly more H_2O_2 after MV treatment, compared to wild-type leaves (Figure 3.5B). Together with the greater reduction in PSII efficiency compared to wild-type, these data indicate that CTs contribute to the protection of poplar leaves against oxidative stress and ROS accumulation.

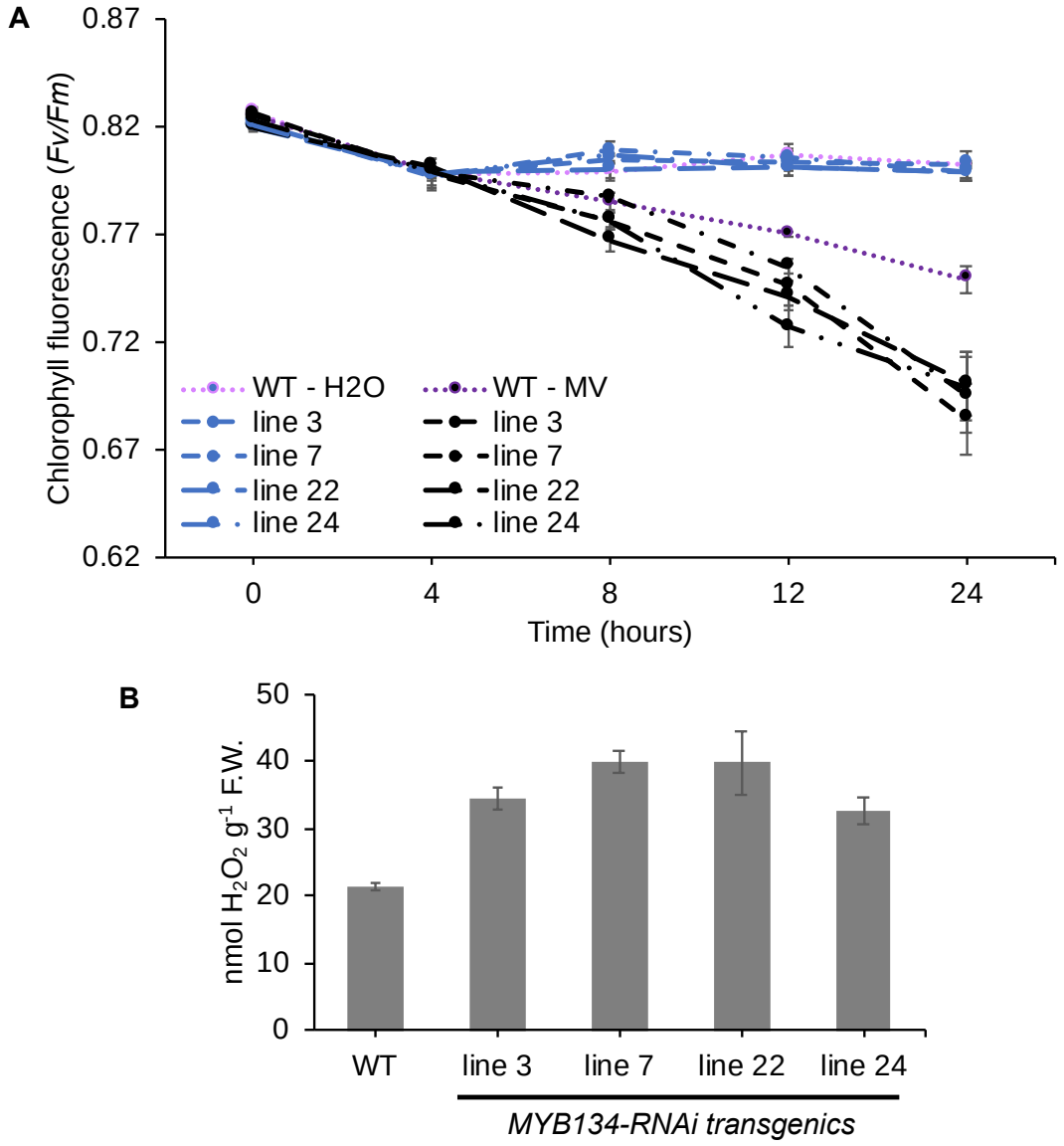

Figure 3.5: Low condensed tannin MYB134-RNAi hybrid poplars show reduced *Fv/Fm* and elevated hydrogen peroxide concentrations following methyl viologen treatment. Duplicate leaves from a MeJa-treated plant were exposed to either water (H_2O) or 200 µM methyl viologen (MV) for 24 hours. The blue lines represent chlorophyll fluorescence in the water treated samples and the black lines represent the same in methyl viologen treated samples (panel A). Concentration of hydrogen peroxide after MV treatment is in panel B (MYB134-RNAi have significantly higher concentrations than WT; $p < 0.001$). Time had a significant effect on fluorescence in MYB134-RNAi lines but not WT ($p < 0.01$; panel A) and was n.s. in the water control group (two-way ANOVA). Data points shown means ± SE; replicated three times.

3.4 Discussion

Due to low MYB134 expression and CT synthesis in plants grown in the protected environment of the greenhouse, we used methyl jasmonate (MeJa) pre-treatments to stimulate MYB134 gene expression and the CT pathway artificially. Following MeJa pre-treatment, MYB134 transcript abundance and CT accumulation was consistently lower in MYB134-RNAi plants compared to controls; this led to reduced antioxidant capacity of the transgenics and a greater susceptibility to MV-induced ROS as seen by reduced chlorophyll fluorescence and elevated H_2O_2 production. These data corroborate our previous results with MYB134-overexpressing poplar, which showed that high CT poplar leaves are more resistant to ROS damage after MV treatment (Gourlay and Constabel, 2019).

The development of RNAi-based methods for generating knock-downs of specific genes has been a great benefit for plant functional genomics (Waterhouse and Helliwell, 2003; Wang *et al*., 2019*b*). RNAi has been applied successfully in many species, including trees and woody plants such as *Pinus radiata* (Wagner *et al*., 2005), *Eucalyptus* spp. (Ziebell *et al*., 2016), and *Populus* spp. (Zhou *et al*., 2018). In *Populus*, several genes and traits have been previously disrupted using this technique, often targeting lignin (Coleman *et al*., 2008; Tian *et al*., 2013; Zhou *et al*., 2018). Here, we used RNAi-suppression of the CT regulator MYB134 to specifically reduce CT synthesis in poplar. As observed previously in RNAi experiments (Behnke *et al*., 2010; Tian *et al*., 2013), target gene expression was suppressed but not eliminated.

The CT pathway in *Populus* has been downregulated previously using CRISPR/Cas9 to target the *MYB115* and *4CL2* genes. Disruption of MYB115 resulted in only a small reduction in CTs in leaves of *P. tomentosa* (Wang *et al.,* 2017), likely because this regulator is less important in leaves compared to roots (see below). Zhou *et al*. (2015) achieved a reduction of CT in roots by as much as 92% by mutating *4CL2* but did not report an effect on leaves. In both cases, CT content was reduced but not eliminated; this could be due to redundancy in gene function, for example the presence of multiple MYB CT activators (see below). With a previous version of the current MYB134-RNAi construct in *P. tremula × alba*, we achieved only a limited reduction of CTs (Ullah *et al*., 2017). However, the overexpression of poplar MYB165 and MYB194 repressors led to strongly reduced CT accumulation (Ma *et al*., 2018). These plants also had a broader

chemical phenotype, with reduced phenolic glycoside and ester content, limiting their utility in experiments targeting CTs.

3.4.1 MYB134-RNAi suppression is specific for the CT pathway

The role of MYB134, a key regulator of the CT pathway in poplar, was first characterized by relying on stable MYB134-overexpressing transgenic poplar (Mellway *et al*., 2009); at a threshold of two-fold differential expression. In these plants 160 genes are more highly expressed compared to wild-type plants (James *et al*., 2017). The most strongly upregulated genes include all the known steps in the flavonoid pathway. Under greenhouse conditions, these transgenics have 50-fold greater foliar CT content but only minor changes in other flavonoids (Mellway *et al*., 2009). However, in such overexpression experiments, primary and secondary effects cannot easily be distinguished. With RNAi-suppressed MYB134, we are more confident that primary effects of MYB134 misregulation can be observed. Consistent with this, we found only 52 genes with reduced expression in MYB134-RNAi plants compared to wild-type after stimulating the plants with natural sunlight. Of these downregulated transcripts, more than half encode functions directly associated with the flavonoid/CT pathway, and all known enzymes of CT synthesis except ANR were represented (Table 3.1). Of the ten most suppressed genes, seven encode flavonoid-related functions. While the RNAi and overexpression experiments cannot be compared directly, our data is consistent with the role of MYB134 as a key regulator of CT pathway.

Interestingly, overexpression of MYB134 and MYB115 strongly upregulates CT synthesis, but simultaneously reduces the accumulation of other phenolics, in particular the salicinoids (*e.g.* tremulacin, salicortin) (Mellway *et al.,* 2009; James *et al*., 2017). By contrast, in the MYB134-RNAi transgenics, salicinoid content was not affected (Supplemental Table 3.2). Therefore, here we observed no evidence of a metabolic trade-off or competition between the salicinoid and flavonoid pathways in the RNAi-suppressed plants. The down-regulation of salicinoids seen after MYB134 overexpression (Mellway *et al*., 2009) is thus likely due to an upregulation of the MYB repressors MYB165 and MYB194 in these plants (Ma *et al.*, 2018). Both

repressors are known to downregulate proposed enzymes of the salicinoid pathway, although they affect the flavonoid enzymes and regulators as well (Ma *et al.,* 2018).

3.4.2 MYB134-RNAi plants provide insight into regulatory network for CTs in poplar

MYB134 and MYB115 are both specific activators of CT synthesis, and share the same set of flavonoid target genes. How their roles overlap is not clear, since in promoter activation assays, they have very similar activities (James *et al.,* 2017). Interestingly, our RNA-seq analysis showed that when induction of MYB134 was suppressed, MYB115 expression was even more reduced (Table 3.1). This is consistent with our previous observation that MYB115 is also strongly up-regulated in MYB134-overexpressors (James *et al*., 2017). In transactivation assays, MYB134 was also shown to directly activate the MYB115 promoter. These results support the hypothesis that MYB134 is the primary determinant of CT synthesis and regulates MYB115 expression. However, additional assays showed that, conversely, MYB115 can also activate the MYB134 promoter, and that MYB115 overexpressors show enhanced MYB134 expression (James *et al.,* 2017). Based on these results, it is plausible that either MYB activator can take the role of primary CT regulator, depending on the tissue and context.

Such organ-specific roles of MYB115 and MYB134 would be consistent with a number of observations. We and others have observed that MYB115 is more highly expressed in roots than MYB134 (James *et al*., 2017; Wang *et al*., 2017). Most flavonoid genes linked to CT biosynthesis, including *DFR*, *LAR*, and *ANR*, also show greater constitutive expression in roots compared to mature leaves (Tsai *et al.*, 2006; James *et al*., 2017). Roots have constitutively high CT content in greenhouse-grown plants, whereas leaves accumulate much less CT unless stimulated by environmental factors such as light or stress. MYB115 could thus be the primary driver of CT synthesis in roots; this hypothesis would also explain why suppression of MYB134 was effective in leaves but did not lead to a reduction of CTs in roots (Figure 3.3). Nevertheless, MYB134 appears to be the main regulator for leaf CTs, particularly in response to environmental stimuli, as evidenced by the results of our MYB134-RNAi experiments.

The hypothesis that MYB115 is important for root CTs could be tested in MYB115 knockout poplars; such transgenics have been generated in a *P. tomentosa* background, but the CT content of roots was not reported (Wang *et al*., 2017). In leaves of these plants, mutation of MYB115 led only to a modest 40% decrease in CTs, consistent with a primary role for MYB115 in roots, and MYB134 in leaves, as suggested here. We cannot rule out involvement of other regulators, however. For example, MYB6 may also participate in CT regulation in roots or leaves (Wang *et al*., 2019*a*). Furthermore, the poplar MYB repressors such as MYB165 and MYB194 also affect CT accumulation in roots (Ma *et al*., 2018). A more precise definition of the role of the suite of MYB factors will therefore require additional knock-out experiments.

3.5 Supplemental Material

3.5.1 Supplemental tables

Supplemental Table 3.1: Differentially expressed genes between WT and MYB134-RNAi transgenic poplar after two weeks exposure to natural sunlight.

Potri number	Potra number	Gene name	Fold-change	*q-value*
Potri|008G116500	Potra002388g18184	LAR1	0.023	8.36E-40
Potri|006G178700	Potra000682g05284	Cinnamoyl-CoA reductase-like protein	0.029	3.95E-29
Potri|002G173900	Potra003711g22520	MYB115	0.030	1.49E-28
Potri|002G033600	Potra194092g28921	DFR1	0.036	3.73E-45
Potri|015G050200	Potra000121g00397	LAR3	0.038	2.30E-10
Potri|009G069100	Potra001804g14599	F3'5'H1	0.042	3.02E-28
Potri|014G019200	Potra166498g27221	Cytochrome B5	0.043	6.48E-30
Potri|015G100600	Potra002731g19860	Chitinase	0.057	1.26E-12
Potri|003G213700	Potra002664g19702	Zinc finger FYVE domain protein	0.060	2.62E-03
Potri|003G176800	Potra161624g34003	CHS4	0.066	2.83E-19
Potri|005G207500	Potra000524g03567	MATE family transporter (AtTT12-like)	0.067	3.68E-14
Potri|006G209000	Potra000895g07258	WD-40 repeat containing protein	0.072	6.77E-15
Potri|016G075800	Potra003770g22777	WD-40 repeat containing protein	0.076	7.37E-14
Potri|005G079200	Potra189073g28655	Prephenate aminotransferase (PAT)	0.080	2.38E-02
Potri|005G113900	Potra000959g07878	F3H3	0.080	1.87E-27
Potri|009G133300	Potra000887g07160	Similar to flavonoid 3-O-galactosyl transferase	0.080	4.08E-09
Potri|004G030700	Potra001988g15626	ANR1	0.080	3.04E-26
Potri|014G019200	Potra000729g05732	Cytochrome b5	0.081	5.48E-06
Potri|005G207500	Potra001057g09070	Transparent testa 12	0.082	3.68E-15
Potri|006G221800	Potra001661g13641	MYB134	0.102	7.36E-06
Potri|009G133300	Potra000887g07161	Similar to flavonoid 3-O-galactosyl transferase	0.107	4.31E-04
Potri|002G095900	Potra001893g15065	Similar to hexose transport protein	0.113	1.62E-06
Potri|002G055100	Potra183086g28278	MATE family transporter (AtTT12-like)	0.143	6.77E-15
Potri|003G176800	Potra010177g26513	CHS4	0.148	2.67E-13
Potri|005G113900	Potra000959g07878	F3H3	0.166	5.95E-05

Potri|001G006700	Potra194932g29001	Acyl-activating enzyme 18	0.168	7.36E-06
Potri|001G051600	Potra002245g17252	CHS3	0.170	3.62E-12
Potri|005G229500	Potra001823g14702	DFR2	0.183	3.82E-04
Potri|001G086700	Potra001048g08913	MYB-related protein	0.210	1.17E-05
Potri|010G129800	Potra002406g18301	LAR2	0.218	3.83E-10
Potri|002G059200	Potra000696g05420	Potassium channel, subfamily K	0.241	4.96E-02
Potri|001G157600	Potra002184g16830	Integral membrane family protein; similar to nodulin MtN21	0.241	4.57E-03
Potri|006G027000	Potra000586g04376	Uncharacterized hydrolase C22A12	0.247	2.21E-05
Potri|019G057800	Potra000801g06348	CHIL2	0.259	2.74E-04
Potri|001G006700	Potra197337g29216	Acyl-activating enzyme 18 (AAE18)	0.262	9.53E-06
Potri|019G008000	Potra003293g21258	Zinc finger FYVE domain containing protein	0.268	7.11E-06
Potri|003G176700	Potra179565g34898	CHS4	0.293	5.60E-06
Potri|004G057700	Potra002435g18478	Similar to AtAGP4C (hydroxyproline-rich glycoproteins)	0.301	1.38E-02
Potri|005G167400	Potra001558g12898	Similar to acetyl-CoA carboxylase	0.308	2.09E-05
Potri|010G012400	Potra163172g27067	Ortholog of At3g16670, At3g16660	0.312	3.53E-04
Potri|006G188300	Potra000968g07978	Class V chitinase	0.328	3.42E-04
Potri|013G073300	Potra009997g26466	F3'H1	0.334	1.42E-10
Potri|014G145100	Potra000539g03787	CHS1	0.334	4.04E-03
Potri|010G213000	Potra000854g35638	CHI1	0.346	3.18E-03
Potri|010G012400	Potra001737g14149	Ortholog of At3g16670, At3g16660	0.366	2.37E-03
Potri|018G100500	Potra000945g07746	Similar to cinnamoyl-CoA reductase	0.387	1.85E-04
Potri|010G145800	Potra001834g14750	ATP-citrate synthase	0.395	3.83E-04
Potri|014G100800	Potra001051g08951	MYB201	0.395	8.83E-04
Potri|005G113900	Potra002038g15935	F3H3	0.415	6.29E-06
Potri|002G057700	Potra000696g05408	Enoyl-CoA hydratase/isomerase family protein; similar to CHY1 (gi:8572760)	0.423	3.69E-04
Potri|009G148100	Potra000358g01441	Stress responsive A/B Barrel Domain	0.444	6.04E-03
Potri|019G049500	Potra177143g27937	4CL4	0.490	2.40E-03
Potri|003G170200	Potra000353g01331	Agamos-like 8 (AGL8)	2.378	4.32E-02
Potri|019G103500	Potra001664g13671	Similar to dwarf in light 2	2.445	5.54E-03
Potri|001G059900	Potra001446g12173	Similar to glucose-6-phosphate dehydrogenase	2.928	3.34E-02
Potri|004G140800	Potra188105g28563	Nitrite reductase PtNIR1.1	2.969	3.79E-02
Potri|010G128900	Potra001973g15562	PtEXT9 (extensin)	2.990	2.74E-02

Potri|009G038300	Potra003973g23885	Ortholog of At5g59080, At5g02020, At3g46880	3.784	2.22E-02
Potri|009G110800	Potra003270g21181	Leghemoglobin related	4.199	1.39E-03
Potri|007G027000	Potra000938g07677	PROLINE-RICH RECEPTOR-LIKE PROTEIN KINASE PERK4; PtPERK9	4.563	6.86E-05
Potri|001G341300	Potra003867g34626	Similar to TBP-binding protein; similar to ABT1	5.736	2.64E-02

Supplemental Table 3.2: Concentrations of key salicinoids and flavonoids in MYB134-RNAi and wild-type leaves as determined using HPLC in greenhouse grown versus natural sunlight exposed poplar plants[1].

	Greenhouse-grown						Two weeks natural sunlight					
Compound	Control[2]	RNAi line 3	RNAi line 7	Control	RNAi line 22	RNAi line 24	Control	RNAi line 3	RNAi line 7	Control	RNAi line 22	RNAi line 24
Salicortin	10.20 ± 0.37	10.98 ± 0.51	10.90 ± 0.89	18.08 ± 1.14	18.03 ± 0.54	18.84 ± 0.52	17.27 ± 1.35	20.15 ± 1.41	17.02 ± 1.29	20.88 ± 0.52	18.10 ± 0.87	18.79 ± 1.11
Tremulacin	13.12 ± 1.09	12.96 ± 1.58	15.10 ± 1.87	17.93 ± 2.11	18.33 ± 2.42	17.11 ± 2.15	16.20 ± 1.52	20.13 ± 0.915	18.05 ± 1.83	24.15 ± 0.897	21.63 ± 2.34	20.61 ± 2.77
Rutin	4.26 ± 0.17	5.01 ± 0.304	4.47 ± 0.607	7.21 ± 0.26	7.28 ± 0.67	6.12 ± 0.71	12.30 ± 1.31	14.15 ± 0.33	13.29 ± 1.16	24.72 ± 1.92	22.14 ± 2.07	23.18 ± 2.09
Catechin	0.16 ± 0.02	0.17 ± 0.018	0.17 ± 0.03	0.17 ± 0.01	0.17 ± 0.01	0.17 ± 0.02	1.73 ± 0.10	**0.93 ± 0.045****	**1.01 ± 0.06***	2.99 ± 0.18	**1.73 ± 0.25***	**1.42 ± 0.22****

[1] Concentrations are expressed as μg mg^{-1} dry weight ± SE. Significant differences from controls were determined using a one-way ANOVA and are indicated by boldface type and asterisks (*, $p < 0.01$; **, $p < 0.001$).

[2] Separate experiments were conducted for MYB134-RNAi lines 3 and 7 from line 22 and line 24, with independent controls for each. Data from these cannot be compared directly.

Chapter 4 : Condensed tannins are antioxidants that protect poplar against oxidative stress and photosystem damage during drought and UV-B exposure

(This chapter is to be submitted to New Phytologist.)

4.1 Introduction

Plants are exposed to a multitude of different stresses, including drought, cold, UV-B, and wounding. Stress can affect growth and development in plants and often involves trade-offs between vegetative and reproductive development (He *et al.,* 2018). The disruption of membranes and organelle compartmentalization due to stress can result in an accumulation of toxic metabolic intermediates. A very common effect of abiotic stress is the production of reactive oxygen species (ROS) (Czarnocka and Karpiński, 2018).

ROS, including hydrogen peroxide (H_2O_2), superoxide (O_2^-), singlet oxygen ($^1O_2$), and the hydroxyl radical (HO*) (Apel and Hirt, 2004) are produced in the peroxisomes, chloroplasts, and mitochondria as a result of natural aerobic reactions. ROS are overproduced during stress events due to the breakdown of cellular components (Choudhury *et al*., 2017), which generally has negative effects on the plant. For example, singlet oxygen is produced from the combination of excited chlorophyll triplets and molecular oxygen during high-light stress (Aro *et al*., 1993). Over-production of ROS in the chloroplasts is associated with damage and disruption to the photosynthetic machinery and can lead to additional damage to photosystem II (PSII). Additionally, electrons leaking from the electron transport chain (ETC) in the chloroplasts and mitochondria react with oxygen, which creates the superoxide radical (O_2^-) (del Rio, 2015). This radical has a short half-life but is responsible for the generation of the highly reactive hydroxyl radical (Demidchik, 2015; del Rio, 2015). H_2O_2 accumulates as a product of superoxide, since O_2^- is dismutated into H_2O_2 by superoxide dismutase (del Rio, 2015). Further, In the presence of transition metals such as iron (Fe) and copper (Cu), the hydroxyl radical is generated from H_2O_2 via the Fenton-reaction; this radical is thought to be responsible for much of the oxidative stress and lipid peroxidation observed in plants (Demidchik, 2015; Choudhury *et al.*, 2017). Since hydroxyl radicals are produced in both photosystem I (PSI) and PSII, the resulting

oxidative damage can lead to an overall disruption of photosynthesis (Demidchik, 2015). Photosystem health can be assessed via measurements of chlorophyll fluorescence on intact plants; this is established as an important non-invasive technique that provides direct insight into the function of the plant's photosystems (Murchie and Lawson, 2013).

The interaction of ROS with membranes, including those of the photosystems, commonly leads to lipid peroxidation. Extreme lipid peroxidation damages membranes, preventing their ability to function as barriers, and can cause the overall break-down of organelles, DNA, and proteins (Farmer and Mueller, 2013; Demidchik, 2015). Lipid peroxidation can also lead to chain reactions, where additional lipid radicals are generated and propagate. A common end-product of lipid peroxidation is malondialdehyde (MDA), a marker for oxidative stress (Noctor *et al.,* 2015). Ultimately, a decrease in photosystem function can result, which can be observed using chlorophyll fluorescence. Assessment of the effects of ROS on photosystems by assaying MDA and measuring chlorophyll fluorescence are important in assessments of plant tolerance and responses to stress.

Plant responses to ROS can include enzymatic and non-enzymatic defense mechanisms. Enzymes that minimize oxidative damage by removing ROS include superoxide dismutase (SOD) or catalase (CAT), and these enzymes typically increase following stress (Cramer *et al*., 2011). The xanthophyll cycle and the water-water cycle are non-enzymatic mechanisms for scavenging ROS produced during photosynthesis (Demmig-Adams, 1990; Asada, 1999). Other compounds that protect against oxidative stress by scavenging ROS include ascorbate, vitamin E, glutathione, and polyphenols (del Rio, 2015). Glutathione plays a pivotal role in the glutathione-peroxidase cycle, which uses glutathione peroxidase to reduce H_2O_2 and glutathione to water (Apel and Hirt, 2004). Many polyphenols, including flavonols and anthocyanins, are strong antioxidants; anthocyanins have been recently shown to act as *in vivo* antioxidants during stress (Nakabayashi *et al*., 2014).

Abiotic stresses that cause the production of ROS and oxidative stress include drought and UV-B exposure. Drought stress can inhibit plant growth by slowing cell expansion, reducing carbon fixation, and increasing membrane instability (Smirnoff, 1993). Drought conditions can lead to stunted leaves, shorter plants, and smaller stems (Smirnoff, 1993; Schneider *et al.,*

2019). A hallmark of the plant response to drought is the release of abscisic acid (ABA) as a signal to close the stomata (Zeevaart and Creelman, 1988; Ren *et al.,* 2007). When stomata are closed, the concentration of carbon dioxide (CO_2) inside the leaf decreases (Chaves, 1991; Cramer *et al.,* 2011) which leads to a reduction in carbon fixation and an accumulation of excitation energy (Smirnoff, 1993; Cruz de Carvalho, 2008). Low internal CO_2 concentration, coupled with continued irradiance leads to the generation of ROS, in particular superoxide (Cruz de Carvalho, 2008). This is due to the Mehler reaction, which is an alternate sink for electrons that reduce oxygen but produce superoxide as a side effect (Cruz de Carvalho, 2008; Miller *et al*., 2010). As with most stresses, plants respond to drought with both enzymatic and non-enzymatic mechanisms. The latter includes metabolites important for osmotic adjustment, for example proline or trehalose (Hare *et al*., 1998; Kosar *et al*., 2019).

UV-B is highly damaging to all parts of the plant as it causes lesions in DNA via dimerization between base pairs (Aro *et al.,* 1993). UV-B stress also induces the generation of ROS, but through different mechanisms than drought. UV-B exposure can lead to direct ROS generation when UV-B photons are absorbed by proteins (Kataria *et al.,* 2014), and the generated ROS then interact with lipids and other cellular components (Foyer *et al*., 1994). A primary consequence of UV-B exposure is damage to the photosynthetic machinery (Czégény *et al.*, 2016), as well as nucleic acids and Calvin cycle enzymes (Kataria *et al.,* 2014). The most common ROS generated under UV-B exposure is superoxide, which leads to the disruption of PSII (Foyer *et al*., 1994; Asada, 2006). Hydroxyl radicals are important ROS in the thylakoid membranes and result from malfunction of the electron transport chain (ETC) (Kataria *et al*., 2014; Czégény *et al.*, 2016). Under excessive UV-B, antioxidant systems that scavenge ROS and maintain homeostasis are disrupted and overwhelmed (Foyer *et al.*, 1994). Similar to drought, UV-B lipid peroxidation generates MDA, but instead of beginning with a lipid radical, a primary radical (R*) is produced when UV-B photons are directly absorbed (Foyer *et al*., 1994). The primary radical then reacts with lipids to form lipid radicals and continues the chain reaction (Foyer *et al*., 1994). As in drought stress, increases in MDA are an indicator of oxidative damage caused by UV-B (Kataria *et al*., 2014).

Responses of plants to UV-B stress include morphological, physiological, biochemical, and molecular adaptations (Kataria *et al*., 2014). For example, decreased leaf size and increased leaf thickness help to reduce the amount of light penetrating the cells. Physiological changes include a decrease in photosynthetic activity to prevent overwhelming the photosystems if the photosystems are damaged directly by the UV-B or by the ROS generated by UV-B (Kataria *et al.*, 2014; Czégény *et al*., 2016). Biochemical changes include the induction of flavonoids to absorb UV-B, and DNA repair to remedy UV-B induced lesions (Kataria *et al*., 2014; Czégény e*t al*., 2016). Although it has been previously shown that UV-B induces CTs (Mellway *et al.*, 2009), how these affect plant tolerance to UV-B is not known.

Condensed tannins (CTs) are widespread polymeric flavonoids found extensively in woody species (Quideau *et al*., 2011), and are end-products of the phenylpropanoid pathway (Dixon *et al*., 2005). They have diverse ecological functions including pathogen defense, modulating soil microbial activity, and herbivore defense (Barbehenn and Constabel, 2011; Ullah *et al.,* 2017). Recent work using methyl viologen (MV) to artificially induce oxidative stress has suggested that CTs can act as cellular antioxidants (Gourlay and Constabel, 2019), which could explain why such diverse stresses all induce CTs in poplar plants. Poplars produce high concentrations of CTs, up to 25% dry weight in some species (Lindroth and Hwang, 1996). By contrast, in most herbaceous plants such as *Arabidopsis*, CTs are present in small concentrations and found only in the seed coat (Gonzalez *et al.,* 2016). In poplar, CTs are induced by multiple stresses including UV-B, high-light stress, pathogens, and herbivory (Peters and Constabel, 2002; Mellway *et al*., 2009). This induction is mediated by MYB134 and MYB115, two poplar transcription factors that specifically regulate CT-biosynthesis (Mellway *et al*., 2009; James *et al*., 2017). When overexpressed in transgenic poplar, these transcription factors lead to a 50-fold higher accumulation of CTs than in wild-type, with minor changes in other flavonoids (Mellway *et al.,* 2009; James *et al.*, 2017). Such CT overexpressing poplar plants are thus an excellent opportunity for testing CT function *in planta*. In addition, we also generated low-CT transgenics by suppressing *MYB134* using RNAi (Chapter 3; Gourlay *et al.,* 2019). These high- and low-CT poplar transgenics were utilized to test the hypothesis that CTs function as *in vivo* antioxidants during drought and UV-B exposure and improve tolerance to these oxidative

stress-generating treatments. We demonstrate that plants with high levels of CTs have greater tolerance to drought and UV-B stress than wild-type plants, while lower levels of CTs compared to wild-type result in greater susceptibility to stress.

4.2 Materials and Methods

4.2.1 Plant growth conditions and treatment

Populus tremula x Populus tremuloides (clone INRA 353-38) wild-type, transgenic MYB134- and MYB115 CT-overexpressing plantlets (Mellway *et al.,* 2009; James *et al*., 2017), and MYB134-RNAi CT-underexpressing plantlets (Gourlay *et al*., 2019) were maintained and micropropagated in tissue culture on Lloyd and McCown's Woody Plant Media (WPM; Caisson) with 1 µM indole-3-butyric acid (IBA). For experiments, tissue culture plantlets were transferred to soil and acclimated in a mist chamber for four weeks, then planted in one-gallon pots with a peat-based soil-less mix (Sunshine Mix 4, Sungro®, Seba Beach, Alberta, Canada) with additional slow-release fertilizer as described by Major and Constabel (2006). Plants were kept in the greenhouse under natural light with supplemental lights to extend day length to 16 h. Temperatures ranged from 18 °C to 26 °C. Plants were two months old with 15-20 leaves when used for experiments.

Experiments were carried out in a greenhouse at the University of Victoria, Victoria, B.C., Canada (Appendix 4.5). For drought stress, eight-week old plants in pots were saturated with water the night before the drought experiment began to ensure all plants started at similar water levels. Subsequently, depending on plant size, well-watered plants received 100-150 ml of water three times daily, and the drought-stressed plants received 20-30 ml of water three times daily. Pot + plant weight was measured daily. When pot weight stabilized in the drought-stressed plants (<10 g difference between days), the plants were considered to be in drought. The drought period was three weeks for MYB134- or MYB115-overexpressors and ten days for MYB134-RNAi plants because RNAi plants were more susceptible to the stress and suffered leaf loss faster than MYB-overexpressors. To end drought stress, plants were watered to saturation and allowed to recover for 7 days. Due to space constraints, several replicate experiments, each

with different sets of transgenic lines, were carried out in succession; each transgenic line was tested at least twice.

For experiments with MYB134-RNAi plants, both RNAi and wild-type plants were first induced with methyl jasmonate (MeJa) on day 0, 2, 4, and 6 and drought experiment started on day 10. MeJa (Sigma Aldrich) was first diluted to 10% in EtOH, then diluted to 0.2% with 0.1% Tween/water. Both sides of leaves were sprayed using a plant mister to the point of run-off. This pre-treatment was intended to stimulate the condensed tannin biosynthesis pathway and thus differentiate RNAi and wild-type plants as described in Gourlay *et al.* (2019).

For UV-B treatments, nodal cuttings from tissue culture were shipped to Helmholtz Zentrum in Munich (Neuherberg, Germany), grown in tissue culture for 12 weeks, and acclimated to the greenhouse. After growing in the greenhouse for eight weeks, plants were moved into environmental simulation chambers (Thiel *et al.,* 1996). Sun simulation chambers at the Helmholtz institution in Munich, Germany were used for this experiment. One chamber had simulated natural sunlight and UV-B exposure similar to levels in Spain, and a second chamber had simulated natural sunlight and no UV-B exposure. The environmental simulation chambers were set to 27 °C during the day and 17 °C at night (relative humidity 40% and 80%, respectively) with natural sunlight, with or without UV-B; however, both chambers continued to receive UV-A. A one-week acclimation period in the growth chamber slowly increased daily photosynthetically active radiation (PAR) from 500 µmol m^{-2} to 1400 µmol m^{-2} (Kaling *et al*., 2015). Plants were exposed to visible wavelengths for 16 h (daily PAR: 60 mol m^{-2}) and UV-B for 13 h (daily biologically effective UV-B: 46.8 kJ m^{-2}). Trays were rotated every day to minimize light differences within the chambers. Plants were in trays filled with water twice a week. Two independent experiments using wild-type, MYB134OE-line 41, and MYB134OE-line 46 were carried out. Leaf samples were harvested at week 0, week 1, and week 2 following UV-B exposure, flash frozen in liquid nitrogen, and stored at -80 °C until analysis.

Chlorophyll fluorescence measurements for drought experiments were conducted with an OPTI-Sciences Modulated Chlorophyll Fluorometer OS1p (Opti-Sciences, Inc., Hudson, NH, USA) as outlined in Gourlay and Constabel (2019). For drought experiments, *Fq'/Fm'* was measured because this parameter represents the amount of absorbed light that is used by PSII

for photochemistry (Murchie and Lawson, 2013). For UV-B experiments, chlorophyll fluorescence was measured with a miniPAM fluorometer (Walz, Effeltrich, Germany). In addition to *Fq'/Fm'*, *Fv/Fm* was also measured, providing data on overall efficiency of PSII (Baker, 2008; Murchie and Lawson, 2013). Leaf plastochron index (LPI) 10 was used for fluorescence measurements. For *Fv/Fm,* dark acclimation clips were placed in three similar locations on each leaf and the chamber was darkened for 30 min prior to fluorescence measurement. To avoid potential circadian effects, all measurements were taken pre-dawn with lights off at the same time of day for each replicated experiment. Due to the sensitivity of *Fq'/Fm'* to light flecks in a greenhouse with natural sunlight, fluorescence measurements during the drought experiment were taken pre-dawn under artificial greenhouse lights (300 µmol m^{-2} s^{-1} at the leaf being measured; PL2000 MIDI 600W, P.L. Light Systems, Beamsville, O.N., Canada). In total, at least two experiments were performed using four different MYB134-RNAi transgenic lines, two MYB134-overexpressing transgenic lines, or two MYB115-overexpressing transgenic lines.

4.2.2 Morphological and physiological measurements

Morphological measurements were taken at key time points during drought experiments at day 0, end of drought, and end of recovery. For UV-B experiments, measurements were taken at day 0, week 1 of UV-B stress, and week 2 of UV-B stress. The change in morphological measurement was defined as the difference between day 0 and end of drought for drought experiments, or day 0 and week 2 of UV-B stress for UV-B experiments. For drought experiments, the number of necrotic leaves (leaves that showed browning at the leaf edges or had necrosis spread throughout) were counted daily. Gas exchange analysis during drought experiments was performed weekly using a LCA 4 portable gas exchange system (ADC Bioscientific Ltd., Global House, Hoddesdon, UK) on LPI 10. Measurements were taken at mid-day for optimal and consistent light intensity. Water use efficiency was recorded as µmol CO_2 / mmol H_2O. For UV-B experiments, gas exchange measurements were taken as described by Kaling *et al.* (2015) on LPI 10 using a portable gas exchange system, GFS-3000 (Walz, Effeltrich, Germany). For UV-B experiments only, anthocyanin, flavonol, and chlorophyll measurements

were taken with a Dualex Scientific+ (Force A, Centre entrepreneurial de l'Institut d'Optique, Orsay, France) every 3-4 days at the same time of day. Three measurements per leaf were taken on the adaxial side of the leaves for mature leaves (LPI 10-11) and young leaves (LPI 2-3).

4.2.3 RNA extraction and RT-qPCR analysis

Total RNA was extracted from poplar leaves as previously described (Yoshida *et al.,* 2015), treated with RQ1 DNase (Promega, Madison, WI, USA), and used to synthesize cDNA using Superscript II reverse transcriptase (Invitrogen, Carlsbad, CA, USA) following the manufacturer's instructions. RT-qPCR was performed in 20 µl reactions using 4 µl homemade qPCR master mix on a CFX96 Real Time system (Bio-Rad). The master mix consisted of (final concentrations): 24.1 mM Tris-HCl, 25.9 mM Tris-base, 25 mM KCl, 1.5 mM $MgCl_2$, 0.5% Tween 20, 4% glycerol, 0.83 mM dNTP, and 5X EVAGreen SYBR (Biotium) in a total volume of 2 ml. MYB134 (Potri.006G221800; Phytozome) transcript abundance data were normalized using the geometric mean of poplar elongation factor (EF1b; Potri.001G224700) and ubiquitin (UBQ10; Potri.014G115100) expression (Yoshida *et al.,* 2015).

4.2.4 Phytochemical and ROS analysis

Twenty-five milligrams of ground, freeze-dried tissue was weighed into 2-ml CryoTubes with four steel beads. Tissue was homogenized and extracted in 1.5 ml of 100% MeOH using a Precellys tissue homogenizer (Bertin Technologies, Rockville, MD, USA) for 2 x 45 s at 5000 shakes per min followed by centrifugation of 10 min at 15,000g. Extractions were repeated twice more with an additional 1 ml MeOH, giving 3.5 ml of total plant extract. The butanol-HCl protocol for CT analysis as outlined in Gourlay and Constabel (2019) (Chapter 2) was used.

Isoprene emission rates were assayed by PTR-MS according to Behnke *et al.* (2010). Three 1-cm leaf discs were excised from leaf 10 at noon and placed in a glass vial with 1 ml of CO_2-infused water. The vial was left open for 30 min while acclimation occurred and then was sealed, and the vials were placed on a light box for 2 h after which the amount of isoprene

emitted was measured. There were six biological replicates per line per treatment. Emission rates were normalized to standard conditions (1000 µmol m^{-2} s^{-1} and 30 °C).

Hydrogen peroxide levels were assayed on harvested leaves as outlined in Gourlay and Constabel (2019) (Chapter 2). Malondialdehyde (MDA) concentrations were determined based on Yu *et al*. (2015) and Yang *et al.* (2015) with modifications as follows. Fifty milligrams of frozen leaf powder was weighed into a cooled 2-ml CryoTube with four steel beads, 1.5 ml of 10% trichloroacetic acid (TCA) was added, and samples homogenized using a Precellys tissue homogenizer (Bertin Technologies, ESBE Ontario) for 2 x 45 s at 5000 shakes per min. Following centrifugation, (10 min at 12,000*g* at 4 °C), 1 ml of 0.6% thiobarbituric acid (TBA) in 10% TCA was added to 1 ml of supernatant, and the assay mixture incubated at 95 °C for 30 min in a water bath. Samples were cooled in an ice bath, centrifuged for 10 min at 4 °C, and absorbance read at 440 nm, 532 nm, 600 nm on a spectrophotometer (ThermoSpectronic Genesys 10uv Scanning spectrophotometer, ThermoFisher Scientific, Waltham, MA, USA). Total MDA content was calculated according to Yang *et al.* (2015). Since high CT content in extracts generated high background absorbance readings in this assay, we also included controls incubated in assay solution but without TBA. These were subtracted from assay readings to correct for the high background absorbances.

4.2.5 Statistical analyses

Data were analyzed using *t*-tests of means, analysis of variance (ANOVA), or repeated measures ANOVA and Tukey honest significant difference (HSD) post-hoc tests in R (https://www.r-project.org); details are presented in the figure legends. Sources of variation for ANOVAs were genotype, treatment and their interaction, or genotype, treatment, time and their interactions.

4.3 Results

4.3.1 Severe drought stress reduces growth in both transgenic and control poplar saplings

Two previously characterized independent transgenic poplar lines with elevated CTs (MYB134OE or MYB115OE) were exposed to drought stress in the greenhouse. Onset of drought occurred between day 8 and day 10, depending on the experiment and ambient greenhouse temperatures. Drought was stopped after approximately three weeks and plants were allowed to recover as necrosis had occurred and severely affected plants lost a substantial number of leaves. All treated plants were clearly affected by the drought treatment, showing reduced size, very low stomatal conductance, and low rates of CO_2 assimilation and transpiration at the end of the experiment compared to well-watered controls (Figure 4.1, Supplemental Figure 4.1, 4.2). There were no differences in size or gas exchange parameters between transgenic lines and wild-type.

4.3.2 CTs protect against drought-induced damage to PSII and reduce ROS concentrations in poplar leaves

Fq'/Fm' remained constant in watered control plants throughout drought experiments (Figure 4.2A, B). Beginning on day 11 of drought, wild-type plants showed a steep reduction in *Fq'/Fm'* that continued until the recovery period. In contrast, both high-CT transgenics demonstrated only a moderate decline in fluorescence (Figure 4.2A, B), indicating that PSII in high-CT plants was less affected by drought stress than in wild-type plants. To confirm this, we repeated the experiment with high CT-poplar overexpressing MYB134 in a different genetic background, *Populus tremula x P. alba* (clone 717-B4) (Mellway *et al*., 2009). The same protective effect of the CTs against drought was observed: *Fq'/Fm'* chlorophyll fluorescence remained higher in these MYB134-overexpressing plants compared to controls (Supplemental Figure 4.3).

To test whether that the reduced PSII damage in MYB134- and MYB115-overexpressors after drought stress is due to lower concentrations of ROS, we quantified H_2O_2 in leaf extracts at the end of drought. In all high-CT lines, significantly lower H_2O_2 concentrations were observed,

compared to wild-types leaves, even in the absence of drought (Figure 4.2C). Drought induced H_2O_2 in wild-type plants as well as MYB overexpressors, but the increase was attenuated in high-CT lines and did not reach levels found in wild-type controls. As a biochemical marker of oxidative damage, we measured malondialdehyde (MDA), a lipid peroxidation by-product that accumulates after oxidative stress. High-CT transgenics contained almost three-fold less MDA compared to wild-type after drought stress (Figure 4.2D), and demonstrated a strong correlation between H_2O_2 and MDA concentrations at $R^2 = 0.9089$. These data confirm that the reduced PSII damage in high-CT plants was correlated with reduced ROS build-up and oxidative damage to lipids.

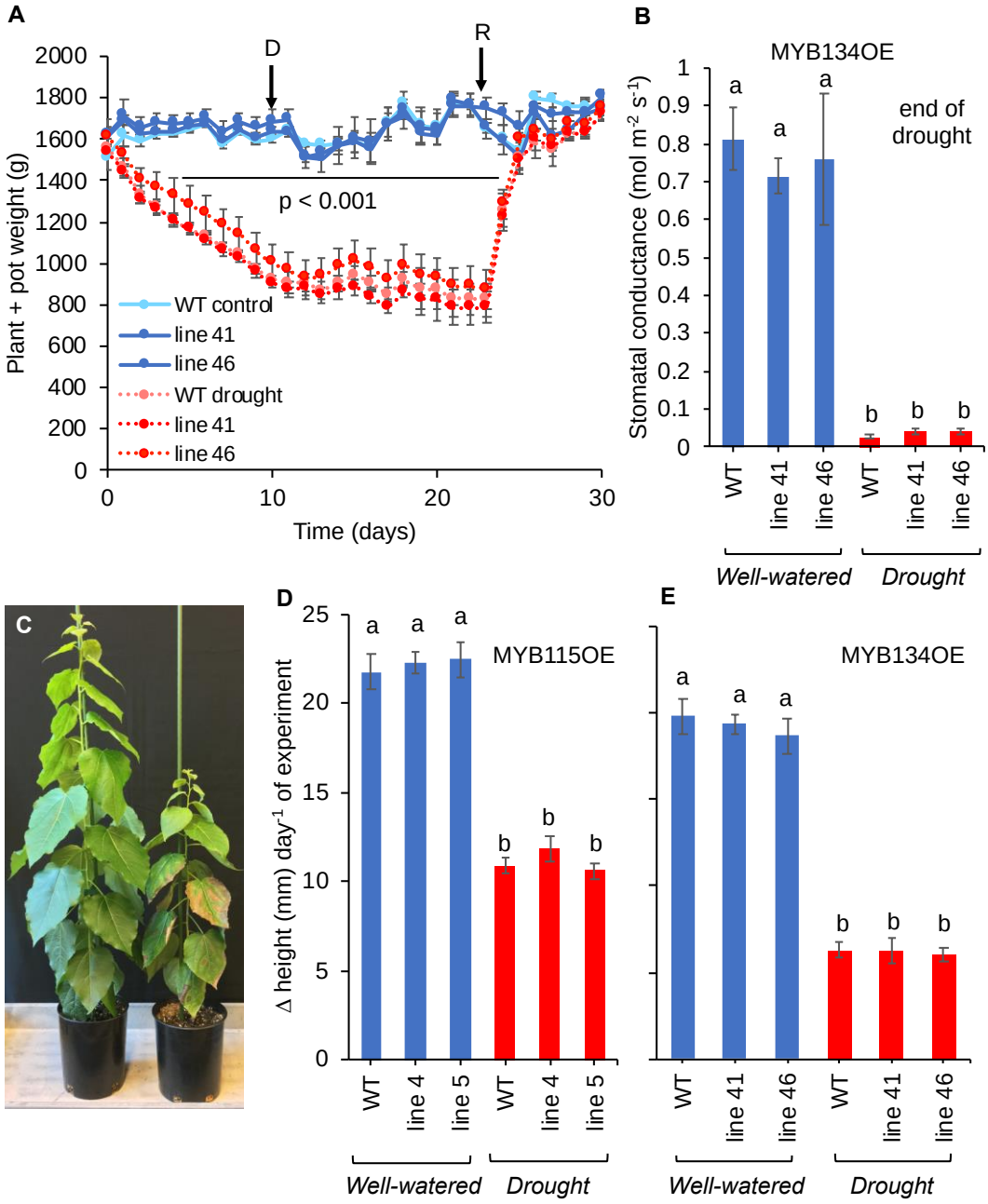

Figure 4.1: Time course and impact of drought stress on growth and stomatal conductance of wild-type and high-CT transgenic poplar. (A) Change in plant + pot weight during imposition of drought stress (as described under Material and Methods). Blue colour corresponds to well-watered plants and red colour corresponds to drought-stressed plants. Solid lines are well-watered and dashed lines are drought-stressed. 'D' indicates beginning of drought as seen in stabilizing of plant and pot weight. 'R' indicates beginning of recovery period. (B) Stomatal conductance for high-CT MYB134-overexpressing and wild-type poplar saplings after drought. (C) Representative image of wild-type well-watered and drought-treated plants. (D) and (E) show impact of drought on growth as the change in height between beginning and end of the drought experiment for high-CT MYB134- and MYB115-overexpressor plants, respectively. Letters indicate significant pair-wise differences using Tukey HSD ($p < 0.05$). Data points are the means of four replicate plants for each independent transgenic line. Error bars represent SE (n = 4).

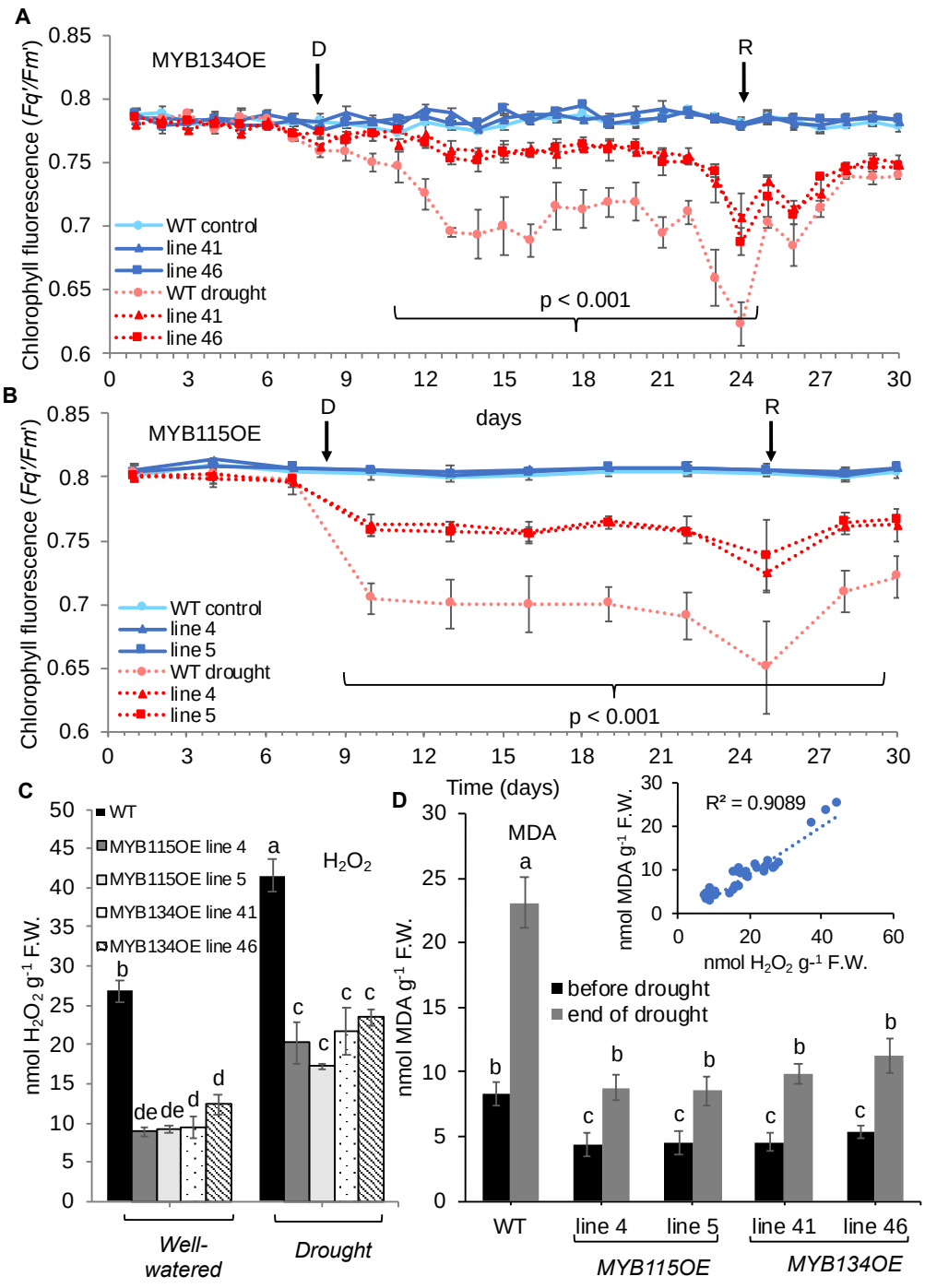

Figure 4.2: Impact of drought on light-adapted chlorophyll fluorescence and ROS content in high-CT transgenics and wild-type plants. (A) and (B) show chlorophyll fluorescence from pre-drought, during drought, and during the recovery period for high-CT MYB134- and MYB115-overexpressing plants, respectively. Red dashed lines correspond to drought-stressed plants and blue solid lines corresponds to well-watered plants. 'D' indicates beginning of drought as seen in stabilizing of plant and pot weight. 'R' indicates beginning of recovery period. Differences between each transgenic line and wild-type are significant after 12 days (A) and 8 days (B) but before recovery period which began on day 25 (A), day 26 (B) (repeated measures ANOVA; $p < 0.001$). (C) H_2O_2 levels for high-CT and wild-type saplings after drought. (D) MDA levels before (black bars) and after (grey bars) drought stress for high-CT and wild-type plants. Letters indicate significant pair-wise differences using Tukey HSD ($p < 0.05$). All data points are the means of four replicate plants for each independent line. Error bars represent SE ($n = 4$).

4.3.3 Reduced foliar CT content makes transgenic poplar more susceptible to oxidative damage caused by drought

Our results with high-CT plants suggested that poplar with a reduced capacity to synthesize CTs should be more susceptible to the effects of oxidative stress caused by drought. We therefore conducted additional drought experiments with a set of previously generated MYB134-RNAi transgenic poplars (Gourlay *et al*., 2019; Chapter 3). After MeJa pre-treatment to induce CTs above baseline levels, plants were subjected to drought stress as above. In these experiments, the onset of drought generally occurred at day 6, and the drought treatment was stopped after 10-12 days because the MYB134-RNAi plants were more sensitive to drought and had lost more than 15 leaves. All drought-treated plants showed reduced size, low stomatal conductance, and low rates of CO_2 assimilation and transpiration compared to well-watered controls (Supplemental Figure 4.4, 4.5).

Chlorophyll fluorescence measurements showed that the MYB134-RNAi transgenics had a greater reduction in *Fq'/Fm'* than wild-type under drought, a trend which continued through to the recovery period (Figure 4.3A). MYB134-RNAi plants were clearly more susceptible to drought than wild-type controls, although the difference to wild-type was less pronounced than MYB134 overexpressors. To test if the PSII damage in the MYB134-RNAi plants correlated with ROS, both H_2O_2 and MDA were quantified. Under drought stress, three out of the four independently transformed low-CT lines had significantly higher H_2O_2 concentrations than wild-type, whereas under well-watered conditions, only line 3 had significantly elevated H_2O_2 concentrations (Figure 4.3B). Prior to the drought stress, there was no difference in MDA concentrations among the different lines, but following drought stress, all four RNAi lines had significantly higher MDA concentrations than wild-type (Figure 4.3C). Again, we observed a strong correlation between H_2O_2 and MDA content. However, the correlation was weaker in the RNAi lines than high-CT plants, likely due to the smaller difference in CT concentrations to wild-type plants. These data suggest that damage to PSII in the MYB134-RNAi low-CT transgenics could be the result of greater ROS accumulation and oxidative damage relative to wild-type.

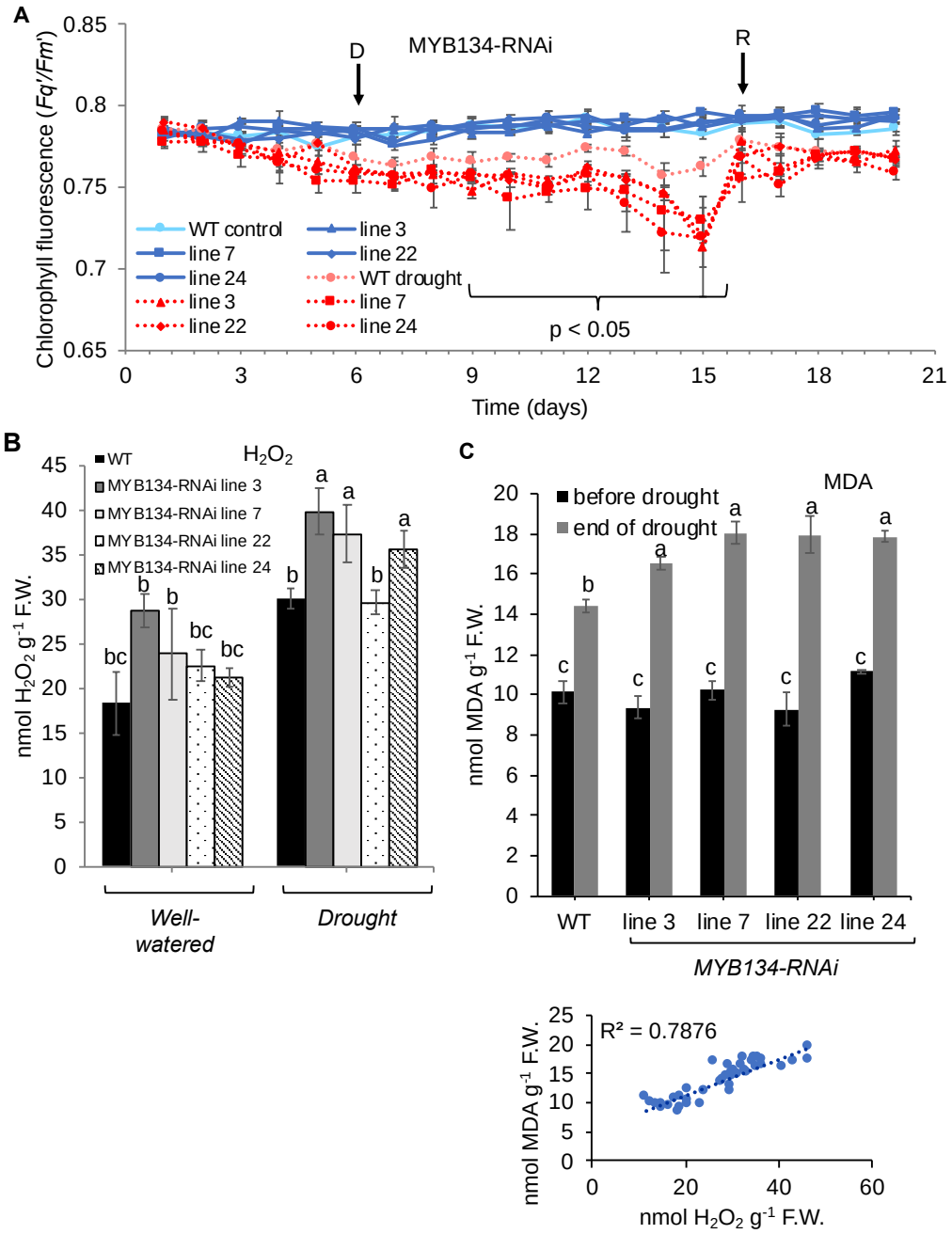

Figure 4.3: Impact of drought on light-adapted chlorophyll fluorescence and ROS of low-CT MYB134-RNAi and control plants. (A) Chlorophyll fluorescence from pre-drought, during drought, and during the recovery period for low MYB134-RNAi and wild-type plants. Red dashed lines correspond to drought-stressed plants and blue solid lines corresponds to well-watered plants. 'D' indicates beginning of drought as seen in stabilizing of plant and pot weight. 'R' indicates beginning of recovery period. Differences between each transgenic line and wild-type are significant after 10 days up to the recovery period at day 16 (repeated measures ANOVA; $p < 0.05$). (B) H_2O_2 levels for low-CT and wild-type saplings after drought. (C) MDA levels before (black bars) and after (grey bars) drought stress for low-CT and wild-type plants. Correlation between MDA and H_2O_2 levels is shown sub-graph. Letters indicate significant pair-wise differences using Tukey HSD ($p < 0.05$). Data points are the means of four replicate plants for each independent line. Error bars represent SE ($n = 4$).

4.3.4 Leaf necrosis is inversely proportional to CT content in transgenic poplar plants

In addition to better physiological performance of the high-CT transgenics, we observed reduced leaf necrosis during drought stress (Figure 4.4). Leaves were defined as showing necrosis if they showed a distinct zone of brown tissue along the leaf lamina edge. Severity of necrosis was quantified by the number of new necrotic leaves appearing per week. This parameter was inversely proportional to CT concentration. High-CT transgenic poplar saplings had fewer necrotic leaves develop during drought stress than wild-type plants (Figure 4.4C). Similarly, the high-CT transgenics needed between 17 and 27 days to show any necrosis on leaves, whereas wild-type required only 10 days (Supplemental Figure 4.6). Overall, under similar conditions, high-CT plants were clearly slower to show visible effects of the drought stress compared to the wild-type plants.

In the MYB134-RNAi experiments, the CT concentrations were 4-5-fold lower compared to the wild-type. This compared to a 50-fold increase in CT content in MYB over-expressors compared to wild-type. This could explain why some effects observed were less pronounced between MYB134-RNAi transgenic lines and wild-type. For example, the number of days before visible symptoms of necrosis were similar for wild-type and all four MYB134-RNAi lines (Supplemental Figure 4.6). However, the severity of the necrosis was greater in the MYB134-RNAi lines, which had more necrotic leaves per week of drought than wild-type (Figure 4.4D). In general, the greater the leaf CT concentration, the less necrosis was observed for each experiment.

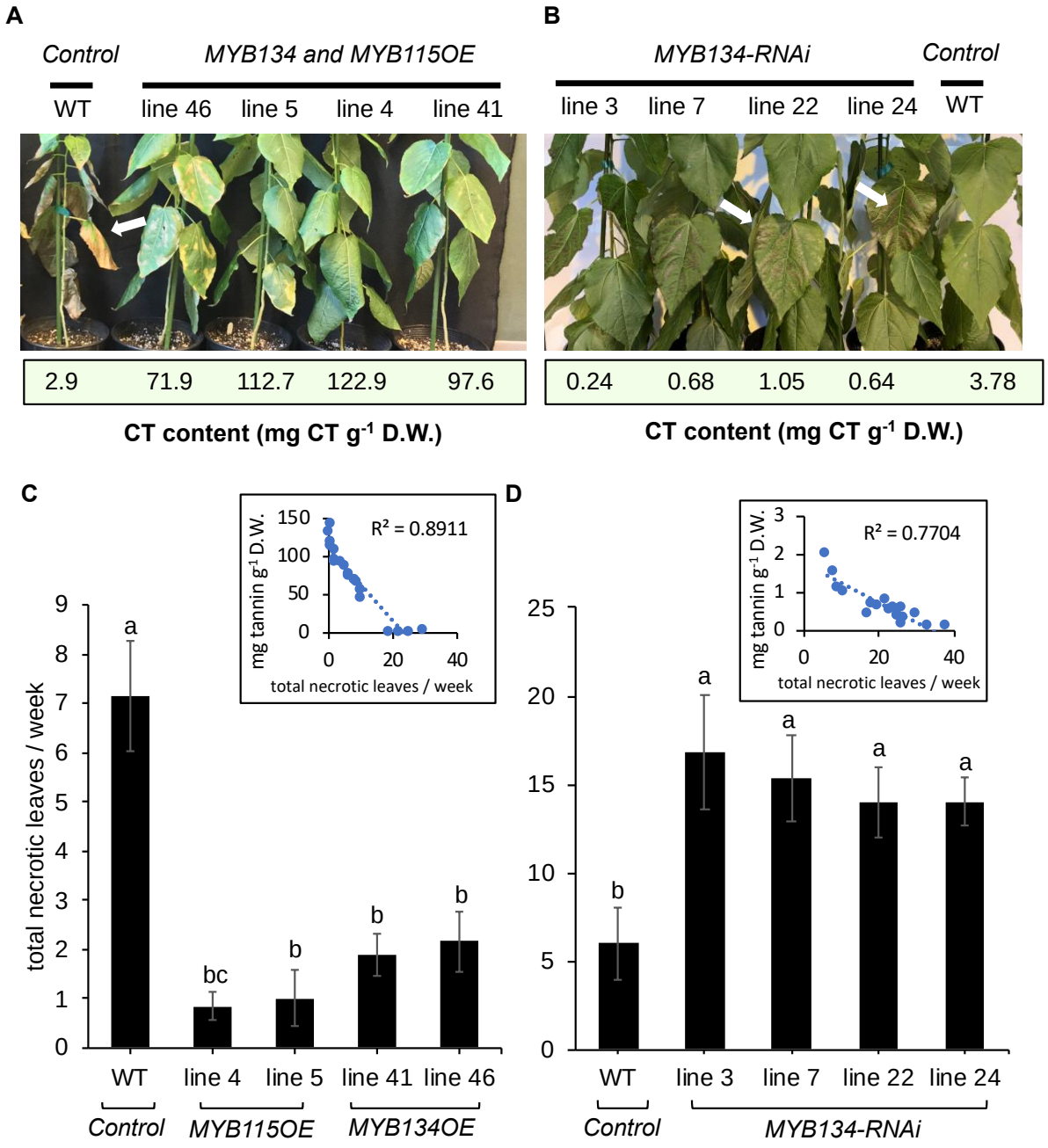

Figure 4.4: CT content reduces necrosis development during drought stress. Top panels show representative images of necrosis on leaves of high-CT following three weeks of drought (A) and RNAi-suppressed low-CT transgenics following ten-days of drought (B) compared to wild-type after drought. Corresponding CT concentrations are shown below each plant. The total number of necrotic leaves per week of drought are visible in panel (C) for high-CT transgenics and panel (D) for low-CT transgenics. Letters indicate significant pair-wise differences using Tukey HSD ($p < 0.05$). All data points are the means of four replicate plants of each independent line. Error bars represent SE (n = 4).

4.3.5 Impact of UV-B exposure on plant growth, photosynthetic parameters, and phenolic compounds on MYB134-overexpressing and wild-type plants

We next exposed high-CT transgenic plants to UV-B light, in order to determine if CTs can protect poplar leaves against oxidative conditions caused by a different stress. These experiments were carried out in custom-built sun simulation environmental chambers; due to logistical constraints of transporting plant material, only the MYB134 overexpressor lines were used for these experiments. We first corroborated the effects of UV-B exposure on MYB134 transcript abundance and CT content in wild-type plants. Consistent with previous observations (Mellway *et al*., 2009), we observed a strong increase in MYB134 transcript abundance as well as a 5-fold increase in CT levels after two weeks of UV-B exposure (Figure 4.5), indicating a clear response to UV-B. No induction of CTs was found in either of the high-CT transgenic lines, which already had very elevated CT levels (Figure 4.5). We also observed a slight increase in anthocyanin and flavonol content in younger leaves for both transgenics and controls, but only flavonols were significantly higher in mature leaves (Figure 4.6). Isoprene emission rates, which are often affected by high temperature and strong light, were not significantly affected by UV-B exposure (Supplemental Figure 4.7). Interestingly, high CT transgenics emitted less isoprene than wild-type plants.

We observed no effect of UV-B on growth, and no significant differences in plant height or stem diameter between wild-type or high-CT lines (Supplemental Figure 4.8 A, B). Stem diameter appeared to be slightly lower in both line 41 and line 46 compared to wild-type, irrespective of treatment, but this difference was not significant. There were also no differences in lamina length between different transgenic lines or in response to UV-B (Supplemental Figure 4.8 C, D). Photosynthetic rate and water use efficiency were not affected by UV-B exposure, but transpiration rate and stomatal conductance showed a slight decrease under UV-B stress (Supplemental Figure 4.9). However, there were no differences between the transgenic lines and the wild-type, and both showed similar responses to UV-B.

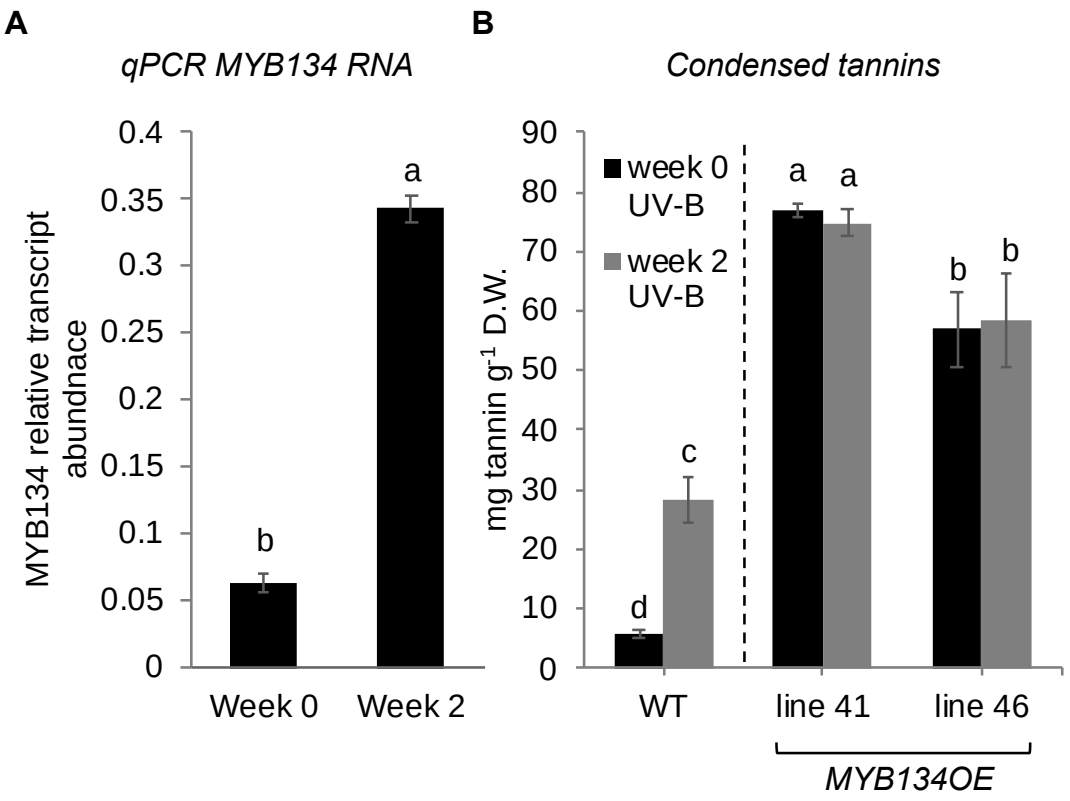

Figure 4.5: Impact of UV-B on MYB134 transcript levels and condensed tannins in wild-type plants. After UV-B exposure for two weeks, plants were assayed for MYB134 transcript abundance from wild-type using qPCR (A) and CTs (B). qPCR values are normalized with elongation factor 1β and ubiquitin. Two high-CT lines (line 41 and line 46) were used in these experiments against wild-type. Letters indicate significant pair-wise differences using Tukey HSD ($p < 0.05$). Data points are the means of six biological replicates. Error bars are SE ($n = 6$).

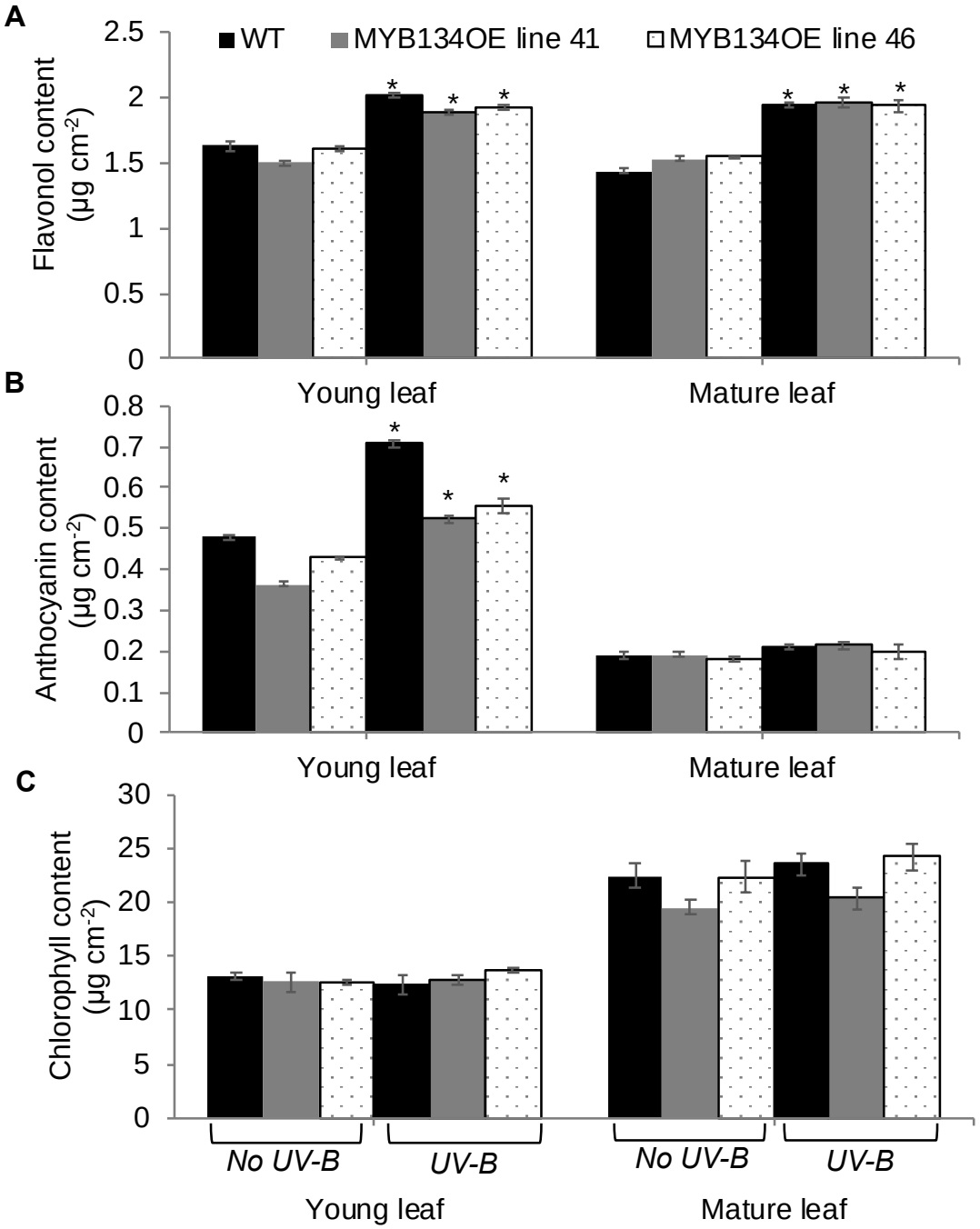

Figure 4.6: Effect of a two-week UV-B exposure on chlorophyll, flavonol, and anthocyanin content of wild-type and high-CT MYB134-overexpressing plants. (A) Flavonol content in poplar leaves as measured using a Dualex (outlined under Materials and Methods). (B) Anthocyanin content in poplar leaves. (C) Chlorophyll content in poplar leaves. Asterisks correspond to significantly different levels than non-UV-B conditions (two-way ANOVA; $p < 0.01$). Data points are the means of six biological replicates. Error bars are SE ($n = 6$).

4.3.6 High CT content protects leaves against photosystem damage by UV-B

Plants grown in sun simulation chambers under visible light without UV-B showed relatively stable chlorophyll fluorescence measurements for both light-adapted (*Fq'/Fm'*) and dark-adapted (*Fv/Fm*) parameters throughout the 2-week experimental period (Figure 4.7). However, wild-type plants grown with UV-B showed a dramatic reduction in fluorescence for both parameters, falling from 0.78 at the beginning to around 0.7 by the end of the experiment. By contrast, no reduction in chlorophyll fluorescence was observed in high CT transgenics under UV-B (Figure 4.7A). This indicated that the high-CT transgenics were less susceptible to the damaging effects of UV-B than the wild-type. The same effect was seen using both *Fq'/Fm'* and *Fv/Fm,* and in both cases only the wild-type showed a decrease in fluorescence due to UV-B exposure (Figure 4.7B). Thus, our data for both light- and dark-adapted fluorescence parameters indicated that high CT plants retained greater PSII function during UV-B stress.

As observed for drought stress, quantification of H_2O_2 in poplar leaves after the UV-B experiment demonstrated a lower H_2O_2 content in the high-CT transgenics, compared to wild-type. The effect was observed with or without UV-B. Although the UV-B did induce higher H_2O_2 levels in the high-CT transgenics, the increase was greater in wild-type plants (Figure 4.7C). Likewise, the wild-type leaves had significantly higher levels of MDA, a biomarker for oxidative damage, compared to the high-CT transgenics (Figure 4.7D). In both transgenic and wild-type plants, MDA levels increased following UV-B stress. In general, the increase in H_2O_2 and MDA after UV-B stress matched the significant reduction in PSII function observed using both *Fq'/Fm'* and *Fv/Fm* in wild-type plants (Figure 4.7).

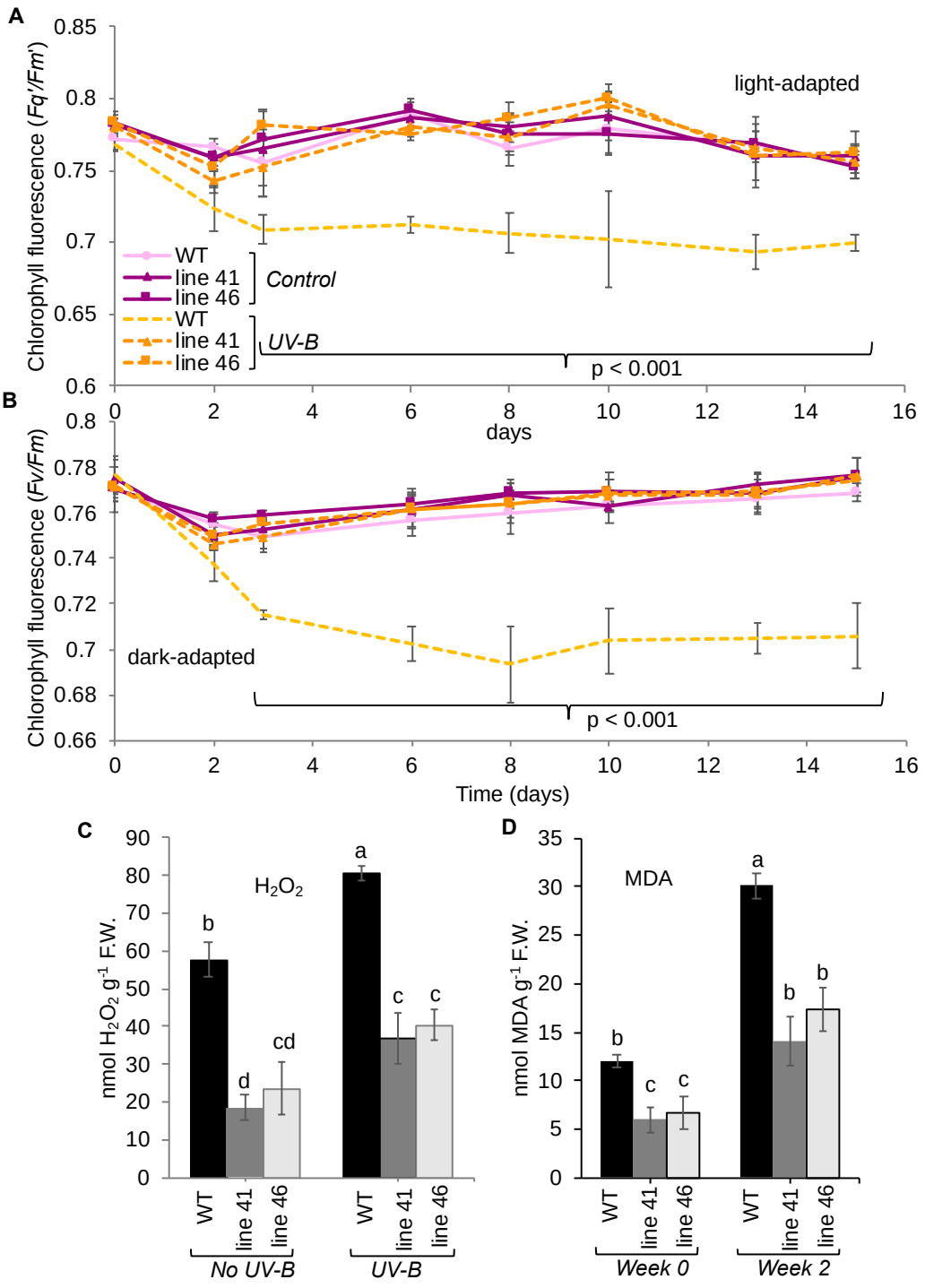

Figure 4.7: Reduced impact of UV-B on chlorophyll fluorescence, MDA, and H_2O_2 content in high-CT transgenics compared to wild-type poplar. (A) and (B) show chlorophyll fluorescence during UV-B exposure between high-CT transgenic and wild-type poplar using *Fq'/Fm'* or *Fv/Fm*, respectively. Wild-type under UV-B exposure had significantly reduced PSII quantum yield when compared to the high-CT transgenics (repeated measures ANOVA; $p < 0.001$). (C) H_2O_2 and (D) MDA levels were assayed from fresh leaf tissue as outlined in the Methods. Letters indicate significant pair-wise differences using Tukey HSD ($p < 0.05$). Data points are the means of six biological replicates. Error bars are SE (n = 6).

4.4 Discussion

4.4.1 CT content in poplar leaves correlates with reduced PSII damage and lower H_2O_2 and MDA content after several ROS-producing stresses

The *in vitro* antioxidant activity of CTs suggests they may contribute to abiotic stress resistance *in vivo*, but this has never been tested directly. Here, we used a combination of transgenic poplar with elevated (MYB134OE, MYB115OE) and suppressed (MYB134-RNAi) CT levels to demonstrate that CTs act as *in planta* antioxidants to counteract oxidative stress during drought and UV-B exposure. Our data with high-CT transgenics during both drought and UV-B stress experiments demonstrated lower accumulation of H_2O_2, less oxidative damage as indicated by MDA content, and reduced PSII damage. Conversely, MYB134-RNAi with suppressed CT synthesis showed the opposite pattern for all parameters. Together with our previous work showing that high-CT plants are more resistant to methyl viologen, an oxidative stress-producing herbicide (Gourlay and Constabel, 2019; Gourlay *et al.,* 2019), our data clearly demonstrate that CTs have the capacity to act as general *in vivo* antioxidants in response to stresses that lead to ROS accumulation.

The mechanism by which CTs can reduce oxidative stress and damage has not yet been elucidated (but see below); however, the strong correlation with H_2O_2 levels and MDA accumulation during very different types of stresses suggests that their antioxidant capacity is involved. We only measured H_2O_2, as this is the most stable and easily assayed ROS; in previous work, however, superoxide was also reduced in high-CT plants under oxidative stress (Gourlay and Constabel, 2019). Similar to our work, Yildirim and Kaya (2017) found a greater increase in H_2O_2 content in drought-sensitive genotype of *Populus nigra* compared to moderately resistant or resistant genotypes. Likewise, a negative correlation between MDA content and chlorophyll fluorescence with drought severity was previously observed in *Populus x euramericana* (Liang *et al*., 2019). MDA is generally used as a measure of lipid peroxidation and a marker for damage to lipids by ROS (Farmer and Mueller, 2013). Importantly, the observation that distinct stresses that cause different types of cellular damage but all lead to enhanced ROS production suggest that it is the antioxidant capacity of CTs that is a key factor. The fact that CT-suppressed RNAi

plants showed the same correlation but in the opposite direction provides additional support for this idea.

4.4.2 Both dark- and light-adapted fluorescence parameters can detect differences in damage to PSII in high-CT and wild-type plants

A primary effect of drought stress is the generation of ROS which causes damage to photosystem membranes (Smirnoff, 1993), the effects of which can be detected by chlorophyll fluorescence. When we monitored *Fq'/Fm'*, a measure of quantum yield in PSII and indicator of the amount of light used for photochemistry (Murchie and Lawson, 2013), we observed a clear and severe reduction in chlorophyll fluorescence in wild-type compared to high-CT transgenics (Figure 4.2A, B). Conversely, low-CT MYB134-RNAi plants were more susceptible to drought stress and showed a greater reduction in *Fq'/Fm'* than the wild-type (Figure 4.3A). Despite very clear effects on *Fq'/Fm'*, we could not detect any impact of drought on *Fv/Fm* as we did for UV-B stress. *Fv/Fm* is a dark-adapted parameter, and reflects the maximum amount of light photosystem II can absorb and effectively utilize for photochemistry. This parameter appears to be less sensitive to drought than *Fq'/Fm'*; one explanation is that ROS are generated only indirectly by drought stress (Cruz de Carvalho, 2008; Miller *et al.,* 2010). Therefore, the negative impacts of drought using dark-adapted parameters (*Fv/Fm*) may only be detectable under extreme stress (Kalaji *et al*., 2017). Our data is consistent with previous observations on willow leaves, where neither a slow 7-day drought nor a quick dehydration produced significant changes in *Fv/Fm* (Ögren, 1990). In rice plants stressed with polyethylene glycol (PEG) to simulate osmotic and drought stress, *Fv/Fm* values were unchanged except at the highest concentration of PEG and under elevated temperatures, whereas *Fq'/Fm'* decreased under all levels of the stress (Wada *et al.*, 2019). By contrast, in other plants such as *Quercus petraea, Fv/Fm* is observed to be more readily affected by drought (Epron *et al*., 1992). In the hybrid *Populus x euramericana* "Neva", both *Fv/Fm* and *Fq'/Fm'* were reduced by drought stress (Liang *et al*., 2019). This poplar hybrid is known to be drought-susceptible, whereas the poplar we used in our work (*Populus tremula x P. tremuloides*), is considered to be more drought tolerant (Dickmann, 2001); this may explain why *Fv/Fm* was not affected in our drought experiments.

Unlike drought stress, in the UV-B experiments the negative effects of this stress on wild-type plants were clearly seen with both fluorescence parameters, and both parameters were clearly reduced in UV-B-exposed wild-type poplar plants (Figure 4.7). This difference could reflect distinct mechanisms by which damage is caused to PSII by UV-B and by drought (Kataria *et al.,* 2014; Czégény *et al*., 2016). Under drought, ROS are generated as a secondary effect of cellular dehydration and stomatal closure (Cramer *et al*., 2011). As membrane stability is weakened under dehydration, electrons are diverted to oxygen from the electron transport chain, which generates ROS in close proximity to the photosystems (Smirnoff, 1993). In addition, when stomata are closed, the reduced ability of leaves to fix carbon leads to a build-up of excitation energy which can generate superoxide (Cruz de Carvalho, 2008). By contrast, UV-B directly impacts the photosystem reaction centres and their corresponding protein complexes, leading to ROS such as singlet oxygen at the oxygen-evolving complex (Foyer *et al.,* 1994; Asada, 2006; Czégény *et al.,* 2016). Further ROS production by UV-B-damaged photosystems results from leakage of electrons from photosynthetic electron transport (Takahashi and Badger, 2011). The effect of UV-B stress on both fluorescence parameters was also observed in *Arabidopsis* Davey *et al.* (2012) where UV-B exposure leads to reductions in both *Fv/Fm* and *Fq'/Fm'*, and that this was more pronounced in the *uvr8* UV-photoreceptor mutant. In beech leaves exposed to UV-B (8.61 kJ m^{-2} day^{-1}), *Fv/Fm* was negatively impacted when compared to leaves in control conditions (Zeuthen *et al.,* 1997). An even greater decrease in *Fv/Fm* was observed when a combination of UV-B and ozone was used on the beech leaves, suggesting that plants experiencing more than one stress suffer more severe negative effects (Zeuthen *et al.,* 1997). In *Populus x canadensis* under UV-A, a decrease in *Fq'/Fm'* with increasing UV-A concentrations (up to 120 W m^{-2} for 100 minutes) was observed (Pallozzi *et al*., 2013). However, dark-adapted parameters were not measured (Pallozzi *et al.,* 2013).

Despite the clear effect of UV-B on wild-type poplar plants, the high-CT transgenics showed no visible reduction in chlorophyll fluorescence, and both *Fq'/Fm'* and *Fv/Fm* time course profiles were indistinguishable from those for wild-type plants under non-UV-B conditions (Figure 4.7). This suggests that PSII was completely protected from detectable UV-B damage in high CT transgenics. This was contrasted by the partial reduction in fluorescence in

the transgenics under drought stress, which indicates at least partial, but not complete protection from PSII damage. These differences could again reflect the distinct mechanisms by which the two stress conditions generate ROS, as described above, with UV-B impacting the photosystems more directly than drought stress. CTs may additionally help to protect against UV-B by absorbing UV-B directly and preventing it from penetrating into the leaf (Czégény *et al*., 2016). We previously showed that in MYB134-overexpressing poplars, CTs accumulate in the upper epidermis of leaves (Mellway *et al.,* 2009). Since chlorophyll fluorescence is measured in the palisade cells located directly below the upper epidermis (Kalaji *et al.,* 2017), these cells in particular might be protected from UV-B. Flavan-3-ols, the precursors to CTs, absorb in the UV-B range and can act as optical filters in plants (Burchard *et al.,* 2000; Huvaere and Skibsted, 2015).

Nevertheless, both wild-type and high-CT plants clearly experienced sufficient UV-B to induce similar concentrations of foliar anthocyanins, a common response to UV-B (Gould, 2004). Furthermore, MDA and H_2O_2 levels in the high-CT transgenics increased in response to UV-B, indicating that cellular damage and lipid peroxidation had occurred. This suggests that a significant amount of UV-B had penetrated the epidermal layers; we propose that CTs could have dual roles against UV-B, by absorbing these wavelengths directly, and by scavenging ROS that is produced by UV-B damage.

4.4.3 A broad role for flavonoids and secondary metabolites in abiotic stress tolerance

The importance of flavonoids in abiotic stress resistance has become more widely appreciated in recent years. Flavonols, flavones, and anthocyanins are known to be effective screens against UV-B (Li *et al*., 1993; Gould, 2004; Treutter, 2006; Petrussa *et al.*, 2013). Indeed, we observed a minor induction of anthocyanins and flavonols in response to the UV-B treatment. In addition, anthocyanins act as filters to visible wavelengths and protect photosystems from overexcitation during early leaf development and senescence (Gould, 2004). Recently, *in planta* antioxidant effects of anthocyanins were reported (Nakabayashi *et al.,* 2014; Li *et al.,* 2017). *Arabidopsis* transgenics with high levels of anthocyanins accumulated less H_2O_2 and were less susceptible to drought stress and methyl viologen (Nakabayashi *et al.,* 2014). Anthocyanins were likewise

shown to be effective in scavenging ROS generated by two other abiotic stresses, excess light and cold stress (Xu *et al.,* 2017). Anthocyanins, like flavan-3-ols and CTs, contain an ortho-hydroxylated B-ring which is responsible for much of their antioxidant activity (Hagerman *et al.,* 1998). Our work with CTs is the first to demonstrate an antioxidant function for CTs within the plant; this has broad implications, as CTs are the most abundant and widespread type of flavonoid and secondary metabolite.

CTs and anthocyanins are both vacuolar compounds (Hernández *et al.,* 2009; Agati *et al.*, 2012). ROS are produced mostly in the chloroplast and mitochondria (Dat *et al*., 2000), but long-lived ROS such as H_2O_2 diffuse into the vacuole where they can be quenched by CTs and other flavonoids (Agati *et al.,* 2012). H_2O_2 moves freely throughout the cell because it can act as a signaling molecule (Mittler, 2017), but under stress conditions proteins on the vacuole membrane can pull H_2O_2 into the vacuole where it can be quenched by CTs (Agati *et al.,* 2012). CTs can function as antioxidants through single-electron transfer or H-atom transfer (Quideau *et al*., 2011). A second potential mechanism is via iron-chelation: CTs are excellent Fe chelators, and by chelating Fe^{2+} CTs could prevent the Fenton reaction, which generates hydroxyl radicals from the interaction of H_2O_2 with Fe^{2+} (Hernández *et al.,* 2009; Mittler, 2017). Hydroxyl radicals are highly reactive ROS (Demidchik, 2015).

We also measured isoprene, a hemiterpene that is formed in chloroplasts and emitted by poplars under some stress conditions, in particular heat stress. It has been linked to increased stress resistance, but how it acts is not known. During the UV-B treatment, we found no change in isoprene emission rates, similar to results previously been observed for grey poplars (*Populus x canescens* syn. *P. alba x P. tremula*) (Kaling *et al.,* 2015). However, higher production of CTs in our transgenic plants were associated with lower rates of isoprene emission (Supplemental Figure 4.7). This could be due to the greater allocation of carbon to the production of CTs, or other metabolic trade-offs.

4.4.4 Summary

Our work demonstrates a novel role for CTs as antioxidants that help protect poplar against the oxidative effects of drought and UV-B stress. This has implications for tolerance to other ROS-

generating stress conditions, for example cold, heavy metal exposure, and high intensity light. CTs are especially abundant and widespread in trees and woody plants, which typically have long lifespans and are adapted to multiple environmental conditions. It will therefore be important to test the function of CTs as antioxidants in the context of additional stresses that face perennial trees over many seasons.

4.5 Supplemental Material

4.5.1 Supplemental figures

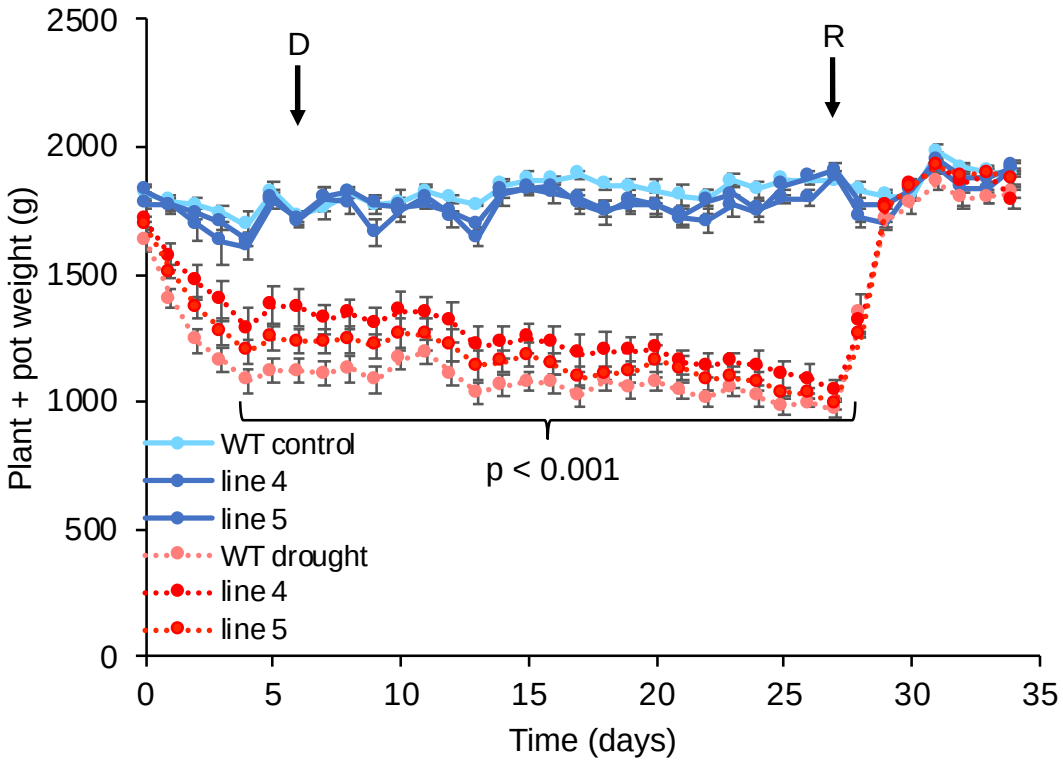

Supplemental Figure 4.1: Plant + pot weight changes for drought experiments using MYB115-overexpressing high-CT transgenics. Change in plant + pot weight during imposition of drought stress (as described under Material and Methods). Blue solid lines corresponds to well-watered plants and red dashed lines correspond to drought-stressed plants. 'D' indicates beginning of drought as seen in stabilizing of plant and pot weight. 'R' indicates beginning of recovery period. There are no statistical differences between wild-type and the transgenics, but the differences between water-treated and drought-stressed are significantly different (two-way ANOVA; $p < 0.001$). Data points are the means of four replicate plants for each independent transgenic line. Error bars represent SE (n = 4).

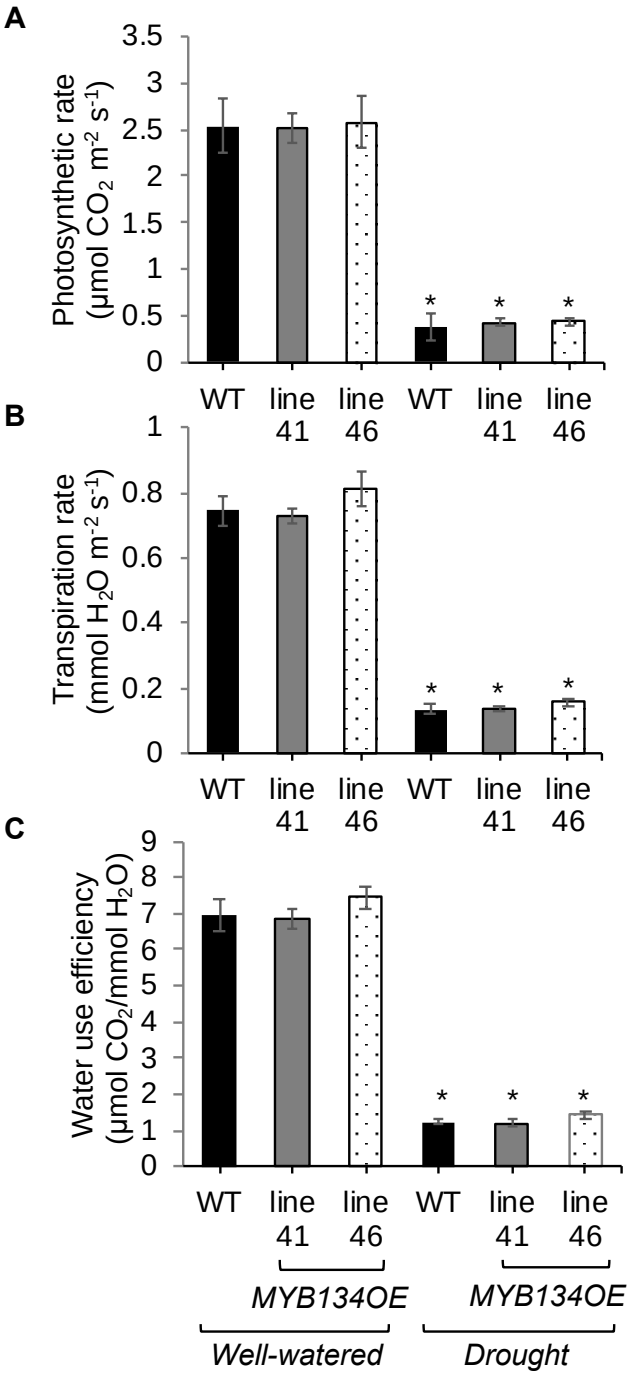

Supplemental Figure 4.2: Effects of drought stress on photosynthetic rate, transpiration rate, and water use efficiency in wild-type and high-CT poplar saplings. (A) Change in photosynthetic rate, (B) transpiration rate, and (C) water use efficiency between well-watered and drought-stressed poplar saplings. Asterisks correspond to significantly different levels than well-watered conditions (t-test; $p < 0.001$); no statistical differences between wild-type or high-CT transgenics in either treatment. Data points are the means of four replicate plants for each independent transgenic line. Error bars represent SE (n = 4).

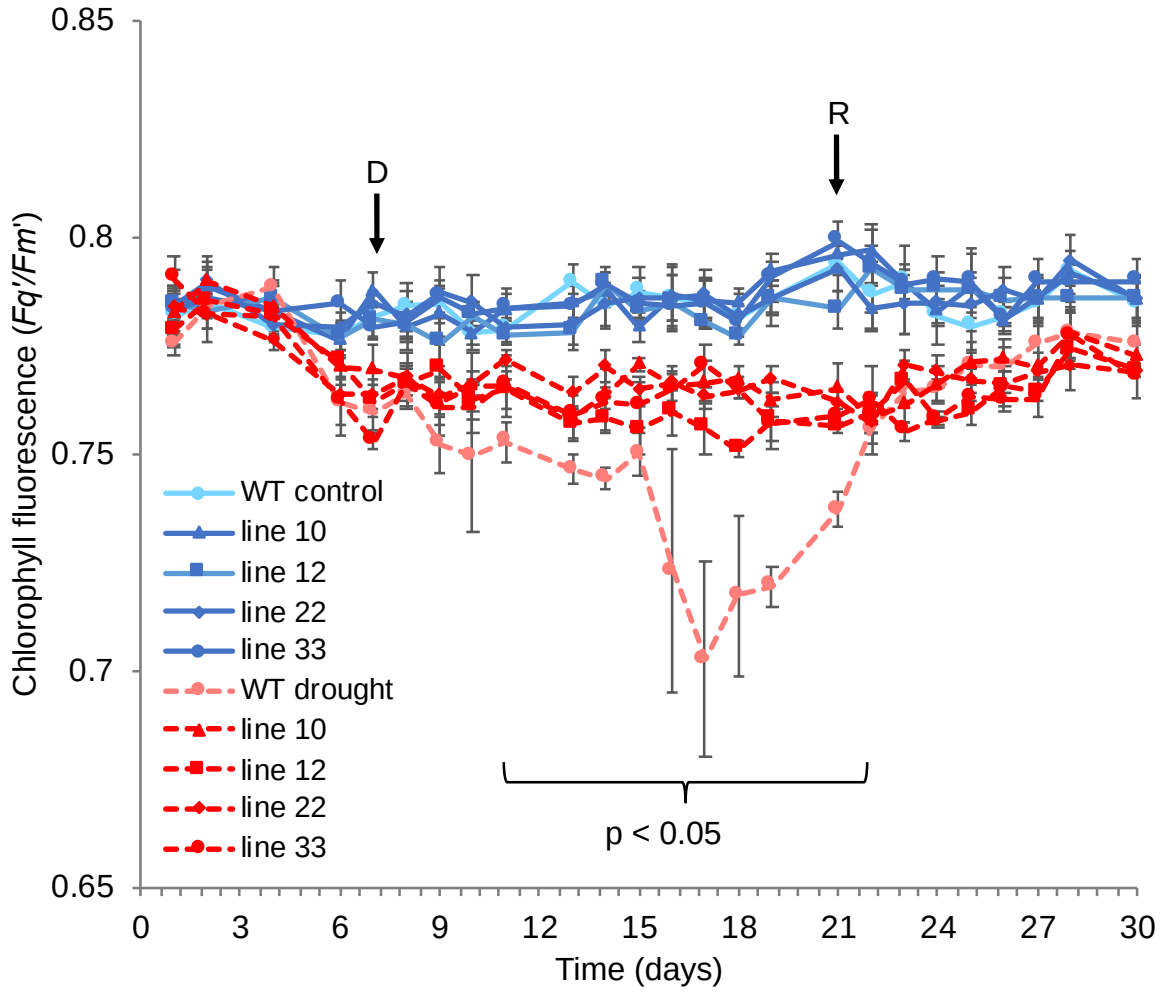

Supplemental Figure 4.3: Effect of drought on high-CT (MYB134-overexpressing) *P. tremula x alba* (clone 717-B4) transgenic poplar. Chlorophyll fluorescence (*Fq'/Fm'*) was measured as outlined in the Methods. Blue solid lines corresponds to well-watered plants and red dashed lines correspond to drought-stressed plants. 'D' indicates beginning of drought as seen in stabilizing of plant and pot weight. 'R' indicates beginning of recovery period. Differences between each transgenic line and wild-type are significant after 11 days up to the recovery period at day 21 (repeated measures ANOVA; $p < 0.05$). Data points are the means of four replicate plants for each independent transgenic line. Error bars represent SE (n = 4).

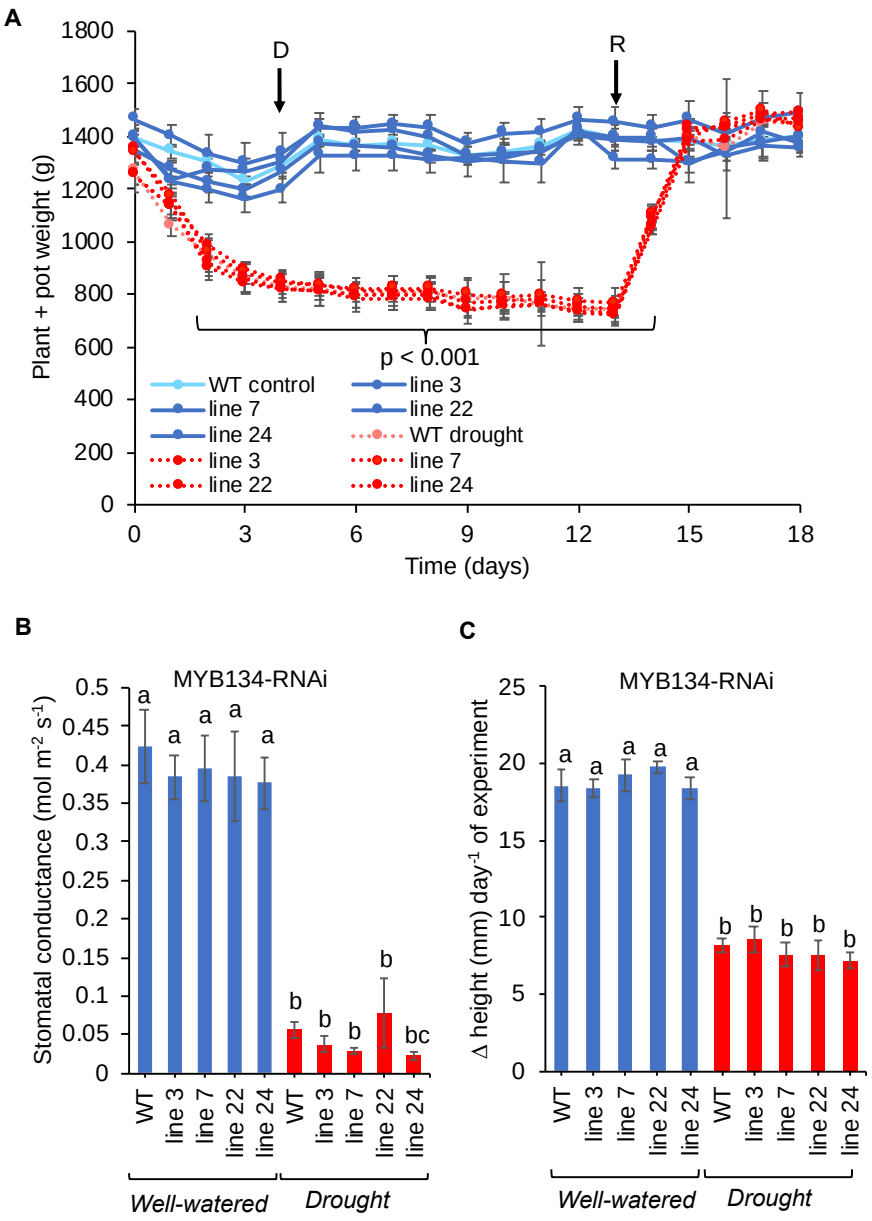

Supplemental Figure 4.4: Time course and impact of drought stress on growth and stomatal conductance of wild-type and low-CT transgenic poplar. (A) Change in plant + pot weight during imposition of drought stress (as described under Material and Methods). Blue colour corresponds to well-watered plants and red colour corresponds to drought-stressed plants. Solid lines are well-watered and dashed lines are drought-stressed. 'D' indicates beginning of drought as seen in stabilizing of plant and pot weight. 'R' indicates beginning of recovery period. (B) Stomatal conductance for low-CT MYB134-RNAi and wild-type poplar saplings after drought. (C) The impact of drought on growth as the change in height between beginning end of the drought experiment for low-CT MYB134-RNAi and wild-type poplar saplings. Letters indicate significant pair-wise differences using Tukey HSD ($p < 0.01$). Data points are the means of four measurements for four replicate plants for each independent transgenic line. Error bars represent SE (n=4).

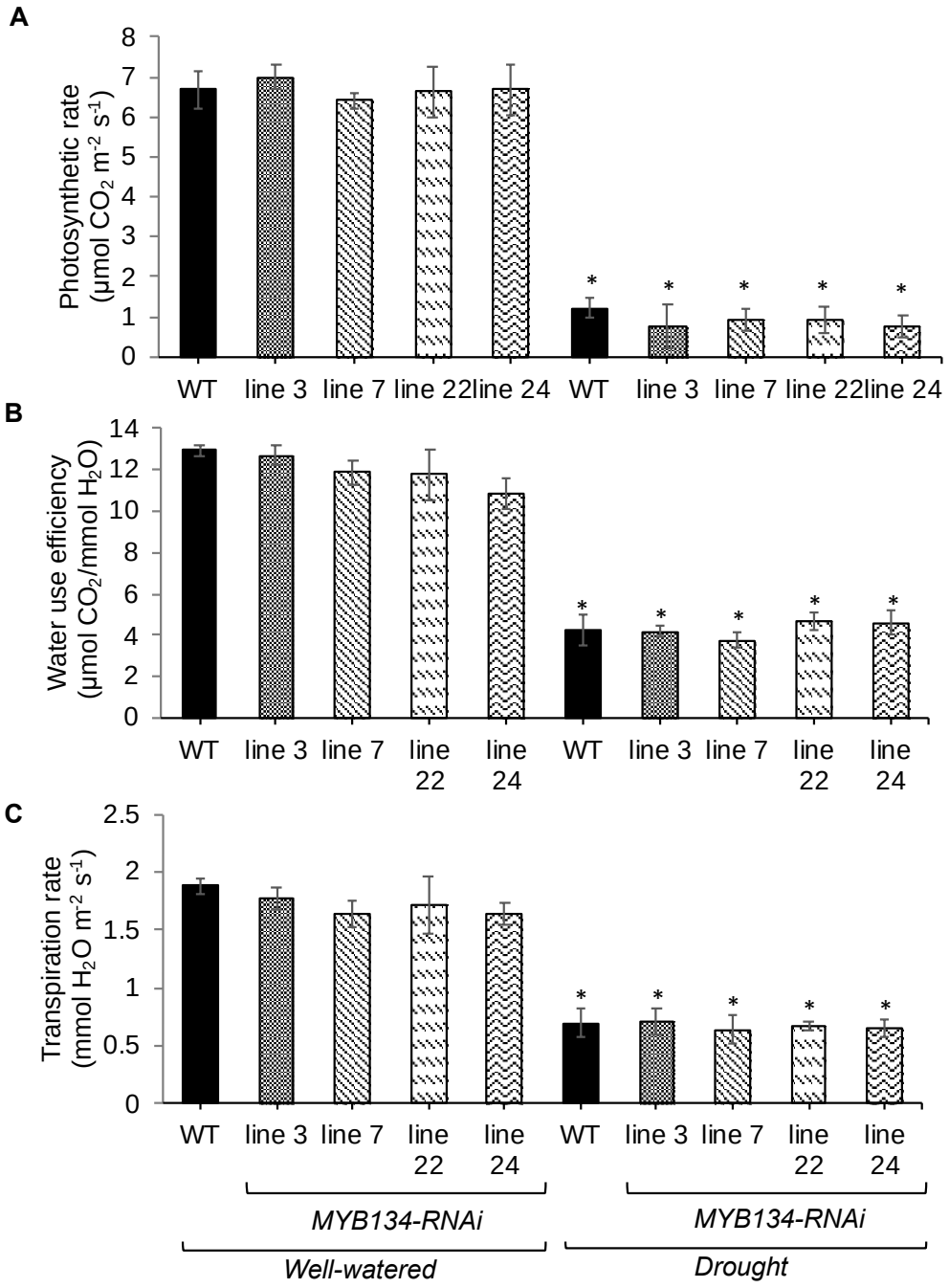

Supplemental Figure 4.5: Effects of drought stress on photosynthetic rate, transpiration rate, and water use efficiency in wild-type and low-CT poplar saplings. (A) Change in photosynthetic rate, (B) transpiration rate, and (C) water use efficiency between well-watered and drought-stressed poplar saplings. Asterisks correspond to significantly different levels compared to well-watered conditions (t-test; $p < 0.001$); no statistical differences between wild-type or high-CT transgenics in either treatment. Data points are the means of four replicate plants for each independent transgenic line. Error bars represent SE (n = 4).

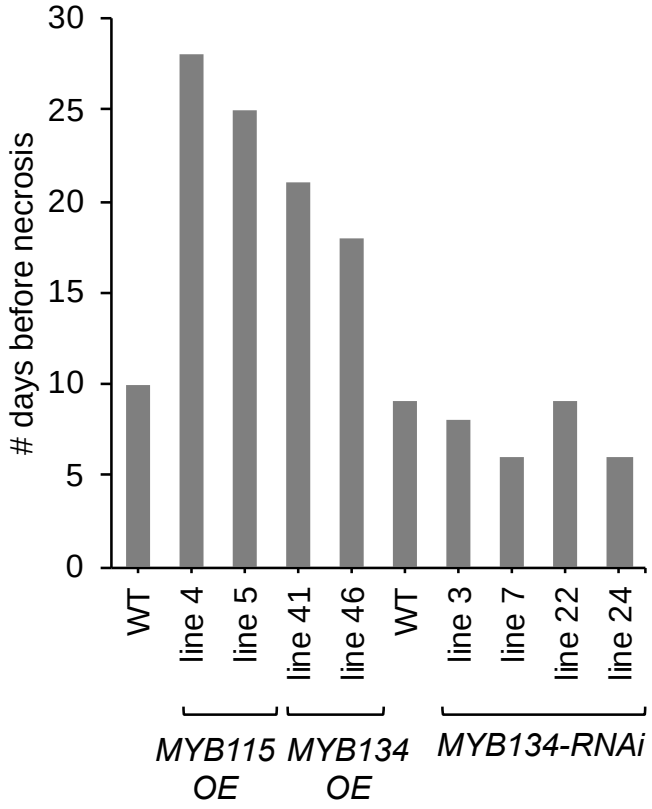

Supplemental Figure 4.6: Impact of drought on appearance of necrotic symptoms in high-CT (OE lines) and suppressed-CT (RNAi) transgenic poplars. The number of days before necrotic symptoms showed on individual plants.

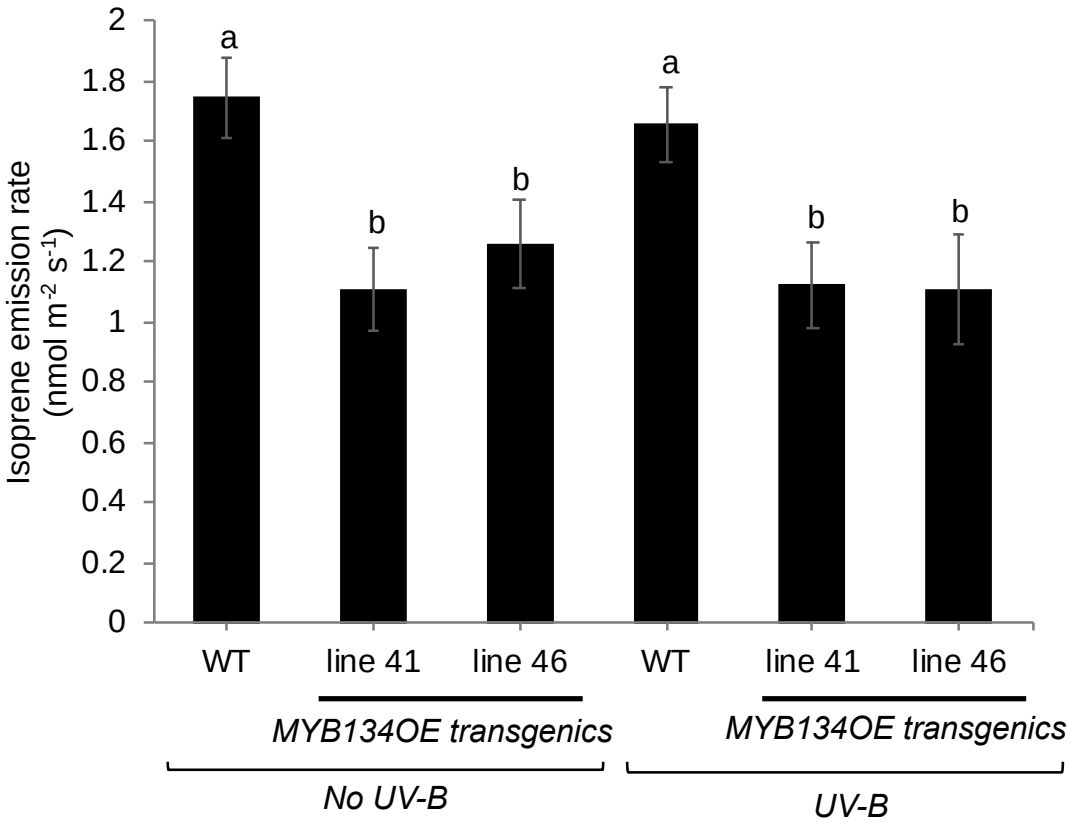

Supplemental Figure 4.7: Isoprene emission rates in high-CT and wild-type poplar plants with and without UV-B exposure. After two weeks of UV-B exposure, isoprene emission rates were measured as described in Material and Methods. Letters indicate significant pair-wise differences using Tukey HSD ($p < 0.05$). Data points are the means six replicate plants for each independent transgenic line. Error bars represent SE (n=6).

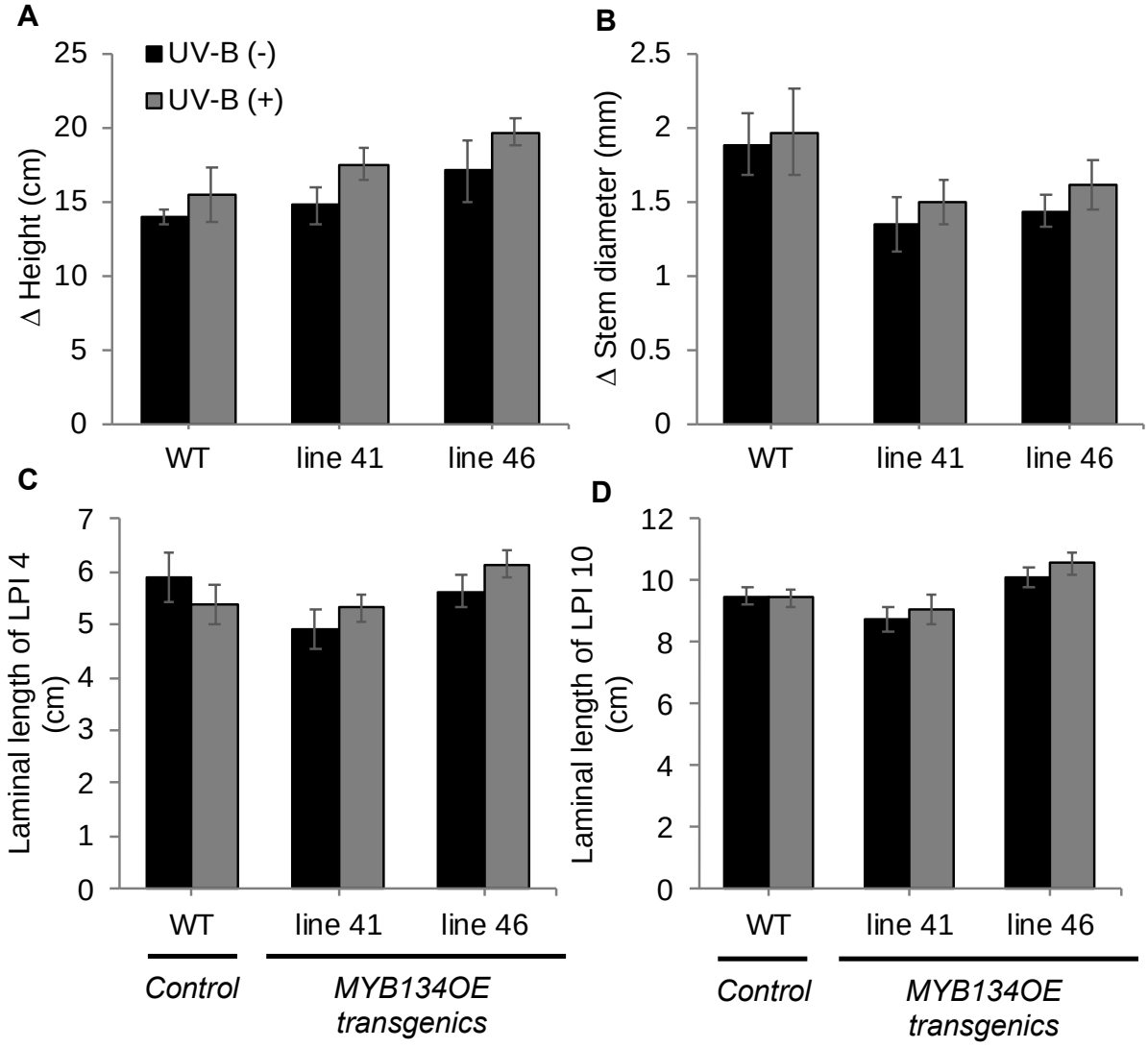

Supplemental Figure 4.8: Effects of UV-B on growth parameters of high-CT MYB overexpressing transgenic and wild-type poplars. (A) and (B) represent the change in height and stem diameter, respectively between time zero measurements and two weeks after UV-B. (C) and (D) are leaf lengths for young and mature leaves, respectively after two weeks UV-B. There are no statistically significant differences between plants treated with or without UV-B, nor between transgenic lines. Data points are the means six replicate plants for each independent transgenic line. Error bars represent SE (n=6).

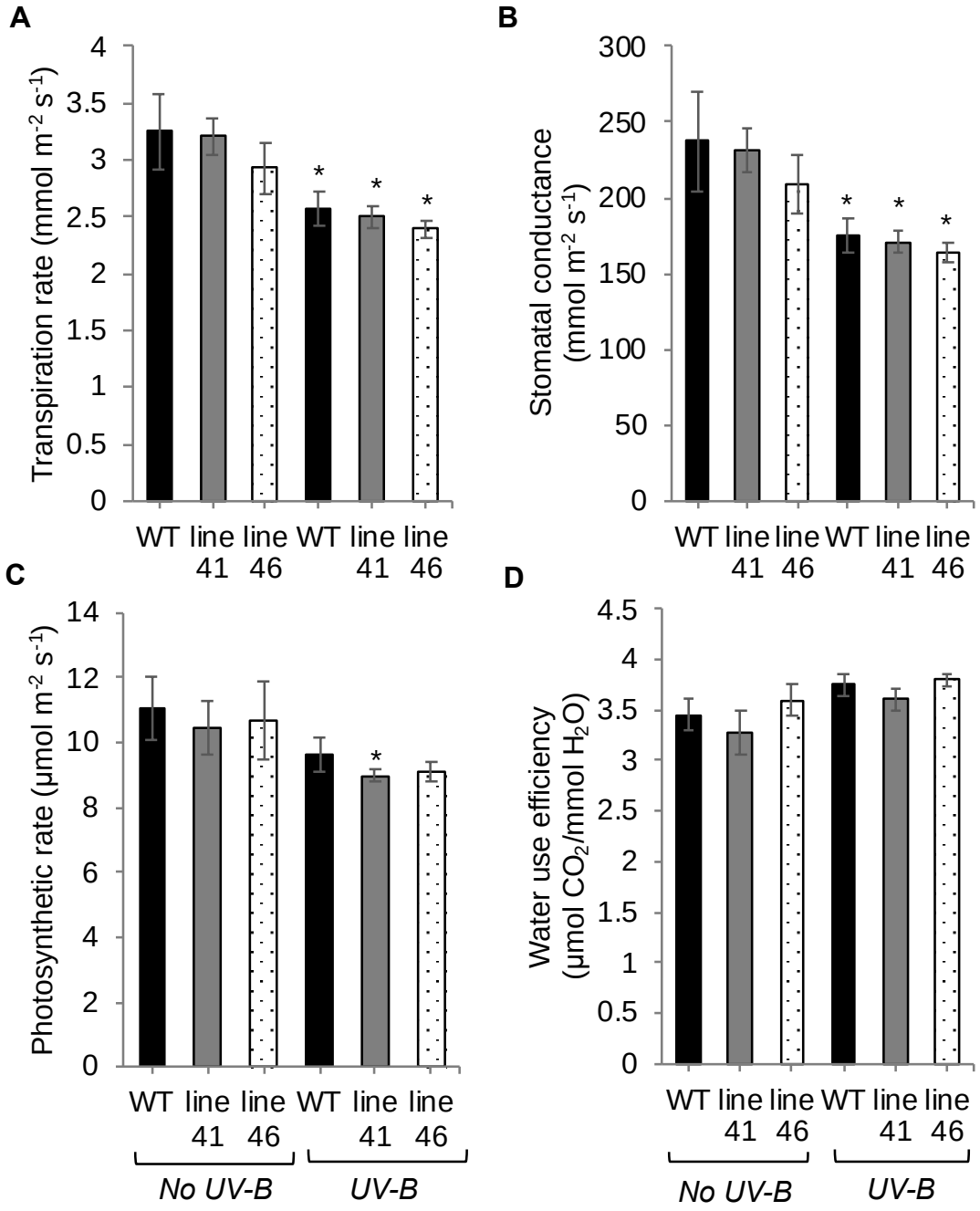

Supplemental Figure 4.9: Effect of UV-B light on photosynthetic parameters and stomatal conductance of wild-type and high-CT poplar saplings. (A) Transpiration rate, (B) stomatal conductance, (C) photosynthetic rate, (D) water use efficiency measured after two weeks UV-B exposure. Asterisks correspond to significant difference between control and UV-B conditions (t-test; $p < 0.05$). There are no differences in any of the parameters between wild-type and the high-CT transgenics in either treatment. Data points are the means six replicate plants for each independent transgenic line. Error bars represent SE (n=6).

Chapter 5 : Overall conclusions

5.1 Summary of major findings

This study aimed to determine if condensed tannins (CTs) function as *in vivo* antioxidants against oxidative stress caused by methyl viologen (MV), drought stress, and UV-B stress. High-CT (MYB134- and MYB115-overexpressing) and low-CT (MYB134-RNAi) poplar lines in the hybrid *Populus tremula x Populus tremuloides* (INRA353-38) were used to investigate tolerance to these different stresses. Chlorophyll fluorescence, hydrogen peroxide (H_2O_2), and malondialdehyde (MDA) levels were measured for each poplar line under each stress. In general, plants with higher CT concentrations were better protected from the stresses. Major findings of this work will be summarized in the following sections.

5.2 CT concentration affects susceptibility to oxidative stress

This research showed that in poplar leaves, the concentration of CTs correlates with overall antioxidant activity (Chapter 2). Utilizing MV, which can generate oxidative stress in a plant, I showed that the high-CT transgenics were more resistant than wild-type (Chapter 2; Gourlay and Constabel, 2019). Using chlorophyll fluorescence, a technique that allows non-invasive assessment of a plant's overall photosystem function (Baker, 2008), I was able to track the relative health of the high-CT plants' photosystems over the course of the experiment. There was a clear difference between the fluorescence levels of the high-CT plants and the wild-type, with the wild-type suffering a greater reduction in chlorophyll fluorescence (Chapter 2; Gourlay and Constabel, 2019). I conclude that the high levels of CTs are responsible for protecting the photosystems of the high-CT transgenics. When I measured H_2O_2 concentrations, one species of reactive oxygen (ROS), I found that the high-CT transgenics had significantly less H_2O_2 under control conditions and following application of MV (Chapter 2; Gourlay and Constabel, 2019). The results of the MV experiments suggest that the high-CT transgenics are better-able to scavenge the ROS generated under MV, and therefore have lower H_2O_2 accumulation and a greater retention of photosystem function (Chapter 2; Gourlay and Constabel, 2019).

Under two different abiotic stresses, drought and UV-B, I saw a similar trend in the high-CT transgenics. Both drought and UV-B impact a plant and generate ROS via different mechanisms (Chapter 4). Results from my work showcase that high-CT plants are better protected from the negative impacts of both stresses, and lower levels of H_2O_2 and MDA (a biomarker of lipid peroxidation; Farmer and Mueller, 2013) are associated with a greater retention of photosystem function (Chapter 4). I thus conclude that the concentration of CTs are an important factor in the maintenance of plant photosystem function and overall tolerance to abiotic stress.

In general, when low-CT transgenic (MYB134-RNAi) plants are exposed to oxidative stress, they exhibit an increase in oxidative damage as seen through increases in H_2O_2 and MDA (Chapter 3 (Gourlay *et al.*, 2019), Chapter 4). Under MV conditions, these low-CT plants have reduced chlorophyll fluorescence and a general increase in H_2O_2 (Chapter 3; Gourlay *et al.*, 2019). When exposed to drought stress, the low-CT plants have a significant impairment in their photosystem coupled with an increase in H_2O_2 and MDA, which is indicative of increased oxidative damage (Chapter 4).

The summary of my work with the high-CT transgenics is that these plants are more tolerant to ROS-producing stresses and oxidative damage. That is partially due to the decrease in ROS and the ability to maintain higher photosystem function than wild-type under the different stresses. The low-CT RNAi plants show an opposite effect, which corroborates the evidence that CTs protect plants under oxidative stress. Therefore, CTs could be important to plant adaptations in natural forest ecosystems.

5.3 Characteristics of CTs as strong antioxidants

It has been previously established that flavonoids such as anthocyanins, CTs, and flavanols, produced from the phenylpropanoid pathway, are very strong *in vitro* antioxidants (Hagerman *et al.*, 1998; Hernández *et al.*, 2009). In fact, many flavonoids are observed to be better *in vitro* antioxidants than well-known antioxidants such as vitamin C (ascorbate) (Hernández *et al.*, 2009; Fini *et al.*, 2011). This is due to the basic flavonoid structure which includes hydroxyl groups arranged in an *ortho* pattern on the B-ring (Hagerman, 2002). Two proposed

mechanisms by which CTs and other flavonoids may function in quenching and scavenging ROS are referred to as single-electron transfer or hydrogen atom transfer (Wright *et al.*, 2001; Quideau *et al.*, 2011). Upon donation of either a hydrogen or an electron, the *ortho* organization of the hydroxyl groups allows the phenolic structure to maintain non-reactivity due to resonance of the B-ring (Rice-Evans *et al.*, 1996; Seyoum *et al.*, 2006). The decoration of compounds, including glycosylation or hydroxylation, and the location of that decoration will affect the overall antioxidant capacity of flavonoids and will factor into which specific ROS will be scavenged (Rice-Evans *et al.*, 1997; Burda and Oleszek, 2001). Free hydroxyl groups in the flavonoid B-ring in 3' position have been shown to contribute *in vitro* to the scavenging ability of flavonoids (Burda and Oleszek, 2001). For overall antioxidant activity and scavenging ability, the number and location of the hydroxyl groups are important (Chen *et al.*, 2002).

The high molecular weight polyphenolic structure of CTs should result in CTs having high antioxidant function. These compounds are among the largest polyphenolics, with polymer sizes between 2-20 (Quideau *et al.*, 2011). CTs have a higher degree of hydroxylation in their structures and this could lead to enhanced overall antioxidant capacity due to more opportunities for ROS scavenging and quenching.

CTs are a mixture of procyanidin and prodelphinidin components; prodelphinidin is trihydroxylated while procyanidin is dihydroxylated. Epigallocatechin (with three hydroxyl groups) has significantly higher antioxidant activity than catechin (with two hydroxyl groups) (Rice-Evans *et al.*, 1997; Wright *et al.*, 2001). In the high-CT transgenics, the CTs have a slightly shifted procyanidin:prodelphinidin ratio compared to wild-type with a higher proportion of prodelphinidin (James *et al.*, 2017). Nevertheless, the large differences in CT concentration between wild-type and the high-CT transgenics may have more impact on overall plant tolerance to stress than the influence of the hydroxylation pattern.

In addition to scavenging and quenching ROS, CTs could function in protecting the plant against ROS by other mechanisms. Utilizing their ability to chelate heavy metals, such as iron (Fe) and copper (Cu), CTs may function as an antioxidant within the plant. In particular, chelating Fe could minimize the occurrence of the Fenton reaction, thus minimizing the production of the most harmful ROS, the hydroxyl radical (Mittler, 2002; Demidchik, 2015). This

would be especially beneficial to plants because the hydroxyl radical participates in chain reactions which continue to produce ROS and lead to even greater damage in plants (Demidchik, 2015).

CTs could also prevent ROS accumulation by serving as UV absorption screens (discussed in Chapter 4). Flavonoids such as anthocyanins and some flavonols are known to function as UV-screens (Hernández *et al.*, 2009), but whether CTs function in this role is not fully explored. This could explain why the high-CT transgenics' chlorophyll fluorescence measurements under UV-B stress were unaffected (Chapter 4). Mellway *et al.* (2009) found that one location where CTs localize in the high-CT plants is the upper epidermis. In that location, they could strongly absorb UV-B photons, preventing too much transmission of UV-B causing further damage.

It has been highlighted that CTs are vacuolar compounds (Agati *et al.*, 2012). The connection between CTs as antioxidants located in the vacuole and the ROS generated under stress in the chloroplasts or mitochondria (Apel and Hirt, 2004) still needs to be discovered. I hypothesize that CTs mitigate creation of ROS such as H_2O_2 which is the most mobile ROS and can cross membranes, potentially diffusing into the vacuole (Dat *et al.*, 2000). The mechanism by which CTs minimize the damaging effects of H_2O_2 in the vacuole could be to chelate Fe and prevent the Fenton reaction which requires both Fe and H_2O_2 to produce the hydroxyl radical (Mittler, 2017). Another possibility is that the polymerization of CTs could play a role in their overall antioxidant activity. For stresses that disrupt membranes directly, localization of CTs is not as important because CTs could come into contact with ROS within the cytosol and exert their function as antioxidants.

5.4 Impacts of my research

My research is the first to connect CTs with tolerance to abiotic stress, and in particular, tolerance through their antioxidant activity and reduction of oxidative damage. Biotic stresses such as herbivory and pathogen attack have been shown to be mitigated by CTs, which serve as feeding deterrents to herbivores (Chapter 1). Although my work has focused primarily on CTs in leaves, many species also synthesize CTs in roots and the antioxidant functions proposed for CTs could be applied to both root and shoot stresses. Oxidative stress in the roots can be

caused by hypoxia, freezing, and salt stress. The function of CTs as *in planta* antioxidants is not restricted only to the stresses outlined in this research, but to other abiotic stresses that generate ROS, such as heavy metal stress. The production of ROS from heavy metals may be an interaction between the metals and oxygen in the cell, or ROS may be produced through the cytotoxic effects of the accumulation of metal ions (Chen *et al.*, 2014; Jiang *et al.*, 2017). Heavy metal stress, in particular from zinc (Zn), cadmium (Cd), lead (Pb), or aluminum (Al) have been shown to increase CT concentrations in the roots of mangrove, *Aegiceras corniculatum*, with CT levels rising from 22 mg g^{-1} D.W. to 40 mg g^{-1} D.W. at the highest concentrations of metals (30 mg/L Zn or 4mg/L Cu) (Guangqiu *et al.*, 2007; Jiang *et al.*, 2017). Although the induction of CTs depends on the heavy metal involved and its concentration (Guangqiu *et al.*, 2007), high CT levels would likely increase plant tolerance to heavy metal stress.

Some heavy metals can replace essential nutrients in signaling proteins and disrupt essential processes like photosynthesis or enzymes that are important for cellular function, thus leading to oxidative stress (Naik *et al.*, 2009). For example, under Zn stress, Pb stress, and the combination stress in *Populus beijingensis* and *Populus cathayana*, both superoxide and MDA levels were elevated (Chen *et al.*, 2014), suggesting enhanced ROS and oxidative damage. CTs could function in scavenging the ROS produced under Zn or Pb stress, and CTs may also function in chelating the heavy metal itself to form complexes. Chelating the heavy metals would lower the overall concentration of those metals within the cell, which could minimize cellular damage and cytotoxicity. For example, aluminum (Al) accumulates in the vacuole within the leaves of plants (Poschenrieder *et al.*, 2008), and since CTs also accumulate in the vacuole, they could help plants tolerate Al stress via chelation or ROS scavenging. When CTs chelate Al, it minimizes overall growth defects in the root system of plants, such as a decrease in root:shoot ratio in biomass and total length, and reduces ROS production (Poschenrieder *et al.*, 2008). Aluminum toxicity may also be mitigated by CTs by Al exclusion at the tips of roots, where cells accumulating CTs act as shields and protecting the inner epidermal cells during their expansion, as in the camphor tree (*Cinnamomum camphora*) (Osawa *et al.*, 2011). If Al complexes with CTs, it would not be easily taken up by the root apices.

Anoxic stress is another stress that generates a large quantity of ROS in plants. When anoxic conditions recede, plants are exposed to oxygen again, and cellular processes resume. This is associated with an increase in ROS (Sairam *et al.*, 2009, 2011). I previously tested the high-CT and wild-type poplar trees under hypoxic conditions (which leads to anoxia) but saw no increase in CTs, most likely due to technical issues with the experimental setup. However, CTs already synthesized by the plants can function as quenchers or scavengers of ROS. Further studies that expand on more specific and carefully controlled hypoxia conditions should be conducted with the high-CT plants.

Salt stress also leads to significant ROS production, as high concentrations of salt cause membrane breakdown and protein denaturation, as well as cytotoxicity due to a buildup of intracellular sodium (Na^+) and chloride (Cl^-) ions (Lutts *et al.*, 1996). High salinity causes ROS to increase, and MDA levels and CT concentrations have been shown to increase in safflower (*Carthamus tinctoriua*) following salt stress, indicating enhanced oxidative damage to the membranes (Abdallah *et al*., 2013). The induction of CTs by salt stress further suggests that these compounds may serve as antioxidants within the plant.

My work has contributed to the understanding of plant strategies of tolerance to abiotic stresses, many of which are known to induce CTs. CTs are important in protection of the plant during abiotic stresses due to their function as antioxidants, either as an ROS scavenger or as an ROS preventer. Even if the stress does not induce CTs, the constitutive levels of CTs in species such as poplar, tea, *Eucalyptus*, and mangroves will function as an additional antioxidant system to help minimize the oxidative damage.

5.5 Future research

Although my work has shown that CTs do function as antioxidants in plants, there are still pressing questions left to be answered. In addition to the suggestions above, future research could work to elucidate CTs particular mechanisms of action as an antioxidant, since every stress is different. CTs mode of action as antioxidants may be associated with cellular Fe, and therefore co-localization studies between Fe and CTs would be illuminating. The location and concentration of Fe may also be a factor in minimizing the frequency of the Fenton reaction,

which lowers the overall ROS concentrations within the cell. Additionally, if ROS such as H_2O_2 make it into the vacuole, CTs could quench and remove the H_2O_2 so it is not available to react with any cellular components. CTs could also function to prevent the stress by chelating heavy metals such as Zn or Al, preventing those compounds from passing further into the roots of plants. Determining how different sizes of CTs (dimers, trimers, polymers) impact the absorption of UV-B pigments will be important in uncovering the role of CTs in protecting plant cells outside of scavenging and quenching, and in particular during stresses that can led to UV damage or photoinhibition. Testing the role of CTs at the root-soil interface with heavy metal toxicity would be interesting to discover the concentration of CTs needed in shield-like cells to effectively complex with the heavy metals in the soil and prevent damage to the cell, as in the camphor tree.

This research has focused on the impacts of CTs as *in planta* antioxidants under oxidative stress generated by MV, drought, and UV-B stress. The observed effects of CTs as antioxidants within the plant may differ in different stresses and the link between CTs and oxidative tolerance have not yet been made in heavy metal stress or anoxic stress. CTs have been proposed to play a role in cellular processes such as senescence (Harding, 2019) where nutrients are re-allocated from the leaves to the plant's stem and roots (Khana-Chopra, 2012). However, senescence is a strong oxidative process due to an increase in ROS production during the break-down of proteins, an increase in lipid peroxidation, and a reduction of antioxidant enzyme activities (Khana-Chopra, 2012; Petrov *et al.*, 2015). ROS can also trigger programmed cell death which assists in the remobilization of nutrients within a plant and is also a part of senescence (Petrov *et al.*, 2015). It is possible that CTs slow down senescence by decreasing the amount of ROS present and thus minimizing oxidative damage to plants during senescence. This would be important to investigate because CTs cannot be broken-down during senescence due to their large polymeric structure (Zhang *et al.*, 2008). In senescing branchlets of mangrove (*Casuarina equisetifolia*), total phenolic levels and protein precipitation capacity was decreased while protein-bound CTs increased, suggesting a role in nutrient cycling within the plant (Zhang *et al.*, 2008). Investigating if elevated CTs lead to reduced oxidative damage and stress during

senescence will be important in forest ecosystems where trees with CTs are prevalent because it may impact forest leaf litter and microbial communities.

In conclusion, my research supports the hypothesis that CTs serve as antioxidants within plants, helping plants tolerate and survive drought and UV-B stress by reducing cellular oxidative stress. This provides persuasive evidence of a new function for CTs in plants.

References

Abdallah S, Rabhi M, Harbaoui F, Zar-kalai F, Lachâal M, Karray-Bouraoui N. 2013. Distribution of phenolic compounds and antioxidant activity between young and old leaves of *Carthamus tinctorius* L. and their induction by salt stress. Acta Physiologiae Plantarum **35**, 1161–1169.

Aebi H. 1984. Catalase *in vitro*. Methods in Enzymology **105**, 121–126.

Agati G, Azzarello E, Pollastri S, Tattini M. 2012. Flavonoids as antioxidants in plants: location and functional significance. Plant Science **196**, 67–76.

Allakhverdiev SI, Feyziev YM, Ahmed A, Hayashi H, Aliev JA, Klimov VV, Murata N, Carpentier R. 1996. Stabilization of oxygen evolution and primary electron transport reactions in photosystem II against heat stress with glycinebetaine and sucrose. Journal of Photochemistry and Photobiology B: Biology **34**, 149–157.

Anders S, Huber W. 2010. Differential expression analysis for sequence count data. Genome Biology **11**, R106.

Apel K, Hirt H. 2004. Reactive oxygen species: metabolism, oxidative stress, and signal transduction. Annual Review of Plant Biology **55**, 373–399.

Aro EM, Virgin I, Andersson B. 1993. Photoinhibition of photosystem II: inactivation, protein damage and turnover. Biochimica et Biophysica Acta **1143**, 113–134.

Asada K. 1999. The water-water cycle in chloroplasts: scavenging of active oxygens and dissipation of excess photons. Annual Review of Plant Physiology and Plant Molecular Biology **50**, 601–639.

Asada K. 2006. Production and scavenging of reactive oxygen species in chloroplasts and their functions. Plant Physiology **141**, 391–396.

Assefa A, Kechero Y, Tolemariyam T. 2017. Antimicrobial activity of condensed tannin extracts from indigenous fodder plants of Gambella region on *Mastitis* pathogens. **11**, 79–82.

Baker NR. 2008. Chlorophyll fluorescence: a probe of photosynthesis *in vivo*. Annual review of Plant Biology **59**, 89–113.

Baker NR, Rosenqvist E. 2004. Applications of chlorophyll fluorescence can improve crop production strategies: an examination of future possibilities. Journal of Experimental Botany **55**, 1607–1621.

Barbehenn R, Constabel C. 2011. Tannins in plant-herbivore interactions. Phytochemistry **72**, 1551–1565.

Barbehenn R, Jaros A, Lee G, Mozola C, Weir Q, Salminen JP. 2009. Tree resistance to *Lymantria dispar* caterpillars: importance and limitations of foliar tannin composition. Oecologia **159**, 777–788.

Barbehenn R, Jones CP, Karonen M, Salminen J. 2006. Tannin composition affects the oxidative activities of tree leaves. Journal of Chemical Ecology **32**, 2235–2251.

Behnke K, Kaiser A, Zimmer I, *et al.* 2010. RNAi-mediated suppression of isoprene emission in poplar transiently impacts phenolic metabolism under high temperature and high light intensities: a transcriptomic and metabolomic analysis. Plant Molecular Biology **74**, 61–75.

Benzie IFF, Strain JJ. 1996. The ferric reducing ability of plasma (FRAP) as a measure of "antioxidant power": the FRAP assay. Analytical Biochemistry **239**, 70–76.

Bittsánszky A, Gyulai G, Humphreys M, *et al.* 2006. RT-PCR analysis and stress response capacity of transgenic gshl-poplarclones (*Populus x canescens*) in response to paraquat exposure. Zeitschrift fur Naturforschung - Section C Journal of Biosciences **61**, 699–703.

Blois M. 1958. Antioxidant determination by use of a stable free radical. Nature **181**, 1199–1200.

Boeckler GA, Gershenzon J, Unsicker SB. 2011. Phenolic glycosides of the Salicaceae and their role as anti-herbivore defenses. Phytochemistry **72**, 1497–1509.

Boeckler GA, Towns M, Unsicker SB, Mellway RD, Yip L, Hilke I, Gershenzon J, Constabel CP. 2014. Transgenic upregulation of the condensed tannin pathway in poplar leads to a dramatic shift in leaf palatability for two tree-feeding *Lepidoptera*. Journal of Chemical Ecology **40**, 150–158.

Bogeat-Triboulot M-B, Brosche M, Renaut J, *et al.* 2007. Gradual soil water depletion results in reversible changes of gene expression, protein profiles, ecophysiology, and growth performance in *Populus euphratica*, a poplar growing in arid regions. Plant Physiology **143**, 876–892.

Bogs J, Downey MO, Harvey JS, Ashton AR, Tanner GJ, Robinson SP. 2005. Proanthocyanidin synthesis and expression of genes encoding leucoanthocyanidin reductase and anthocyanidin reductase in developing grape berries and grapevine leaves. Plant Physiology **139**, 652–663.

Bowler C, van Montagu M, Inze D. 1992. Superoxide dismutase and stress tolerance. Annual Reivew of Plant Physiology and Plant Molecular Biology **43**, 83–116.

Braatne JH, Rood SB, Heilman PE. 1996. Life history, ecology, and conservation of riparian cottonwoods in North America. In: Stettler RF, Bradshaw HD, Heilman PE, Hinckley TM (Eds.) Biology of *Populus* and its implications for management and conservation. Part I, Chapter 3. NRC Research Press, National Research Council of Canada, Ottawa, ON, Canda: 57–85.

Bradshaw HD, Ceulemans R, Davis J, Stettler R. 2000. Emerging model systems in plant biology: poplar (*Populus*) as a model forest tree. Journal of Plant Growth Regulation **19**, 306–313.

Brunner AM, Busov VB, Strauss SH. 2004. Poplar genome sequence: functional genomics in an ecologically dominant plant species. Trends in Plant Science **9**, 49–56.

Bryant JP, Chapin SFI, Klein DR. 1983. Carbon / nutrient balance of boreal plants in relation to vertebrate herbivory. Nordic Society Oikos **40**, 357–368.

Burchard P, Bilger W, Weissenböck G. 2000. Contribution of hydroxycinnamates and flavonoids to, epidermal shielding of UV-A and UV-B radiation in developing rye primary leaves as assessed by ultraviolet-induced chlorophyll fluorescence measurements. Plant, Cell and Environment **23**, 1373–1380.

Burda S, Oleszek W. 2001. Antioxidant and antiradical activities of flavonoids. Journal of Agricultural and Food Chemistry **49**, 2774–2779.

Bus JS, Gibson JE. 1984. Paraquat: model for oxidant-initiated toxicity. Environmental Health Perspectives **55**, 37–46.

Cha JY, Kim WY, Kang S Bin, *et al.* 2015. A novel thiol-reductase activity of *Arabidopsis* YUC6 confers drought tolerance independently of auxin biosynthesis. Nature Communications **6**, 1–13.

Chaves M. 1991. Effects of water deficits on carbon assimilation. Journal of Experimental Botany **42**, 1–16.

Chen L, Gao S, Zhu P, Liu Y, Hu T, Zhang J. 2014. Comparative study of metal resistance and accumulation of lead and zinc in two poplars. Physiologia Plantarum **151**, 390–405.

Chen JW, Zhu ZQ, Hu TX, Zhu DY. 2002. Structure-activity relationship of natural flavonoids in hydroxyl radical-scavenging effects. Acta Physiologiae Sinica **23**, 667–672.

Choudhury FK, Rivero RM, Blumwald E, Mittler R. 2017. Reactive oxygen species, abiotic stress and stress combination. Plant Journal **90**, 856–867.

Coleman HD, Park J-Y, Nair R, Chapple C, Mansfield SD. 2008. RNAi-mediated suppression of p-coumaroyl-CoA 3'-hydroxylase in hybrid poplar impacts lignin deposition and soluble secondary metabolism. Proceedings of the National Academy of Sciences **105**, 4501–4506.

Constabel CP, Lindroth RI. 2010. The impact of genomics on advances in herbivore defense and secondary metabolism in *Populus*. In: Jansson S, Bhaleaero R, Grover A (Eds.), Genetics and Genomics of *Populus*, Springer Verlag Inc., New York, NY, USA: 279–305.

Constabel CP, Yoshida K, Walker V. 2014. Diverse ecological roles of plant tannins: plant defense and beyond. In: Romani A, Lattanzio V, Quideau S (Eds.), Recent Advances in Polyphenol Research Vol 4, John Wiley & Sons Ltd., New Jersey, USA: 115–142.

Constabel CP. 2018. Molecular controls of proanthocyanidin synthesis and structure: prospects for genetic engineering in crop plants. Journal of Agricultural and Food Chemistry **66**, 9882–9888.

Cramer GR, Urano K, Delrot S, Pezzotti M, Shinozaki K. 2011. Effects of abiotic stress on plants: a systems biology perspective. BMC Plant Biology **11**, 163.

Cruz de Carvalho MH. 2008. Drought stress and reactive oxygen species. Plant Signaling & Behavior **3**, 156–165.

Czarnocka W, Karpiński S. 2018. Friend or foe? Reactive oxygen species production, scavenging and signaling in plant response to environmental stresses. Free Radical Biology and Medicine **122**, 4–20.

Czégény G, Mátai A, Hideg É. 2016. UV-B effects on leaves - oxidative stress and acclimation in controlled environments. Plant Science **248**, 57–63.

Dat J, Vandenabeele S, Vranová E, van Montagu M, Inzé D, van Breusegem F. 2000. Dual action of the active oxygen species during plant stress responses. Cellular and Molecular Life Sciences **57**, 779–795.

Daudi A, O'Brien JA. 2012. Detection of hydrogen peroxide by DAB staining in *Arabidopsis* leaves. Bio-Protocol **2**, 1–4.

Davey MP, Susanti NI, Wargent JJ, Findlay JE, Paul Quick W, Paul ND, Jenkins GI. 2012. The UV-B photoreceptor UVR8 promotes photosynthetic efficiency in *Arabidopsis thaliana* exposed to elevated levels of UV-B. Photosynthesis Research **114**, 121–131.

Demidchik V. 2015. Mechanisms of oxidative stress in plants: from classical chemistry to cell biology. Environmental and Experimental Botany **109**, 212–228.

Demmig-Adams B. 1990. Carotenoids and photoprotection in plants: a role for the xanthophyll zeaxanthin. Biochimica et Biophysica Acta **1020**, 1–24.

Demmig-Adams B, Adams WW. 1992. Responses of plants to high light stress. Annual Reivew of Plant Physiology and Plant Molecular Biology **43**, 599–626.

Dickmann DI (2001) An overview of the genus *Populus*. In: Dickmann DI, Isebrands JG, Eckenwalder JE, Richardson J (Eds.), Poplar Culture in North America. Part A. NRC Research Press, Ottawa, ON, Canada: 1–42.

Dixon RA, Xie DY, Sharma SB. 2005. Proanthocyanidins - a final frontier in flavonoid research? New Phytologist **165**, 9–28.

Ellis B, Jansson S, Strauss SH, Tuskan GA. 2010. Why and how *Populus* became a "model tree". In: Jansson S, Bhalerao R, Groover A (Eds.), The genetics and genomics of *Populus*. Plant genetics and genomics, Springer-Verlag Inc., New York, NY, USA: 3-14.

Epron P, Dreyer E, Breda N. 1992. Photosynthesis of oak trees during drought under field conditions: diurnal course of net CO2 assimilation and photochemical efficiency of photosystem II. Plant, Cell and Environment **15**, 809-820.

Farmer RE. 1996. The genecology of *Populus*. In: Stettler RF, Bradshaw HD, Heilman PE, Hinckley TM (Eds.) Biology of *Populus* and its implications for management and conservation. Part I, Chapter 2. NRC Research Press, National Research Council of Canada, Ottawa, ON, Canda: 33-55.

Farmer EE, Mueller MJ. 2013. ROS-mediated lipid peroxidation and RES-activated signaling. Annual Review of Plant Biology **64**, 429–450.

Feeny PP. 1968. Effect of oak leaf tannins on larval growth of the winter moth *Operophtera brumata.* Journal of Insect Physiology **14**, 805–817.

Fini A, Brunetti C, Ferdinando M Di, Ferrini F, Tattini M. 2011. Stress-induced flavonoid biosynthesis and the antioxidant machinery of plants. Plant Signaling and Behavior **6**, 709–711.

Fournand D, Vicens A, Sidhoum L, Souquet JM, Moutounet M, Cheynier V. 2006. Accumulation and extractability of grape skin tannins and anthocyanins at different advanced physiological stages. Journal of Agricultural and Food Chemistry **54**, 7331–7338.

Foyer C, Lelandais M, Kunert K. 1994. Special review: photooxidative stress in plants. Physiologia Plantarum **92**, 696–717.

Fraga CG, Galleano M, Verstraeten S, Oteiza PI. 2010. Basic biochemical mechanisms behind the health benefits of polyphenols. Molecular Aspects of Medicine **31**, 435–445.

Gesell A, Yoshida K, Tran LT, Constabel CP. 2014. Characterization of an apple TT2-type R2R3 MYB transcription factor functionally similar to the poplar proanthocyanidin regulator PtMYB134. Planta **240**, 497–511.

Gill SS, Tuteja N. 2010. Reactive oxygen species and antioxidant machinery in abiotic stress tolerance in crop plants. Plant Physiology and Biochemistry **48**, 909–930.

Gonzalez A, Brown M, Hatlestad G, *et al.* 2016. TTG2 controls the developmental regulation of seed coat tannins in *Arabidopsis* by regulating vacuolar transport steps in the proanthocyanidin pathway. Developmental Biology **419**, 54–63.

Gould KS. 2004. Nature's Swiss army knife: the diverse protective roles of anthocyanins in leaves. Journal of Biomedicine and Biotechnology **2004**, 314–320.

Gourlay G, Constabel CP. 2019. Condensed tannins are inducible antioxidants and protect hybrid poplar against oxidative stress. Tree Physiology **39**, 345–355.

Gourlay G, Ma D, Schmidt A, Constabel CP. 2019. RNAi suppression of MYB134 transgenic poplar inhibits biosynthesis of leaf CTs and increases susceptibility to oxidative stress. *Submitted to Journal of Experimental Botany.*

Guangqiu Q, Chongling Y, Haoliang L. 2007. Influence of heavy metals on the carbohydrate and phenolics in mangrove, *Aegiceras corniculatum* L., seedlings. Bulletin of Environmental Contamination and Toxicology **78**, 440–444.

Hagerman AE. 2002. Condensed tannin structural chemistry. The Tannin Handbook **2**, 1–8.

Hagerman A, Riedl K, Jones G, Kara N, Rit T, Hartz P, Rie L. 1998. High molecular weight polyphenolics (tannins) as biological antioxidants. Journal of Agricultural Food Chemistry **46**, 1887–1892.

Hamilton JG, Zangerl AR, DeLucia EH, Berenbaum MR. 2001. The carbon-nutrient balance hypothesis: its rise and fall. Ecology Letters **4**, 86–95.

Harding SA, Jiang H, Jeong ML, Casado FL, Lin H-W, Tsai C-J. 2005. Functional genomics analysis of foliar condensed tannin and phenolic glycoside regulation in natural cottonwood hybrids. Tree Physiology **25**, 1475–86.

Hare PD, Cress WA, Van Staden J. 1998. Dissecting the roles of osmolyte accumulation during stress. Plant, Cell and Environment **21**, 535–553.

Hättenschwiler S, Hagerman AE, Vitousek PM. 2003. Polyphenols in litter from tropical montane forests across a wide range in soil fertility. Biogeochemistry **64**, 129–148.

He M, He C-Q, Ding N-Z. 2018. Abiotic stresses: general defenses of land plants and chances for engineering multistress tolerance. Frontiers in Plant Science **9**, 1–18.

Hernández I, Alegre L, Van Breusegem F, Munné-Bosch S. 2009. How relevant are flavonoids as antioxidants in plants? Trends in Plant Science **14**, 125–132.

Hernández I, Alegre L, Munné-Bosch S. 2006. Enhanced oxidation of flavan-3-ols and proanthocyanidin accumulation in water-stressed tea plants. Phytochemistry **67**, 1120–1126.

Hewitt EJ. 1966. Sand and water culture methods used in the study of plant nutrition. Technical Communication No. 22 (2nd Ed). Commonwealth Bureau of Horticulture and Plantation Crops East Mailing, Maidstone, Kent, UK.

Hikosaka K, Takashima T, Kabeya D, Hirose T, Kamata N. 2005. Biomass allocation and leaf chemical defence in defoliated seedlings of *Quercus serrata* with respect to carbon-nitrogen balance. Annals of Botany **95**, 1025–1032.

Huvaere K, Skibsted LH. 2015. Flavonoids protecting food and beverages against light. Journal of the Science of Food and Agriculture **95**, 20–35.

James AM, Ma D, Mellway R, *et al.* 2017. Poplar MYB115 and MYB134 transcription factors regulate proanthocyanidin synthesis and structure. Plant Physiology **174**, 154–171.

Jenkins GI. 2009. Signal transduction in responses to UV-B radiation. Annual Review of Plant Biology **60**, 407–431.

Jia LG, Sheng ZW, Xu WF, Li YX, Liu YG, Xia YJ, Zhang JH. 2012. Modulation of anti-oxidation ability by proanthocyanidins during germination of *Arabidopsis thaliana* seeds. Molecular Plant **5**, 472–481.

Jiang S, Weng B, Liu T, Su Y, Liu J, Lu H, Yan C. 2017. Response of phenolic metabolism to cadmium and phenanthrene and its influence on pollutant translocations in the mangrove plant *Aegiceras corniculatum* (L.) Blanco (Ac). Ecotoxicology and Environmental Safety **141**, 290–297.

Kalaji HM, Schansker G, Brestic M, *et al.* 2017. Frequently asked questions about chlorophyll fluorescence, the sequel. Photosynthesis Research **132**, 13–66.

Kaling M, Kanawati B, Ghirardo A, Albert A, Winkler JB, Heller W, Barta C, Loreto F, Schmitt-Kopplin P, Schnitzler JP. 2015. UV-B mediated metabolic rearrangements in poplar revealed by non-targeted metabolomics. Plant, Cell and Environment **38**, 892–904.

Kant S, Bi Y-M, Rothstein SJ. 2011. Understanding plant response to nitrogen limitation for the improvement of crop nitrogen use efficiency. Journal of Experimental Botany **62**, 1499–1509.

Kataria S, Jajoo A, Guruprasad KN. 2014. Impact of increasing ultraviolet-B (UV-B) radiation on photosynthetic processes. Journal of Photochemistry and Photobiology B: Biology **137**, 55–66.

Kennedy JA, Hayasaka Y, Vidal S, Waters EJ, Jones GP. 2001. Composition of grape skin proanthocyanidins at different stages of berry development. Journal of Agricultural and Food Chemistry **49**, 5348–5355.

Khanna-Chopra R. 2012. Leaf senescence and abiotic stresses share reactive oxygen species-mediated chloroplast degradation. Protoplasma **249**, 469–481.

Kim MD, Kim YH, Kwon SY, Jang BY, Lee SY, Yun DJ, Cho JH, Kwak SS, Lee HS. 2011. Overexpression of 2-cysteine peroxiredoxin enhances tolerance to methyl viologen-mediated oxidative stress and high temperature in potato plants. Plant Physiology and Biochemistry **49**, 891–897.

Kosar F, Akram NA, Sadiq M, Al-Qurainy F, Ashraf M. 2019. Trehalose: a key organic osmolyte effectively invovlved in plant abiotic stress tolerance. Journal of Plant Growth Regulation **38**, 606–618.

Kosola KR, Parry D, Workmaster BAA. 2006. Responses of condensed tannins in poplar roots to fertilization and gypsy moth defoliation. Tree Physiology **26**, 1607–1611.

Kraus TEC, Dahlgren RA, Zasoski RJ. 2003. Tannins in nutrient dynamics of forest ecosystems - a review. Plant Soil **256**, 41–66.

Kraus TEC, Zasoski RJ, Dahlgren RA. 2004. Fertility and pH effects on polyphenol and condensed tannin concentrations in foliage and roots. Plant and Soil **262**, 95–109.

Krieger-Liszkay A. 2005. Singlet oxygen production in photosynthesis. Journal of Experimental Botany **56**, 337–346.

Kumari M, Jain S. 2012. Tannin: an antinutrient with positive effects to manage diabetes. Research Journal of Recent Sciences **1**, 1–8.

Lavola A, Julkunen-Tiitto R, Aphalo P, de la Rosa T, Lehto T. 1997. The effect of UV-B radiation on UV-absorbing secondary metabolites in birch seedlings grown under simulated forest soil conditions. New Phytologist **137**, 617–621.

Levée V, Major I, Levasseur C, Tremblay L, MacKay J, Séguin A. 2009. Expression profiling and functional analysis of *Populus* WRKY23 reveals a regulatory role in defense. New Phytologist **184**, 48–70.

Li P, Li YJ, Zhang FJ, Zhang GZ, Jiang XY, Yu HM, Hou BK. 2017. The *Arabidopsis* UDP-glycosyltransferases UGT79B2 and UGT79B3, contribute to cold, salt and drought stress tolerance via modulating anthocyanin accumulation. Plant Journal **89**, 85–103.

Li J, Ou-Lee TM, Raba R, Amundson RG, Last RL. 1993. *Arabidopsis* flavonoid mutants are hypersensitive to UV-B irradiation. Plant Cell **5**, 171–179.

Liang G, Bu J, Zhang S, Jing G, Zhang G, Liu X. 2019. Effects of drought stress on the photosynthetic physiological parameters of *Populus × euramericana* "Neva". Journal of Forestry Research **30**, 409–416.

Lindroth RL, Hwang SY. 1996. Clonal variation in foliar chemistry of quaking aspen (*Populus tremuloides* Michx.). Biochemical Systematics and Ecology **24**, 357–364.

Liu J, Osbourn A, Ma P. 2015. MYB transcription factors as regulators of phenylpropanoid metabolism in plants. Molecular Plant **8**, 689–708.

Lutts S, Kinet JM, Bouharmont J. 1996. NaCl-induced senescence in leaves of rice (*Oryza sativa* L.) cultivars differing in salinity resistance. Annals of Botany **78**, 389–398.

Ma D, Constabel CP. 2019. MYB repressors as regulators of phenylpropanoid metabolism in plants. Trends in Plant Science **24**, 275–289.

Ma D, Reichelt M, Yoshida K, Gershenzon J, Constabel CP. 2018. Two R2R3-MYB proteins are broad repressors of flavonoid and phenylpropanoid metabolism in poplar. Plant Journal **96**, 1–17.

Madritch MD, Hunter MD. 2005. Phenotypic variation in oak litter influences short- and long-term nutrient cycling through litter chemistry. Soil Biology and Biochemistry **37**, 319–327.

Madritch MD, Lindroth RL. 2015. Condensed tannins increase nitrogen recovery by trees following insect defoliation. New Phytologist **208**, 410–420.

Major I, Constabel C. 2006. Molecular analysis of poplar defense against herbivory: comparison of wound- and insect elicitor-induced gene expression. New Phytologist **172**, 617–635.

Maxwell K, Johnson G. 2000. Chlorophyll fluorescence - a practical guide. Journal of Experimental Botany **51**, 659–668.

McKiernan AB, Potts BM, Brodribb TJ, Hovenden MJ, Davies NW, McAdam SM, Ross JJ, Rodemann T, O'Reilly-Wapstra JM. 2015. Responses to mild water deficit and rewatering differ among secondary metabolites but are similar among provenances within *Eucalyptus* species. Tree Physiology **36**, 133–147.

Meilan R, Ma C. 2006. *Agrobacterium* protocols: poplar (*Populus* spp.). In: Wang K (Ed.), Methods in Molecular Biology Vol 344. Humana Press Inc., Totowa, NJ, USA: 143–151.

Mellway RD, Tran LT, Prouse MB, Campbell MM, Constabel CP. 2009. The wound-, pathogen-, and ultraviolet B-responsive MY134 gene encodes an R2R3 MYB transcription factor that regulates proanthocyanidin synthesis in poplar. Plant Physiology **150**, 924–941.

Miller G, Suzuki N, Ciftci-Yilmaz S, Mittler R. 2010. Reactive oxygen species homeostasis and signalling during drought and salinity stresses. Plant, Cell and Environment **33**, 453–467.

Mittler R. 2002. Oxidative stress, antioxidants and stress tolerance. Trends in Plant Science **7**, 405–410.

Mittler R. 2017. ROS are good. Trends in Plant Science **22**, 11–19.

Murchie EH, Lawson T. 2013. Chlorophyll fluorescence analysis: a guide to good practice and understanding some new applications. Journal of Experimental Botany **64**, 3983–3998.

Naik D, Smith E, Cumming JR. 2009. Rhizosphere carbon deposition, oxidative stress and nutritional changes in two poplar species exposed to aluminum. Tree Physiology **29**, 423–436.

Nakabayashi R, Yonekura-Sakakibara K, Urano K, *et al.* 2014. Enhancement of oxidative and drought tolerance in *Arabidopsis* by overaccumulation of antioxidant flavonoids. Plant Journal **77**, 367–379.

Nakajima J, Tanaka I, Seo S, Yamazaki M, Saito K. 2004. LC/PDA/ESI-MS profiling and radical scavenging activity of anthocyanins in various berries. Journal of Biomedicine and Biotechnology **5**, 241–247.

Nelson N, Ben-Shem A. 2004. The complex architecture of oxygenic photosynthesis. Nature Reviews Molecular Cell Biology **5**, 971–982.

Noctor G, Foyer CH. 1998. Ascorbate and glutathione: keeping active oxygen under control. Annual Review of Plant Physiology and Plant Molecular Biology **49**, 249–279.

Noctor G, Lelarge-Trouverie C, Mhamdi A. 2015. The metabolomics of oxidative stress. Phytochemistry **112**, 33–53.

Nybakken L, Hörkkä R, Julkunen-Tiitto R. 2012. Combined enhancements of temperature and UVB influence growth and phenolics in clones of the sexually dimorphic *Salix myrsinifolia*. Physiologia Plantarum **145**, 551–564.

Ögren E. 1990. Evaluation of chlorophyll fluorescence as a probe for drought stress in willow leaves. Plant Physiology **93**, 1280–1285.

Oo CW, Kassim MJ, Pizzi A. 2009. Characterization and performance of *Rhizophora apiculata* mangrove polyflavonoid tannins in the adsorption of copper (II) and lead (II). Industrial Crops and Products **30**, 152–161.

Osawa H, Endo I, Hara Y, Matsushima Y, Tange T. 2011. Transient proliferation of proanthocyanidin-accumulating cells on the epidermal apex contributes to highly aluminum-resistant root elongation in camphor tree. Plant Physiology **155**, 433–446.

Osier TL, Lindroth RL. 2001. Effects of genotype, nutrient availability, and defoliation on aspen phytochemistry and insect performance. Journal of Chemical Ecology **27**, 1289–1313.

Pallozzi E, Fortunati A, Marino G, Loreto F, Agati G, Centritto M. 2013. BVOC emission from *Populus × canadensis* saplings in response to acute UV-A radiation. Physiologia Plantarum **148**, 51–61.

Peng K, Jin L, Niu YD, *et al.* 2018. Condensed tannins affect bacterial and fungal microbiomes and mycotoxin production during ensiling and upon aerobic exposure. Applied and Environmental Microbiology **84**, 1–20.

Pertea M, Kim D, Pertea G, Leek JT, Steven L. 2016. Transcript-level expression analysis of RNA-seq experiments with HISAT, StringTie, and Ballgown. Nature Protocols **11**, 1650–1667.

Peters DJ, Constabel CP. 2002. Molecular analysis of herbivore-induced condensed tannin synthesis: cloning and expression of dihydroflavonol reductase from trembling aspen (*Populus tremuloides*). Plant Journal **32**, 701–712.

Petrov V, Hille J, Mueller-Roeber B, Gechev TS. 2015. ROS-mediated abiotic stress-induced programmed cell death in plants. Frontiers in Plant Science **6**, 1–16.

Petrussa E, Braidot E, Zancani M, Peresson C, Bertolini A, Patui S, Vianello A. 2013. Plant flavonoids - biosynthesis, transport and involvement in stress responses. International Journal of Molecular Sciences **14**, 14950–14973.

Popović BM, Štajner D, Ždero-Pavlović R, Tumbas-Šaponjac V, Čanadanović-Brunet J, Orlović S. 2016. Water stress induces changes in polyphenol profile and antioxidant capacity in poplar plants (*Populus* spp.). Plant Physiology and Biochemistry **105**, 242–250.

Porter LJ, Hrstich LN, Chan BG. 1986. The conversion of procyanidins and prodelphinidins to cyanidin and delphinidin. Phytochemistry **25**, 223–230.

Poschenrieder C, Gunsé B, Corrales I, Barceló J. 2008. A glance into aluminum toxicity and resistance in plants. Science of the Total Environment **400**, 356–368.

Prior RL, Gu L. 2005. Occurrence and biological significance of proanthocyanidins in the American diet. Phytochemistry **66**, 2264–2280.

Quideau S, Deffieux D, Douat-Casassus C, Pouységu L. 2011. Plant polyphenols: chemical properties, biological activities, and synthesis. Angewandte Chemie - International Edition **50**, 586–621.

Ramsay NA, Glover BJ. 2005. MYB-bHLH-WD40 protein complex and the evolution of cellular diversity. Trends in Plant Science **10**, 63–70.

Randriamanana TR, Lavola A, Julkunen-Tiitto R. 2015. Interactive effects of supplemental UV-B and temperature in European aspen seedlings: implications for growth, leaf traits, phenolic defense and associated organisms. Plant Physiology and Biochemistry **93**, 84–93.

Re R, Pellegrini N, Proteggente A, Pannala A, Yang M, Rice-Evans C. 1999. Antioxidant activity applying an improved ABTS radical cation decolorization assay. Free Radical Biology and Medicine **26**, 1231–1237.

Redondo LM, Chacana PA, Dominguez JE, Fernandez Miyakawa ME. 2014. Perspectives in the use of tannins as alternative to antimicrobial growth promoter factors in poultry. Frontiers in Microbiology **5**, 1–7.

Ren J, Dai W, Xuan Z, Yao Y, Korpelainen H, Li C. 2007. The effect of drought and enhanced UV-B radiation on the growth and physiological traits of two contrasting poplar species. Forest Ecology and Management **239**, 112–119.

Rice-Evans CA, Miller NJ, Paganga G. 1996. Structure-antioxidant activity relationships of flavonoids and phenolic acids. Free Radical Biology and Medicine **20**, 933–956.

Rice-Evans CA, Miller NJ, Paganga G. 1997. Antioxidant properties of phenolic compounds. Trends in Plant Science **2**, 152–159.

del Río LA. 2015. ROS and RNS in plant physiology: an overview. Journal of Experimental Botany **66**, 2827–2837.

Ristivojević P, Trifković J, Andrić F, Milojković-Opsenica D. 2015. Poplar-type propolis: chemical composition, botanical origin, and biological activity. Natural Product Communications **10**, 1869–1876.

Sairam RK, Dharmar K, Chinnusamy V, Lekshmy S, Joshi R, Bhattacharya P. 2011. NADPH oxidase as the source of ROS produced under waterlogging in roots of mung bean. Biologia Plantarum **55**, 741–746.

Sairam RK, Kumutha D, Ezhilmathi K, Chinnusamy V, Meena RC. 2009. Waterlogging induced oxidative stress and antioxidant enzyme activities in pigeon pea. Biologia Plantarum **53**, 493–504.

Saito K, Yonekura-Sakakibara K, Nakabayashi R, Higashi Y, Yamazaki M, Tohge T, Fernie AR. 2013. The flavonoid biosynthetic pathway in *Arabidopsis*: structural and genetic diversity. Plant Physiology and Biochemistry **72**, 21–34.

Santos-Buelga C, Scalbert A. 2000. Proanthocyanidins and tannin-like compounds-nature, occurrence, dietary intake and effects on nutrition and health. Journal of the Science of Food and Agriculture **80**, 1094–1117.

Scalbert A. 1991. Antimicrobial properties of tannins. Phytochemistry **30**, 3875–3883.

Schneider JR, Caverzan A, Chavarria G. 2019. Water deficit stress, ROS involvement, and plant performance. Archives of Agronomy and Soil Science **65**, 1160–1181.

Schulz E, Tohge T, Zuther E, Fernie AR, Hincha DK. 2015. Natural variation in flavonol and anthocyanin metabolism during cold acclimation in *Arabidopsis thaliana* accessions. Plant, Cell and Environment **38**, 1658–1672.

Schwanz P, Polle A. 2001. Growth under elevated CO2 ameliorates defenses against photo-oxidative stress in poplar (*Populus alba x tremula*). Environmental and Experimental Botany **45**, 43–53.

Schweitzer JA, Bailey JK, Rehill BJ, Martinsen GD, Hart SC, Lindroth RL, Keim P, Whitham TG. 2004. Genetically based trait in a dominant tree affects ecosystem processes. Ecology Letters **7**, 127–134.

Seyoum A, Asres K, El-Fiky FK. 2006. Structure-radical scavenging activity relationships of flavonoids. Phytochemistry **67**, 2058–2070.

Shay PE, Constabel CP, Trofymow JA. 2018. Evidence for the role and fate of water-insoluble condensed tannins in the short-term reduction of carbon loss during litter decay. Biogeochemistry **137**, 127–141.

Shirley BW. 1996. Flavonoid biosynthesis: 'new' function for an 'old' pathway. Trends in Plant Science **1**, 377–382.

Sjödin A, Street NR, Sandberg G, Gustafsson P, Jansson S. 2009. The *Populus* Genome Integrative Explorer (PopGenIE): a new resource for exploring the *Populus* genome. New Phytologist **182**, 1013–1025.

Slavov, GT, Zhelev, P. 2010. Salient biological features, systematics, and genetic variation of *Populus*. In: Jansson S, Bhalerao R, Groover A (Eds.), The genetics and genomics of Populus. Plant genetics and genomics, Springer-Verlag Inc., New York, NY, USA: 15-38.

Smirnoff N. 1993. The role of active oxygen in the response of plants to water deficit and desiccation. New Phytologist **125**, 27–58.

Smirnoff N, Arnaud D. 2019. Hydrogen peroxide metabolism and functions in plants. New Phytologist **221**, 1197–1214.

Smith AH, Zoetendal E, Mackie RI. 2005. Bacterial mechanisms to overcome inhibitory effects of dietary tannins. Microbial Ecology **50**, 197–205.

Stanton, BJ, Neale, DB, Li, S. 2010. *Populus* breeding: from the classical to the genomic approach. In: Jansson S, Bhalerao R, Groover A (Eds.), The genetics and genomics of *Populus*. Plant genetics and genomics, Springer-Verlag Inc., New York, NY, USA: 309-348.

Stevens, CE and Hume, ID. 2004. Comparative physiology of the vertebrate digestive system. Cambridge University Press, New York, NY, USA: 11-23.

Takagi D, Takumi S, Hashiguchi M, Sejima T, Miyake C. 2016. Superoxide and singlet oxygen produced within the thylakoid membranes both cause photosystem I photoinhibition. Plant Physiology **171**, 1626–1634.

Takahashi S, Badger MR. 2011. Photoprotection in plants: a new light on photosystem II damage. Trends in Plant Science **16**, 53–60.

Thiel S, Döhring T, Köfferlein M, Kosak A, Martin P, Seidlitz HK. 1996. A phytotron for plant stress research: how far can artificial lighting compare to natural sunlight? Journal of Plant Physiology **148**, 456–463.

Tian XM, Xie J, Zhao YL, Lu H, Liu SC, Qu L, Li JM, Gai Y, Jiang XN. 2013. Sense-, antisense- and RNAi-4CL1 regulate soluble phenolic acids, cell wall components and growth in transgenic *Populus tomentosa* Carr. Plant Physiology and Biochemistry **65**, 111–119.

Treutter D. 2006. Significance of flavonoids in plant resistance: a review. Environmental Chemistry Letters **4**, 147–157.

Tsai CJ, Harding SA, Tschaplinski TJ, Lindroth RL, Yuan Y. 2006. Genome-wide analysis of the structural genes regulating defense phenylpropanoid metabolism in *Populus*. New Phytologist **172**, 47–62.

Tuskan GA, Difazio S, Jansson S, *et al.* 2006. The genome of black cottonwood, *Populus trichocarpa* (Torr. & Gray). Science **313**, 1596–1604.

Ullah C, Unsicker SB, Fellenberg C, Constabel CP, Schmidt A, Gershenzon J, Hammerbacher A. 2017. Flavan-3-ols are an effective chemical defense against rust infection. Plant Physiology **175**, 1560–1578.

Utkhao W, Yingjajaval S. 2015. Changes in leaf gas exchange and biomass of *Eucalyptus camaldulensis* in response to increasing drought stress induced by polyethylene glycol. Trees **29**, 1581–1592.

Wada S, Takagi D, Miyake C, Makino A, Suzuki Y. 2019. Responses of the photosynthetic electron transport reactions stimulate the oxidation of the reaction center chlorophyll of photosystem I, P700, under drought and high temperatures in rice. International Journal of Molecular Sciences **20**, 1–16.

Wagner A, Phillips L, Narayan RD, Moody JM, Geddes B. 2005. Gene silencing studies in the gymnosperm species *Pinus radiata*. Plant Cell Reports **24**, 95–102.

Wallis IR, Edwards MJ, Windley H, Krockenberger AK, Felton A, Quenzer M, Ganzhorn JU, Foley WJ. 2012. Food for folivores: nutritional explanations linking diets to population density. Oecologia **169**, 281–291.

Wang L, Lu W, Ran L, Dou L, Yao S, Hu J, Fan D, Li C, Luo K. 2019*a*. R2R3 - MYB transcription factor MYB 6 promotes anthocyanin and proanthocyanidin biosynthesis but inhibits secondary cell wall formation in Populus tomentosa. The Plant Journal **99**, 733–751.

Wang J, Mei J, Ren G. 2019*b*. Plant microRNAs: biogenesis, homeostasis, and degradation. Frontiers in Plant Science **10**, 1–12.

Wang L, Ran L, Hou Y, Tian Q, Li C, Liu R, Fan D, Luo K. 2017. The transcription factor MYB115 contributes to the regulation of proanthocyanidin biosynthesis and enhances fungal resistance in poplar. New Phytologist **215**, 351–367.

Waterhouse PM, Helliwell CA. 2003. Exploring plant genomes by RNA-induced gene silencing. Nature Reviews Genetics **4**, 29–38.

Westley R. 2015. Investigating potential physiological roles of condensed tannins in roots of *Populus*: localization and distribution in relation to nutrient ion uptake. *Master's thesis.*

Wilkins O, Nahal H, Foong J, Provart NJ, Campbell MM. 2009. Expansion and diversification of the *Populus* R2R3-MYB family of transcription factors. Plant Physiology **149**, 981–993.

Wohlgemuth H, Mittelstrass K, Kschieschan S, Bender J, Weigel H, Overmyer K, Kangasjärvi J, Sandermann H, Langebartels C. 2002. Activation of an oxidative burst is a general feature of sensitive plants exposed to the air pollutant ozone. Environment **25**, 717–726.

Wright JS, Johnson ER, DiLabio GA. 2001. Predicting the activity of phenolic antioxidants: theoretical method, analysis of substituent effects, and application to major families of antioxidants. Journal of the American Chemical Society **123**, 1173–1183.

Wullschleger SD, Weston DJ, Difazio SP, Tuskan GA. 2013. Revisiting the sequencing of the first tree genome: *Populus trichocarpa*. Tree Physiology **33**, 357–364.

Xu W, Dubos C, Lepiniec L. 2015. Transcriptional control of flavonoid biosynthesis by MYB-bHLH-WDR complexes. Trends in Plant Science **20**, 176–185.

Xu Z, Mahmood K, Rothstein SJ. 2017. ROS induces anthocyanin production via late biosynthetic genes and anthocyanin deficiency confers the hypersensitivity to ROS-generating stresses in *Arabidopsis*. Plant and Cell Physiology **58**, 1364–1377.

Yan JX, Lu YF, Yan SC. 2014. The effects of irradiance on the production of phenolic compounds and condensed tannins in *Larix gmelinii* needles. Biologia Plantarum **58**, 159–163.

Yang Y, Li X, Yang S, Zhou Y, Dong C, Ren J, Sun X, Yang Y. 2015. Comparative physiological and proteomic analysis reveals the leaf response to cadmium-induced stress in poplar (*Populus yunnanensis*). PLoS ONE **10**, 1–20.

Yıldırım K, Kaya Z. 2017. Gene regulation network behind drought escape, avoidance and tolerance strategies in black poplar (*Populus nigra* L.). Plant Physiology and Biochemistry **115**, 183–199.

Yoshida K, Ma D, Constabel CP. 2015. The MYB182 protein down-regulates proanthocyanidin and anthocyanin biosynthesis in poplar by repressing both structural and regulatory flavonoid genes. Plant Physiology **167**, 693–710.

Yu B, Zhao CY, Li J, Li JY, Peng G. 2015. Morphological, physiological, and biochemical responses of *Populus euphratica* to soil flooding. Photosynthetica **53**, 110–117.

Zeevaart JAD, Creelman RA. 1988. Metabolism and physiology of abscisic acid. Annual Review of Plant Physiology and Plant Molecular Biology **39**, 439–473.

Zeuthen J, Mikkelsen TN, Paludan-Müller G, Ro-Poulsen H. 1997. Effects of increased UV-B radiation and elevated levels of tropospheric ozone on physiological processes in European beech (*Fagus sylvatica*). Physiologia Plantarum **100**, 281–290.

Zhang S, Jiang H, Zhao H, Korpelainen H, Li C. 2014. Sexually different physiological responses of *Populus cathayana* to nitrogen and phosphorus deficiencies. Tree Physiology **34**, 343–354.

Zhang LH, Lin YM, Ye GF, Liu XW, Lin GH. 2008. Changes in the N and P concentrations, N:P ratios, and tannin content in *Casuarina equisetifolia* branchlets during development and senescence. Journal of Forest Research **13**, 302–311.

Zhang LH, Shao HB, Ye GF, Lin YM. 2012. Effects of fertilization and drought stress on tannin biosynthesis of *Casuarina equisetifolia* seedlings branchlets. Acta Physiologiae Plantarum **34**, 1639–1649.

Zhang X, Zang R, Li C. 2004. Population differences in physiological and morphological adaptations of *Populus davidiana* seedlings in response to progressive drought stress. Plant Science **166**, 791–797.

Zhou X, Jacobs TB, Xue L-J, Harding SA, Tsai C-J. 2015. Exploiting SNPs for biallelic CRISPR mutations in the outcrossing woody perennial *Populus* reveals 4-coumarate: CoA ligase specificity and redundancy. New Phytologist **208**, 298–301.

Zhou X, Ren S, Lu M, Zhao S, Chen Z, Zhao R, Lv J. 2018. Preliminary study of cell wall structure and its mechanical properties of C3H and HCT RNAi transgenic poplar sapling. Scientific Reports **8**, 1–10.

Ziebell A, Gjersing E, Hinchee M, Katahira R, Sykes RW, Johnson DK, Davis MF. 2016. Downregulation of p-coumaroyl quinate/shikimate 3’-hydroxylase (*C3’H*) or cinnamate-4-hydrolylase (*C4H*) in *Eucalyptus urophylla × Eucalyptus grandis* leads to increased extractability. Bioenergy Research **9**, 691–699.

Appendix

Appendix 1: Representative image of one of my hybrid poplar trees

Appendix 2: Phloroglucinol stains of MYB134-RNAi stem cross-sections

Appendix 2.1: Wild-type

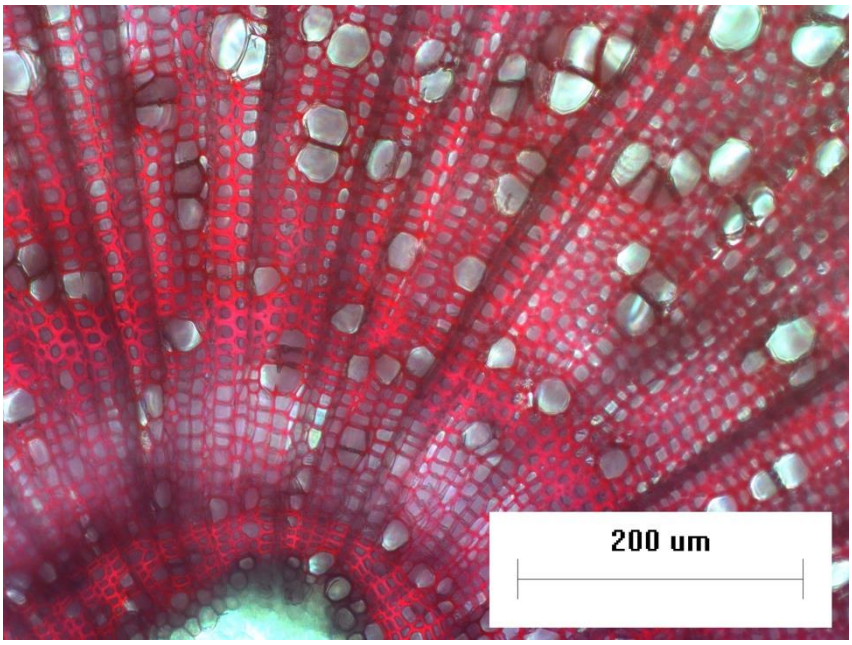

Appendix 2.2: MYB134-RNAi line 3

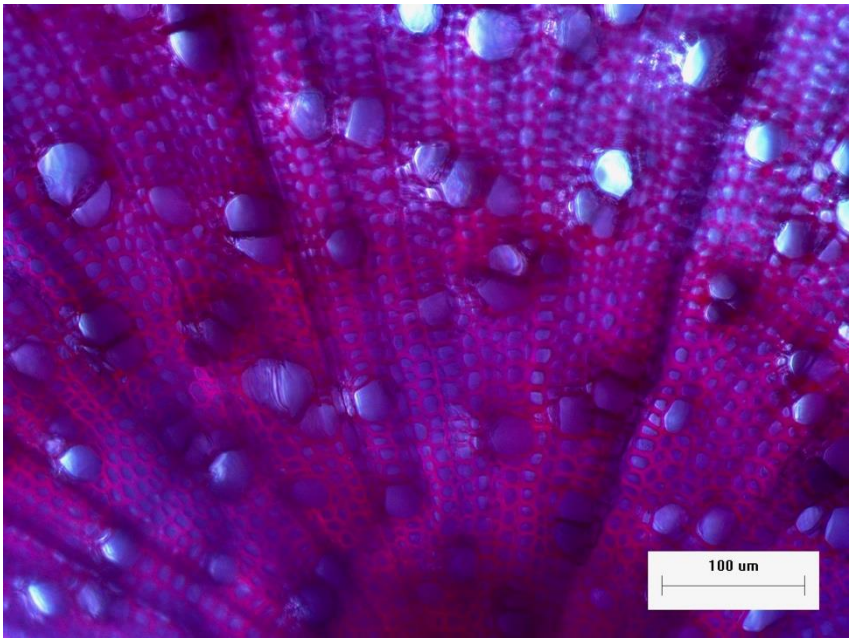

Appendix 2.3: MYB134-RNAi line 7

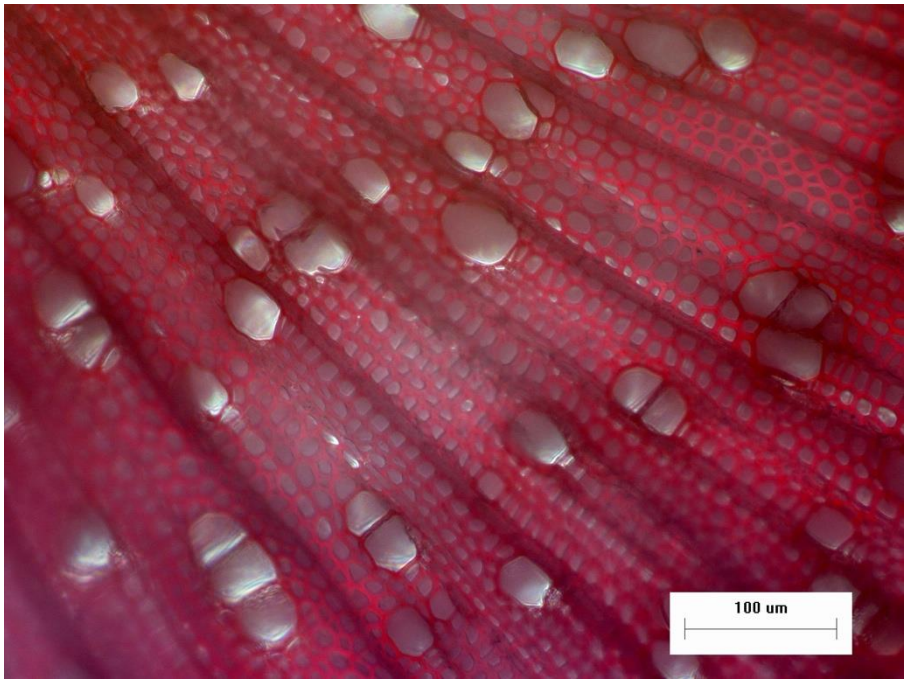

Appendix 2.4: MYB134-RNAi line 22

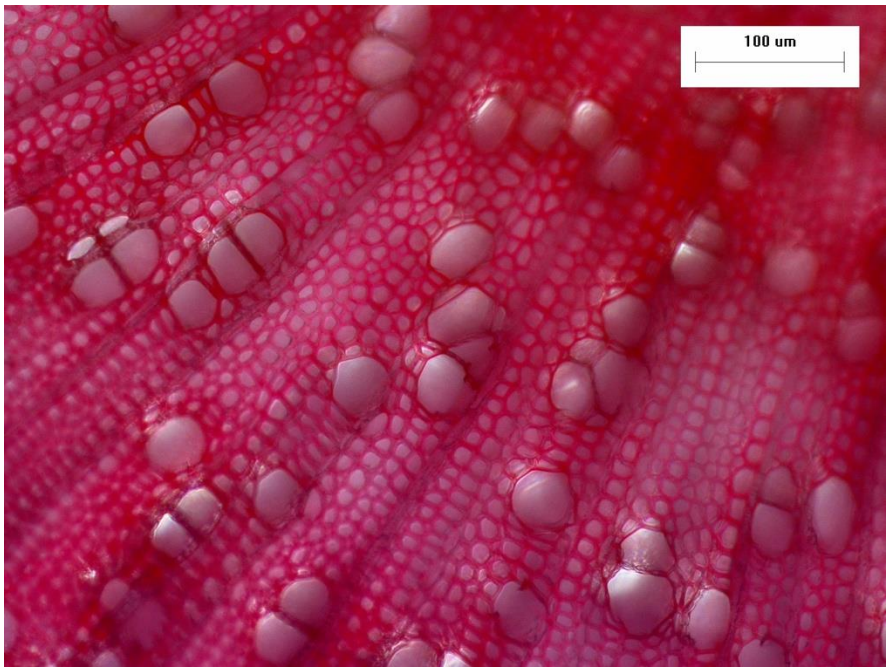

Appendix 2.5: MYB134-RNAi line 24

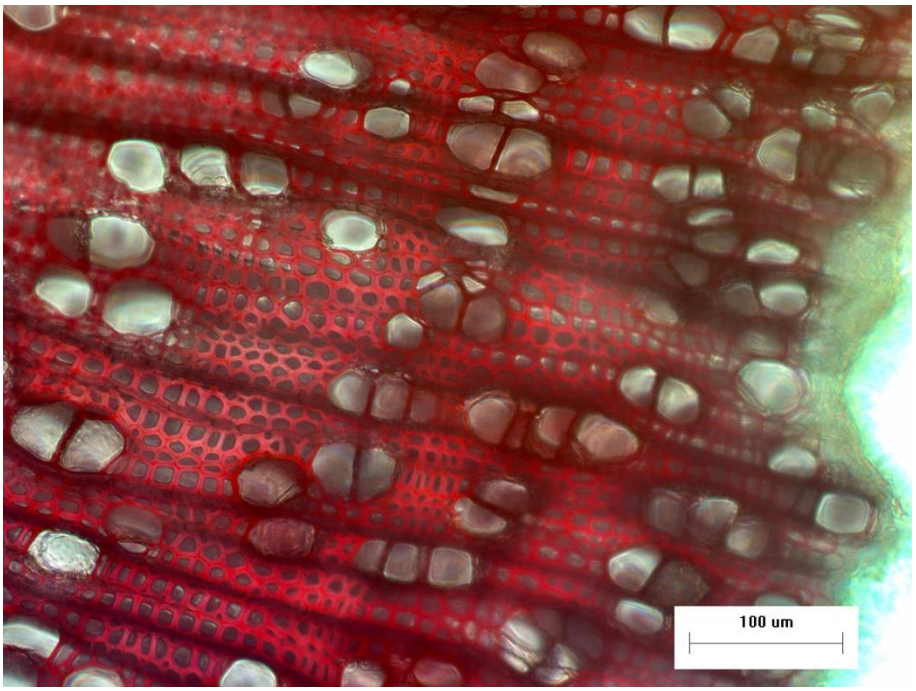

All images were generated with help from Lan Tran. These cross-sections were completed to ensure there were no off-target effects of the RNAi on the plant vasculature.

Appendix 3: Toluidine blue stains of MYB134-RNAi stem cross-sections

Appendix 3.1: Wild-type

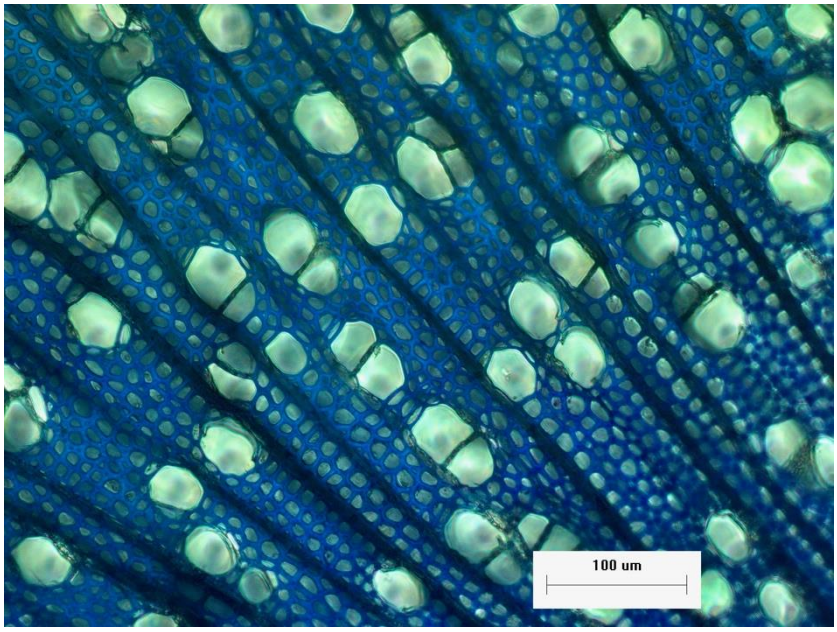

Appendix 3.2: MYB134-RNAi line 3

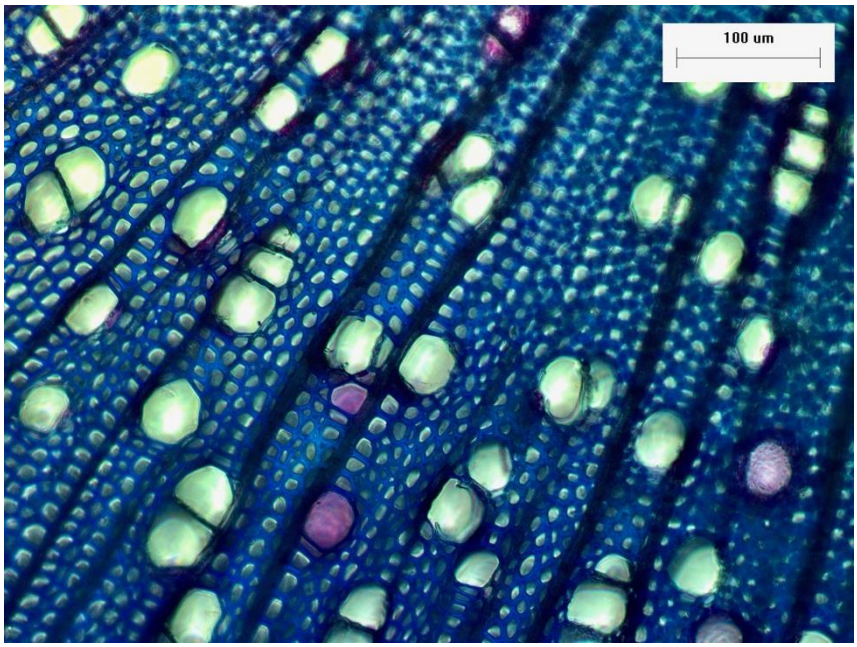

Appendix 3.3: MYB134-RNAi line 7

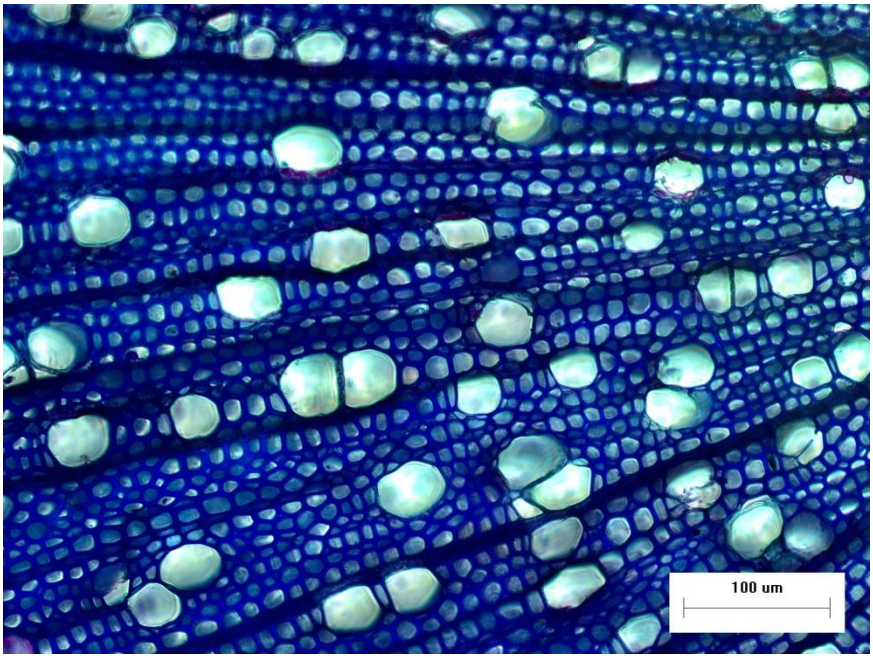

Appendix 3.4: MYB134-RNAi line 22

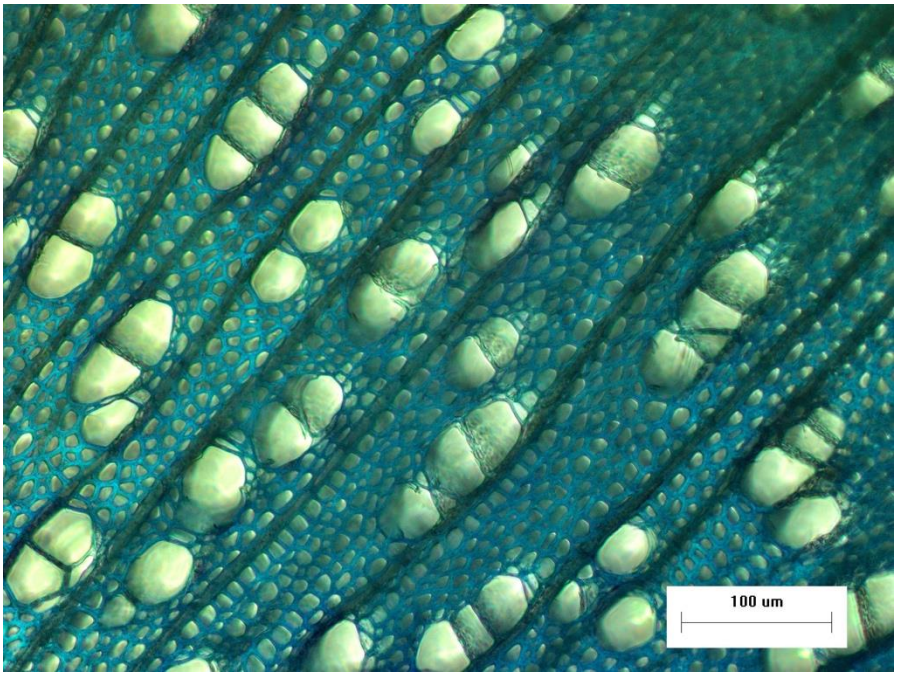

Appendix 3.5: MYB134-RNAi line 24

All images were generated with help from Lan Tran. These cross-sections were completed to ensure there were no off-target effects of the RNAi on the plant vasculature.

Appendix 4: Methods

Appendix 4.1: Plants in mist chamber

Appendix 4.2: Plants in greenhouse #2

Appendix 4.3: Outside experiment setup

Appendix 4.4: Methyl viologen setup

Appendix 4.5: Photo of my final harvest of poplar trees